



UNIVERSITÀ  
DEGLI STUDI  
DI PADOVA

Head Office: Università degli Studi di Padova

Department of Mother and Child Health

---

Ph.D. COURSE IN: Developmental Medicine and Healthcare Planning Sciences

CURRICULUM: Pediatrics: Onco-hematology, human genetics, rare disease and predictive medicine

SERIES XXXV

**UNRAVELLING THE ROLE OF LIPIDS AND NUTRITION IN THE REPLICATION OF ZIKA VIRUS AT THE  
LEVEL OF THE PLACENTA**

Thesis written with the financial contribution of ZIKAction project led by Penta Foundation Italy

**Coordinator:** Prof. Gianni Bisogno

**Supervisor:** Prof. Carlo Giaquinto

**Co-Supervisor:** Dott. Francesco Bonfante

**Ph.D. student :** Eva Mazzetto



# **Unravelling the role of lipids and nutrition in the replication of Zika virus at the level of the placenta**

## ***Abstract***

Before 2007, Zika (ZIKV) virus has been an unknown pathogen, sporadically detected in some African areas and transmitted among humans by mosquito bites, causing moderate symptoms. In late 2013, ZIKV started spreading worldwide, triggering a pandemic that involved South Asiatic, Pacific and American countries. In 2016, ZIKV reached the highest diffusion in Brazil, which counted over 200.000 cases in the human population. In the same year, the World Health Organization declared ZIKV a public health emergency of international concern. In countries affected by the ZIKV epidemic, the biomedical community reported a steep increase in pregnancy impairment, highlighting an alarming correlation between ZIKV infection and fetal malformation. Although many scientific groups have been studying ZIKV vertical transmission, how this virus can damage a fetus during the second and third gestational trimesters is still unknown.

In this context, this project aimed to better understand the ZIKV pathogenic mechanism underpinning the viral crossing of the placenta and the consequent impact that those phenomena have on fetal development at the late stages of pregnancy. To reach this goal, in a first study, we investigated which viral factors, among genome, proteins and lipids, could mainly determine ZIKV pathogenesis in placenta. We replicated three genetically different ZIKV strains in mammalian and mosquito cell lines to obtain viral stocks with a species-specific lipid composition. Then, we characterized the replicative kinetic and infective performance of these viral ZIKV stocks on immortalized placental cell lines and human full-term placenta explants. Our experiments revealed that the lipid composition of the viral envelope more than viral lineage or genetics influenced the ZIKV virus's ability to replicate in the placental tissues during the late stages of pregnancy. derived from mammalian cells displayed higher infectivity in placental villous trophoblasts.

Consequently, we decided to further investigate the role of viral and host lipids by performing a translation *in-vivo* study in immunocompetent mice. In this second experiment, we considered that ZIKV derives its lipids directly from the placental cells and, in turn, these cells constitute their lipid structures using fats derived from food nutrients. From this perspective, we hypothesized that maternal dietary lipids could play a role in determining placental tissue susceptibility to ZIKV infection. To verify this assumption, we formulated four diets reproducing the lipid content of the main human dietary patterns and then, we tailored them for mouse nutrition. The immunocompetent mice were divided into four groups, and fed with experimental diets before and during the pregnancy. At 12 days of gestation, mice were ZIKV or mock-infected and successively sacrificed to collect organs. From the analyses conducted on sampled tissues, we established that dietary lipids influenced the lipid structure of the placenta modulating the expression of the different lipid classes in this tissue. Moreover, we observed a different placental susceptibility to ZIKV infection, depending on the diet administered and the lipid content of the placental tissues. Specifically, we demonstrated that mice fed with a diet characterized by low and unsaturated fatty acids, harboured placentas enriched with phosphatidylserines, which conferred to these tissues a higher resistance to the ZIKV infection.

Collectively, our studies have unveiled maternal diet as a fundamental determinant of ZIKV pathogenesis in a pre-clinical animal model of placental infection. The results not only present new perspectives on the neglected interplay between dietary lipids and Flavivirus pathogenesis, but open the way to a new line of research in the field of prophylaxis for the control of ZIKV.

# **Ruolo dei lipidi e della nutrizione nella replicazione del virus Zika a livello di placenta**

## **Sommario**

Il virus Zika, appartenente alla famiglia dei *Flaviviridae*, è un virus che si trasmette all'uomo tramite puntura di zanzara causando una malattia dal decorso spesso asintomatico. Nel 2013 Zika iniziò a diffondersi velocemente nei territori del Sud-Est asiatico e dell'Oceano Pacifico fino ad arrivare, nel 2016, al Sud e Centro America dove oltre 200.000 casi di infezione vennero registrati nella popolazione locale. Nello stesso anno, l'Organizzazione Mondiale della Sanità (OMS) dichiarò la diffusione del virus Zika emergenza internazionale di salute pubblica. A partire da quel periodo, l'incremento di casi di microcefalia e difetti congeniti nei neonati dei paesi colpiti dal virus Zika destò molta preoccupazione nella comunità medico-scientifica, che poco dopo, confermò la capacità di questo patogeno di trasmettersi verticalmente dalla madre al feto. Dall'apice della pandemia ad oggi, i ricercatori di tutto il mondo hanno compiuto uno sforzo collettivo nell'indagare la patogenesi di Zika; ciononostante, il modo in cui il virus è in grado di infettare la placenta specialmente nelle ultime fasi della gravidanza, rimane tutt'ora da stabilire.

In questo contesto, il seguente progetto di dottorato si è posto come primo obiettivo quello di indagare il ruolo dei principali fattori virali, rappresentati da genoma, proteine e lipidi nel determinare la patogenesi di Zika a livello di placenta. I risultati dei nostri esperimenti hanno evidenziato che i lipidi dell'envelope virale, la membrana di cui è rivestito il virus, più che il genoma o le proteine virali, sono stati capaci di influenzare la capacità replicativa del virus Zika nelle cellule placentari immortalizzate e nelle culture *ex-vivo* di placenta umana. Nello specifico abbiamo osservato, come i ceppi di Zika costituiti da un envelope ricco di fosfatidilcoline possedessero una maggior infettività nelle cellule trofoblastiche del villo placentare. Alla luce di tale evidenza, abbiamo deciso di proseguire il progetto di

ricerca indagando più approfonditamente il ruolo dei lipidi mediante l'applicazione di uno studio *in-vivo* sul modello topo. In questo secondo esperimento, partendo dal presupposto che, sia i lipidi virali, che quelli delle cellule ospite, derivano dai grassi assunti con l'alimentazione, ci siamo chiesti se i lipidi della dieta materna fossero in grado di influenzare la suscettibilità placentare all'infezione da Zika. Per verificare questa ipotesi, abbiamo formulato quattro diete, rappresentative del contenuto lipidico dei principali *pattern* nutrizionali diffusi nel mondo, e le abbiamo adattate al metabolismo del nostro modello animale. Le femmine di topo utilizzate sono state divise in quattro gruppi e alimentate prima e durante la gestazione con le diete sperimentali. A dodici giorni di gestazione, gli animali sono stati infettati con il virus Zika e successivamente sacrificati per la raccolta degli organi. Le analisi condotte hanno evidenziato come, i grassi introdotti con la dieta siano stati in grado di influenzare in modo significativo la suscettibilità della placenta all'infezione da Zika. In particolare, gli animali alimentati con diete dal contenuto lipidico moderato, e ricco in acidi grassi insaturi, avevano placenti con elevate quantità di fosfatidilserine, le quali hanno conferito a questo tessuto una notevole resistenza nei confronti dell'infezione da Zika.

Complessivamente, i risultati ottenuti da questo progetto di dottorato non solo hanno permesso di approfondire l'interazione tra lipidi e *Zika* offrendo nuove prospettive di ricerca nell'ambito della patogenesi dei *Flavivirus*, ma hanno anche posto le basi per un innovativo ed inedito utilizzo dell'alimentazione, quale strumento profilattico di gestione della malattia da Zika nelle donne in gravidanza.

*A tutte le donne,  
che desiderano essere anche madri.*

# Table of contents

<b>Abstract</b> .....	iii
<b>Sommario</b> .....	v
<b>Chapter 1</b> .....	1
<i>General introduction</i> .....	1
1.1 Zika virus epidemiology.....	2
1.2 Zika virus structure.....	4
1.3 Zika virus host-cell interaction.....	6
1.4 Zika virus transmission.....	8
1.5 Zika pathogenesis and clinical manifestations.....	9
1.6 Zika diagnosis.....	11
1.7 Zika prevention and therapy.....	11
1.8 Objective and thesis structure.....	13
<i>References</i> .....	14
<b>Chapter 2</b> .....	17
Host and viral lipids as determinants of Zika virus infectivity in full-term placenta.....	18
Abstract.....	18
2.1 Introduction.....	19
2.2 Methods:.....	21
2.2.1 Cell lines.....	21
2.2.2 BeWo cells syncytialization.....	22
2.2.3 Full-term placenta explant cultures.....	22
2.2.4 Histology and Immunohistochemistry.....	23
2.2.5 Viruses propagation and titration.....	24
2.2.6 Lipidomic analysis.....	25
2.2.7 Next-generation sequencing.....	27
2.2.8 Growth curves of ZIKV strains in immortalized placenta cell lines.....	28
2.2.9 ZIKV strains infectivity and binding capacity in immortalized placenta cell lines.....	29
2.2.10 ZIKV strains fusion efficiency in immortalized placenta cell lines.....	29
2.2.11 ZIKV replication in human placental explants.....	31
2.2.12 Molecular testing by real-time RT-PCR.....	31
2.2.13 Statistical analysis.....	32
2.3 Results.....	32
2.3.1 Genetic analysis of viral stocks generated from ZIKV replication in mammalian and insect-cell lines.....	32
2.3.2 Lipidomic analysis of the envelope of ZIKV strains originated from replication in mammalian or in insect-cell lines.....	33
2.3.3 Replication of ZIKV strains originated from mammalian and mosquito cells in placental immortalized cell lines.....	34
2.3.4 Infectivity of ZIKV strains originated from mammalian and mosquito cells in placental immortalized cell lines.....	37
2.3.5 ZIKV strains fusion efficiency in immortalized placenta cell lines.....	38
2.3.6 Infectivity and replication kinetic of ZIKV stocks derived from mammalian and mosquito cell lines in human full-term placental explants.....	40
2.4 Discussion.....	43
2.5 Supplementary contents.....	51
<i>References</i> .....	55
<b>Chapter 3</b> .....	60
Maternal dietary lipids as risk factor of Zika virus vertical transmission in a rodent model.....	61
Abstract.....	61
3.1 Introduction.....	63
3.2 Methods.....	65
3.2.1 Animals and husbandry.....	65
3.2.2 Diets.....	65
3.2.3 Viruses.....	66
3.2.4 Experimental design: diet administration and ZIKV infection.....	67
3.2.5 Biochemical parameters and hormones.....	68
3.2.6 Lipidomic analysis on placental tissues.....	69
3.2.7 Viral detection by qRT-PCR.....	69



3.2.8 Immunostaining .....	71
3.2.9 Statistical analyses .....	71
<b>3.3 Results</b> .....	<b>72</b>
3.3.1 Dietary impact on mice metabolism .....	72
3.3.2 Dietary impact on mice placental lipid composition .....	75
3.3.3 ZIKV pathogenesis in an immunocompetent mouse model .....	76
3.3.4 Dietary impact on the placental susceptibility to ZIKV infection.....	78
3.3.5 Correlation between placental lipids and ZIKV infection.....	81
3.3.6 ZIKV vertical transmission .....	83
3.4 Discussions .....	83
3.5 Supplementary contents.....	90
<i>References</i> .....	96
<b>Chapter 4</b> .....	<b>99</b>
<i>General discussions</i> .....	99
<b>Annex I</b> .....	<b>104</b>
<b>Acknowledgments</b> .....	<b>105</b>

# **Chapter 1**

## *General introduction*

## 1.1 Zika virus epidemiology

Zika virus (ZIKV) was first isolated in 1947 in the Uganda forest from a sentinel macaque and *Aedes (Stegomyia) africanus* mosquitoes. Results of serologic and entomologic investigations suggest that ZIKV had an extensive geographic distribution in Africa and Asia before 2007 (1). However, a low number of disease cases was reported among the infected population, which all displayed mild or self-limiting clinical manifestations. The first alarm, indicating a change in ZIKV epidemiology, was the ZIKV outbreaks in the Pacific in the Yap Islands, Micronesia, in 2007 and French Polynesia in 2013-2014, which were followed by a pandemic spread of the virus to the Americas, the Caribbean, and Africa (2). In particular, the autochthonous transmission of ZIKV in the north-eastern part of Brazil was first reported in early 2015 and, by the end of the same year, ZIKV activity had expanded into at least 14 South and Central American states (3). In early 2016, local outbreaks were confirmed in Guyana, Ecuador, Bolivia, Peru, Nicaragua, Curacao, Jamaica, Haiti, Santo Domingo and other Caribbean islands. In the first half of the same year, the virus was also detected in Argentina and Cuba and, finally, in spring 2016, it reached the United States (Fig. 1). The epidemics started to decline in various American countries in the second half of 2016 and, although small local outbreaks were still being reported in 2017, their incidence was greatly reduced. During the next 5 years, 2017–2021, infection rates decreased substantially; for example, the United States reported 15 new local cases in 2017 and none since. However, ZIKV did not disappear from the region; >150,000 cases were reported, unadjusted for underreporting, in the Americas through September 2021 (4). Moreover, accurate and up-to-date epidemiologic data on ZIKV are limited in many areas of the world, because the majority of ZIKV infections are asymptomatic and therefore may not be detected or reported. Furthermore, many countries lack or have limited systems for routine surveillance and detection of ZIKV

disease's cases, and in the absence of large outbreaks, available information is often based on clinical case reports, traveller cases, and research studies. Even in settings with laboratory capacity, case detection and surveillance are challenging due to the limited availability of diagnostic tests and difficulties with the interpretation of serologic test results because of known cross-reactivity of ZIKV with related circulating *Flaviviruses*, most notably DENV. Finally, the capacities to detect arbovirus transmission have been further hampered in many countries by the COVID-19 pandemic (<https://www.who.int/publications/m/item/zika-epidemiology-update---february-2022>). From the phylogeny perspective, there were two major lineages of ZIKV, African and Asian. All the contemporary human ZIKV strains share greater sequence homology with the first Asian ZIKV isolated in Malaysia/1966, suggesting that the ZIKV strains responsible for the most recent human outbreak evolved from the Asian lineage (Fig. 2) (5). The differences in the epidemic potential and pathogenicity of these viral lineages and strains remain poorly understood. For example, an earlier report postulated the association of a specific viral mutation of the Asian lineage with the observation of teratogenic effects of ZIKV infection following the outbreaks in French Polynesia and in the Americas in 2015-2016. However, this hypothesis was immediately challenged by the documentation of a case of microcephaly in Thailand after congenital infection with Asian strain ZIKV without that mutation (6). Interestingly, to date, adverse pregnancy outcomes and cases of Congenital ZIKV syndrome caused by ZIKV African lineage viruses have not been recognized and it is not known whether this is because they do not occur, or because of limitations of detection and surveillance (7).

Cases of ZIKV Infection

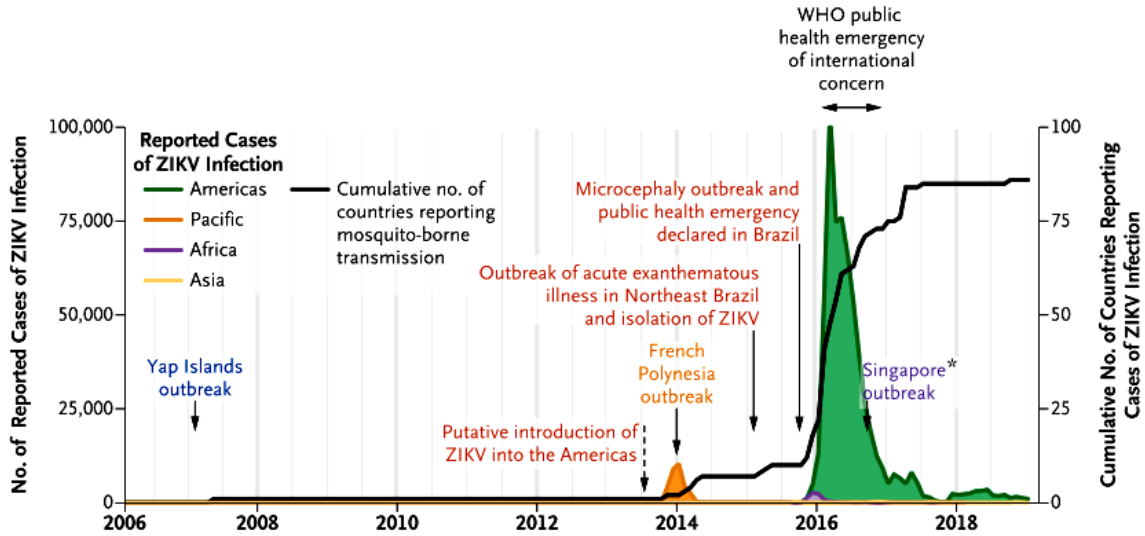


Fig. 1 ZIKV temporal diffusion among countries. Source: Zika Virus Infection — After the Pandemic (8).

A

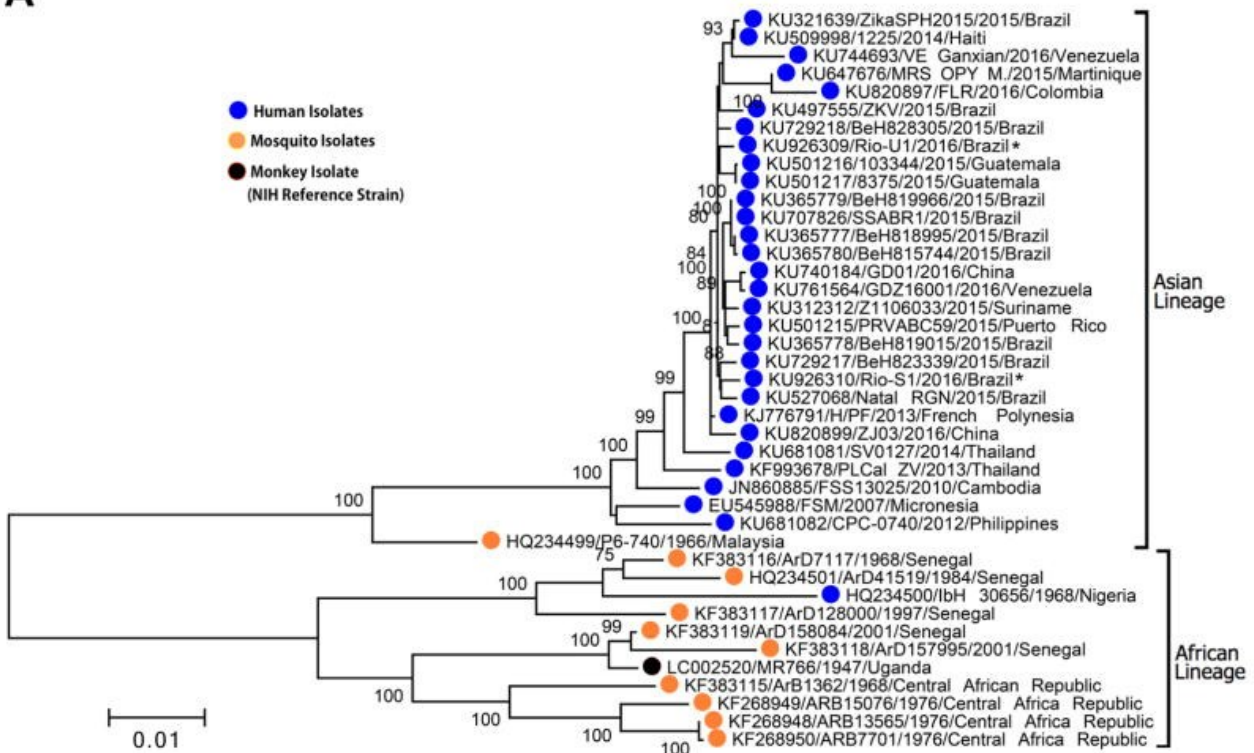


Fig. 2. Phylogenetic tree constructed from nucleotide data from 41 viral complete ORF sequences of ZIKV strains showing ZIKV lineages. Source: From Mosquitos to Humans: Genetic Evolution of Zika Virus (5)

1.2 Zika virus structure

ZIKV is an arbovirus (arthropod-borne virus) classified into the Flavivirus genus within the Flaviviridae family, which includes important human and animal pathogens such as yellow fever virus (YFV), dengue virus (DENV), West Nile virus (WNV), St. Louis encephalitis

virus (SLEV), Japanese encephalitis virus (JEV) and tick-borne encephalitis virus (TBEV) (9). ZIKV is a small enveloped single-stranded positive RNA virus with a size ranging from 30 to 45 nm in diameter. Cryoelectron microscopy reconstructions of *Flavivirus* particles have shown that virions are composed of a central core that contains the capsid (C) or core protein associated with the viral genomic RNA. This nucleocapsid is enclosed in a lipid bilayer derived from the host cell. The pre-membrane/membrane (prM/M) and envelope (E) proteins are anchored into the lipid envelope and conform to the smooth outer shell of the virion (10) (Fig.3). ZIKV genome is constituted by a single-stranded RNA molecule of positive polarity that, similarly to cellular mRNAs, includes a cap structure at its 5'. The genome contains a single open reading frame (ORF) that encodes a polyprotein of about 3400 amino acids that is expected to be cleaved into mature viral proteins. The mature virion's proteins are represented by three structural proteins (C, E, prM/M proteins), and seven non-structural proteins (NS1, NS2A, NS2B, NS3, NS4A, NS4B, and NS5). The structural proteins participate in the assembly of the virions: C associates with the viral genome to constitute the core of the virions and the E protein promotes the attachment/fusion of ZIKV with the host cells. Relative to prM function, this protein assists the folding of the E protein and prevents premature fusion of the particles before being released from the infected cell (11). The cleavage of prM into M protein also promotes the maturation of the viral particles. The role of NS proteins is not well-understood but progress has been made in the study of ZIKV NS proteins in viral pathogenesis (12). NS1, NS3, NS4B and NS5 all inhibit the interferon signaling pathway and NS2B-NS3 impedes the JAK-STAT signaling pathway. NS2A and NS4A may play a role in ZIKV-induced neurological disorders. Moreover, NS2A attenuates the proliferation of radial glial cells and causes defects of adherent junction proteins in the brain cells. Interestingly, co-expression of NS4A and NS4B in fetal neural stem cells inhibits the Akt-mTOR signaling pathway, which is one of the key cellular pathways essential for brain development and autophagy

regulation. Finally, NS4A may also inhibit brain development by inhibiting the function of Ankle2, whose mutations cause autosomal recessive microcephaly in humans.

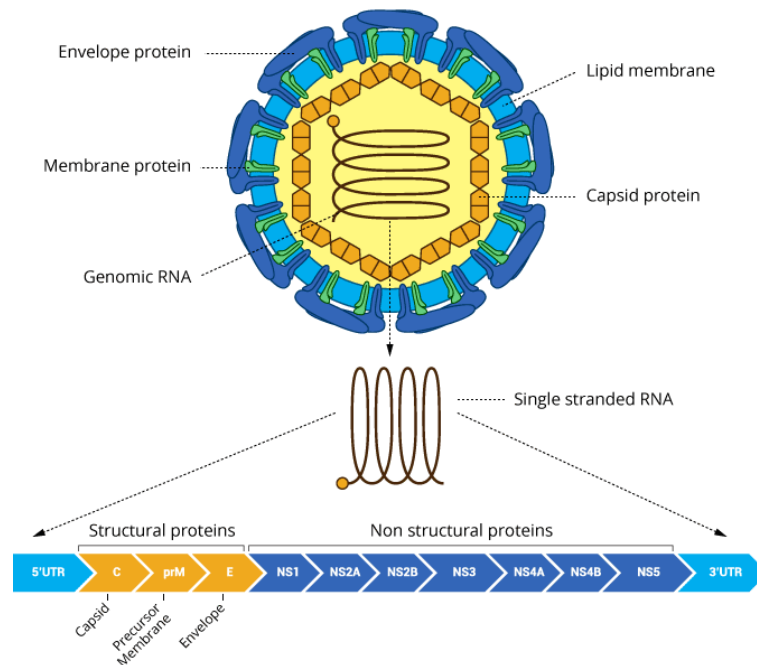


**Fig. 3. ZIKV virions' structure.**

Source: <https://www.promega.com//media/images/inspiration/zika/ZikaVirusStructureIllustration.png>

### 1.3 Zika virus host-cell interaction

ZIKV interacts with the host-cell surface through its surface mature protein E arranged in an icosahedral format. Initially, this viral protein binds to the negatively charged glycosaminoglycans (GAGs), which consist in low-affinity aspecific attachment factors that concentrate the virus on the cell surface. Then the carbohydrate profiles of ZIKV E protein are recognized by C-type lectin (CLR) receptors, a large family of receptors which act as pathogen-associated molecular patterns (PAMPs) (Fig. 4). The most implicated CLR in ZIKV entry is DC-SIGN, which is mainly expressed on macrophages and dendritic cells(13). Moreover, the ZIKV entry process can be mediated by interaction with viral negatively charged lipids and anionic lipid cell receptors belonging to two distinct families of transmembrane phosphatidylserine receptors: TIM (TIM1, TIM3 and TIM4) and

TAM (TYRO3, AXL and MER). The physiological function of these receptors is to recognize negatively charged lipids in apoptotic cells and trigger their endocytosis and disposal. Several pieces of evidence suggest that ZIKV can also use apoptotic mimicry to infect different human tissues, including skin cells, endothelial cells, neural cells and placenta cells (14). Once ZIKV is bound to cell receptors, the viral entry is mediated by the mechanism of clathrin-mediated endocytosis usually used by the cells for nutrient uptake. After clathrin-mediated uptake, the endocytic vesicle, carrying the virus, is delivered to the initial endosomes, which mature into late endosomes, and then the viral membrane fuses with the endosome membrane and viral RNA is released into the host-cell cytoplasm (15). It is important to note that membrane fusion on the host cell depends on the pH of the viral membrane and the interaction among viral and host lipids (13). Once the viral RNA is released in the cytoplasm of the host cell, it is translated into structural and NS proteins and viral replication starts. As plus-stranded RNA viruses, ZIKV remodels intracellular membranes developing organelle-like structures to create adequate platforms for viral replication. Specifically, *Flavivirus* replication produces marked rearrangements of the endoplasmic reticulum (ER) of the infected cells, mainly characterized by invaginations of vesicle-like structures into the lumen of this organelle. The newly synthesized immature ZIKV particles are produced by budding the C protein and the associated genomic RNA (nucleocapsid) into ER-derived membranes that are studded with prM and E. In this way, the membrane of the ZIKV is hijacked from modified portions of the ER and, hence, exhibits a unique lipid composition to achieve its functions. These de novo synthesized immature viral particles traffic along the secretory pathway across the Golgi complex, where they undergo the cleavage of the prM protein by a trans-Golgi resident furin-like protease, that promotes particle maturation before their release from the infected cell (15).



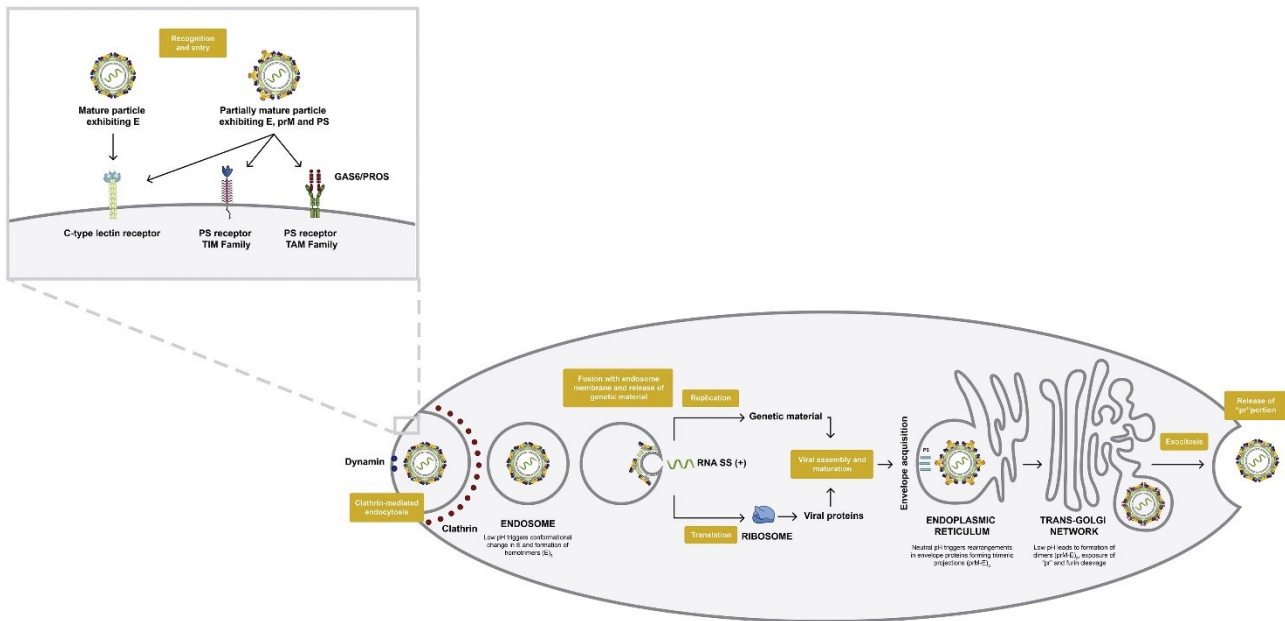


**Fig. 4 ZIKV replicative cycle into the host cell. Source: ZIKA virus entry mechanisms in human cells (13).**

### 1.4 Zika virus transmission

It has been supposed that originally, the ZIKV transmission was restricted to a sylvatic or enzootic cycle involving wild primates and local mosquitoes. Successively, the global spread of the anthropophilic vector *A. Aegypti*, the increase of the urban human population size, and the expansion of international commerce and travel have favored ZIKV diffusion and its establishment into the urban human-mosquito-human transmission cycle (16). Through the vector bite, ZIKV replicates in dendritic and in endothelial cells to further disseminate via blood vessels and reach ZIKV tissue targets such as the uterus, testicles, the brain and other organs (17). Interestingly, testicles, brain, placental tissue and fetal nervous system are immune privileged barriers, difficult to cross. It has been supposed that ZIKV could infect immune cells, as leukocytes, and use them as carriers to reach those tissues. Moreover, Villalobos-Sanchez et al. reviewed the main experimental studies on ZIKV transmission in pregnancy and they pointed out other possible routes exploited by ZIKV to infect the placenta, including antibody-dependent enhancement, transplacental infection, paracellular transmission and ZIKV transcytosis mediated by

extracellular vesicles (18). In addition to the well-characterized mosquito-borne ZIKV transmission, several reports indicated that ZIKV could be transmitted sexually from male to female. ZIKV is present in the semen at higher levels than in urine and blood, which further indicates sexual transmission being a relevant route of virus transmission. Besides, mosquito-bite and sexual transmission, secondary modes of transmission could be represented by contact with body fluids such as blood, breast milk, saliva, urine, sweat and tears (19). However, the impact of these routes in spreading ZIKV disease seems limited, since the presence of ZIKV in these specimens is often low or transient. Differently from other *Flaviviruses*, ZIKV can be transmitted from mother to fetus causing a congenital infection called Congenital ZIKV syndrome (CZS). It has been estimated the mean risk of vertical transmission after mother's infection was 47% in the first trimester, 28% in the second and 25% in the third. However, ZIKV infection during pregnancy is not always associated with an adverse outcome since the impact of ZIKV on fetal development depends on several factors of which many are still unknown (20). However, ZIKV infection damage to the fetus is often underestimated, because, beyond CZS, other potentially ZIKV-related outcomes could impair fetal or newborn health becoming detectable later in the baby's growth (21,22).

## **1.5 Zika pathogenesis and clinical manifestations**

In most cases, ZIKV infection is responsible for an asymptomatic or moderate self-limiting disease. ZIKV has an incubation period of 3 to 14 days and the manifestations of ZIKV disease often consist of cutaneous rash, low-grade fever, arthralgia and myalgia, and conjunctivitis (8). Although ZIKV shows broad cellular tropism, the striking feature of the clinical manifestation is the neurologic complications that result from post-infectious immune response or direct viral neurotropism (23). Among neuronal complications, ZIKV is responsible for an increase in Guillain–Barré syndrome, which is estimated to be 2 to 3 cases per 10.000 ZIKV infections. However, several case series showed that the

prognosis of ZIKV-associated Guillain–Barré syndrome was similar to that of Guillain–Barré syndrome associated with other infectious or non-infectious processes, although with higher morbidity in ZIKV-associated cases. In pregnant women, ZIKV causes a spectrum of fetal and birth defects. The congenital ZIKV syndrome (CZS) includes fetal brain disruption sequence with the subsequent collapse of the fetal skull and severe microcephaly, subcortical calcifications; pyramidal and extrapyramidal signs; ocular lesions of chorioretinal atrophy and focal pigmented mottling of the retina (Fig. 5). The absence of clinical and radiologic abnormalities indicative of CZS at birth does not exclude the risk of abnormalities such as seizures, hearing loss, visual impairment, dysphagia, and developmental delay later in life (24).

<b>Table 1. Key Features of Congenital Zika Syndrome.</b>	
<b>Lesion Type</b>	<b>Manifestations</b>
<b>Structural lesions</b>	
Fetal brain disruption sequence*	Severe microcephaly, premature closure of fontanelles, collapsed skull, overlapping sutures, redundant scalp skin
Brain abnormalities	Cortical atrophy with decreased myelination, cerebellar hypoplasia Neuronal migration disorder — lissencephaly, agyria, pachygyria, polymicrogyria, heterotopia, dysgenesis of corpus callosum Calcifications, mainly subcortical* Ventriculomegaly, increased posterior fossa and pericerebral spaces
Ocular abnormalities	Pigmented retinal mottling*, chorioretinal atrophy*, macular scarring, glaucoma, optic nerve atrophy and abnormalities, intraocular calcifications Microphthalmia, anophthalmia Iris coloboma, lens subluxation, cataract
Congenital contractures	Arthrogryposis, talipes equinovarus, hip dislocation
Intrauterine growth restriction	
<b>Functional lesions</b>	
Seizures	
Pyramidal or extrapyramidal abnormalities*	Body tone abnormalities (mainly hypertonia), swallowing disorder, movement abnormalities (dyskinesia, dystonia), hyperexcitability, impatient crying, sleep disorders
Neurodevelopmental abnormalities	Visual impairment (strabismus, nystagmus, vision loss) Hearing loss or deafness Developmental delay

\* Lesions are rarely observed in other congenital infections.

**Fig. 5. Key features of Congenital ZIKV Syndrome. Source: Zika Virus Infection — After the Pandemic (8).**

## **1.6 Zika diagnosis**

ZIKV symptoms are not specific, for this reason a definitive diagnosis is assessed by using nucleic acid testing (PCR) or serological testing. PCR is performed on whole blood or serum specimens obtained during the first days of illness because of transient viremia (25). Semen or urine could be used as samples alternative to blood given the potentially prolonged duration of ZIKV RNA in these fluids. In ZIKV diagnosis, the result of serologic tests is often complicated by the high cross-reactivity in persons who have been exposed to other Flaviviruses, like DENV. Among serological tests, the most specific is the plaque reduction neutralization test (PRNT), which is considered the reference gold standard (<https://www.cdc.gov/zika/pdfs/laboratory-guidance-zika.pdf>). In pregnant women, a complex algorithm is applied to time ZIKV infection and predict the viral replication outcome in the mother and fetus. Moreover, in some countries such as Brazil, besides serum and urine collection, mothers were monitored for the presence of ZIKV by analysis of placental tissue sampled at the delivery. It was demonstrated that a placental biopsy, conducted using a systematic collection and adequate storage could be a further diagnostic tool to define the impact of ZIKV replication during pregnancy (26).

## **1.7 Zika prevention and therapy**

To date, the best tool to prevent ZIKV infection is the reduction of contact between mosquito vectors and susceptible humans. To reach this goal, Latin America aimed to limit the mosquito insect population through eradication campaigns using toxic insecticides which were not sustainable from an environmental point of view. However, several alternative methods could be applied to safely control the mosquitos population: i) elimination or protection of water containers, ii) application of larvicides, iii) the release of genetically modified male mosquitoes that express a dominant, lethal gene at the larval stage, resulting in the death of all offspring from mating with wild females, leaving no risk

for persistence of the transgene in nature, iv) the release of mosquitoes infected with endo-symbiotic *Wolbachia* bacteria, which can spread through natural populations. Finally, a low-cost and near-term way to reduce *A. Aegypti* populations is the use of lethal autocidal gravid ovitraps (16). Beyond mosquito control, another prophylactic approach is the development of a vaccine against ZIKV. To date, more than 10 candidate vaccines have advanced to phase 1 clinical trial and 2 have begun phase 2 (VRC5288 and mRNA-1893) (27). However, a major barrier to evaluating vaccine effectiveness is the waning incidence of ZIKV after the pandemic, which in turn has hampered the implementation of phase 2 and phase 3 clinical trials. Alternative approaches, such as controlled human challenge infection models, are being considered to obtain efficacy data for regulatory approval of a vaccine (28). ZIKV prevention relies also on abstinence or protected sexual intercourse after suspected infection for 2 months if the partner with suspected infection is female and for 3 months if the partner with suspected infection is male (8). In addition, therapeutic vaccination for ZIKV has been extensively explored as an alternative to vaccines. A total of 461 monoclonal antibodies (mAbs) that bind to E proteins have been identified, with 70 of them displaying moderate to high neutralizing activities in animal models (27). Finally, several compounds were investigated as potential anti-ZIKV drugs and classified based on their mode of action, such as host-directed antivirals, which focus on modulating host cellular processes used for the viral life cycle, or direct-acting antivirals, which target viral components. However, all these compounds have shown activity against ZIKV *in-vitro* but none of them has yet been evaluated in clinical trials. Moreover, recommended therapies for ZIKV infection would require the ability to cross the placenta and blood-brain barrier (BBB), and should be safe to use during pregnancy.

## 1.8 Objective and thesis structure

The goal of this project was to investigate ZIKV pathogenesis at the level of the human placenta trying to identify undiscovered viral and host determinants of ZIKV infectivity. In particular, we focused our research on studying the interaction between ZIKV and a fully-developed placenta in the late stages of pregnancy. It is well-known that, during the first trimester, placental cells are highly susceptible to ZIKV infection since the developing placenta is not structurally and functionally complete in its role of protective barrier (29). On the contrary, it was demonstrated that a full-term placenta characterized by fused syncytiotrophoblast cells and antiviral secretion represents a resistant tissue to this virus (30). Nevertheless, several longitudinal studies reported that ZIKV can impair fetal development also during the second and third trimester of gestation (21, 22, 29). In the last years, scientists suggested different pathogenic mechanisms exploited by ZIKV to overcome a fully-developed placental barrier, including antibody enhancement effect, paracellular route and transcytosis pathway; however, to date, how ZIKV impairs this tissue remains to be established (18). Notably, the lack of knowledge in this field not only compromises the fight against ZIKV, but also hinders the possibility to define an efficient preventive approach for pregnant women. In our study, we tried to investigate ZIKV pathogenesis in the human placenta, taking into account the important role that lipids have in *Flavivirus* replicative cycle. Lipids can influence viral attachment, entry and fusion into the host cells; moreover, the cell lipid availability and metabolism determine the success of *Flavivirus* replication (15).

Therefore, we firstly investigated if viral lipids more than proteins and genomes could affect ZIKV infectivity at the level of the placenta using *in-vitro* and *ex-vivo* assays. Secondly, we corroborated the findings of the previous study, using a translational *in-vivo* model. Specifically, we formulated four experimental diets, reproducing the lipid content of the main human dietary patterns and tailored them for mouse nutrition. Our

goal was to verify if the maternal dietary lipid could change the lipid profile of placental cells and consequently affect the susceptibility of this tissue to ZIKV infection.

The structure of this thesis is mainly composed of the first and the second study performed for this PhD project. The general introduction to the ZIKV virus (Chapter 1) is followed by Chapter 2, which describes the study entitled “Host and viral lipids as determinants of Zika virus infectivity in the full-term placenta.” In Chapter 3, the thesis reports the second study titled “Maternal dietary lipids as a risk factor of Zika virus vertical transmission in a rodent model”. Finally, the thesis concludes with Chapter 4, in which, there is a general discussion of the overall findings.

## **References**

1. Musso D, Gubler DJ. Zika Virus. *Clin Microbiol Rev.* luglio 2016;29(3):487–524.
2. Duffy MR, Chen TH, Hancock WT, Powers AM, Kool JL, Lanciotti RS, et al. Zika Virus Outbreak on Yap Island, Federated States of Micronesia. *N Engl J Med.* 11 giugno 2009;360(24):2536–43.
3. Ebranati E, Veo C, Carta V, Percivalle E, Rovida F, Frati ER, et al. Time-scaled phylogeography of complete Zika virus genomes using discrete and continuous space diffusion models. *Infection, Genetics and Evolution.* settembre 2019;73:33–43.
4. Yakob L. Zika Virus after the Public Health Emergency of International Concern Period, Brazil. *Emerg Infect Dis.* aprile 2022;28(4):837–40.
5. Wang L, Valderramos SG, Wu A, Ouyang S, Li C, Brasil P, et al. From Mosquitos to Humans: Genetic Evolution of Zika Virus. *Cell Host & Microbe.* maggio 2016;19(5):561–5.
6. Grubaugh ND, Ishtiaq F, Setoh YX, Ko AI. Misperceived Risks of Zika-related Microcephaly in India. *Trends in Microbiology.* maggio 2019;27(5):381–3.
7. Sheridan MA, Balaraman V, Schust DJ, Ezashi T, Michael Roberts R, Franz AWE. African and Asian strains of Zika virus differ in their ability to infect and lyse primitive human placental trophoblast. *PLoS ONE.* 2018;13(7):1–18.
8. Musso D, Ko AI, Baud D. Zika Virus Infection — After the Pandemic. Longo DL, curatore. *N Engl J Med.* 10 ottobre 2019;381(15):1444–57.

9. Saiz JC, Vázquez-Calvo Á, Blázquez AB, Merino-Ramos T, Escribano-Romero E, Martín-Acebes MA. Zika Virus: the Latest Newcomer. *Frontiers in microbiology*. 2016;7(April):496.
10. Sirohi D, Chen Z, Sun L, Klose T, Pierson TC, Rossmann MG, et al. The 3.8 Å resolution cryo-EM structure of Zika virus. *Science*. 22 aprile 2016;352(6284):467–70.
11. Roby JA, Hall RA, Setoh YX, Khromykh AA. Post-translational regulation and modifications of flavivirus structural proteins. *Journal of General Virology*. 1 luglio 2015;96(7):1551–69.
12. Yu Y, Gao C, Wen C, Zou P, Qi X, Cardona CJ, et al. Intrinsic features of Zika Virus non-structural proteins NS2A and NS4A in the regulation of viral replication. Dimopoulos G, curatore. *PLoS Negl Trop Dis*. 6 maggio 2022;16(5):e0010366.
13. Agrelli A, de Moura RR, Crovella S, Brandão LAC. ZIKA virus entry mechanisms in human cells. *Infection, Genetics and Evolution*. aprile 2019;69:22–9.
14. Nobrega GM, Samogim AP, Parise PL, Venceslau EM, Guida JPS, Japécanga RR, et al. TAM and TIM receptors mRNA expression in Zika virus infected placentas. *Placenta*. novembre 2020;101:204–7.
15. Martín-Acebes MA, Vázquez-Calvo Á, Saiz JC. Lipids and flaviviruses, present and future perspectives for the control of dengue, Zika, and West Nile viruses. *Progress in Lipid Research*. 2016;64:123–37.
16. Weaver SC, Costa F, Garcia-Blanco MA, Ko AI, Ribeiro GS, Saade G, et al. Zika Virus: History, Emergence, Biology, and Prospects for Control. *Antiviral Research*. 2016;130:69–80.
17. Khaiboullina SF, Ribeiro FM, Uppal T, Martynova EV, Rizvanov AA, Verma SC. Zika Virus Transmission Through Blood Tissue Barriers. *Frontiers in Microbiology*. 2019;10(July):1–13.
18. Villalobos-Sánchez E, Burciaga-Flores M, Zapata-Cuellar L, Camacho-Villegas TA, Elizondo-Quiroga DE. Possible Routes for Zika Virus Vertical Transmission in Human Placenta: A Comprehensive Review. *Viral Immunology*. 1 luglio 2022;35(6):392–403.
19. Calvet GA, Santos FB dos, Sequeira PC. Zika virus infection: epidemiology, clinical manifestations and diagnosis. *Current Opinion in Infectious Diseases*. ottobre 2016;29(5):459–66.
20. Ades AE, Soriano-Arandes A, Alarcon A, Bonfante F, Thorne C, Peckham CS, et al. Vertical transmission of Zika virus and its outcomes: a Bayesian synthesis of prospective studies. *The Lancet Infectious Diseases*. 2021;21(4):537–45.
21. Brasil P, Vasconcelos Z, Kerin T, Gabaglia CR, Ribeiro IP, Bonaldo MC, et al. Zika virus vertical transmission in children with confirmed antenatal exposure. *Nat Commun*. dicembre 2020;11(1):3510.
22. Einspieler C, Utsch F, Brasil P, Panvequio Aizawa CY, Peyton C, Hydee Hasue R, et al. Association of Infants Exposed to Prenatal Zika Virus Infection With Their Clinical,



Neurologic, and Developmental Status Evaluated via the General Movement Assessment Tool. *JAMA Netw Open*. 18 gennaio 2019;2(1):e187235.

23. Miner JJ, Diamond MS. Zika Virus Pathogenesis and Tissue Tropism. *Cell Host and Microbe*. 2017;21(2):134–42.
24. Pomar L, Vouga M, Lambert V, Pomar C, Hcini N, Jolivet A, et al. Maternal-fetal Transmission and Adverse Perinatal Outcomes in Pregnant Women Infected With Zika Virus: A Prospective Cohort Study in French Guiana. *Obstetric Anesthesia Digest*. giugno 2019;39(2):89–90.
25. Lanciotti RS, Kosoy OL, Laven JJ, Velez JO, Lambert AJ, Johnson AJ, et al. Genetic and Serologic Properties of Zika Virus Associated with an Epidemic, Yap State, Micronesia, 2007. *Emerg Infect Dis*. agosto 2008;14(8):1232–9.
26. Venceslau EM, Guida JPS, Nobrega G de M, Samogim AP, Parise PL, Japicanga RR, et al. Adequate Placental Sampling for the Diagnosis and Characterization of Placental Infection by Zika Virus. *Frontiers in Microbiology*. 2020;11(February):1–11.
27. Tan LY, Komarasamy TV, James W, Balasubramaniam VRMT. Host Molecules Regulating Neural Invasion of Zika Virus and Drug Repurposing Strategy. *Front Microbiol*. 4 marzo 2022;13:743147.
28. Vannice KS, Cassetti MC, Eisinger RW, Hombach J, Knezevic I, Marston HD, et al. Demonstrating vaccine effectiveness during a waning epidemic: A WHO/NIH meeting report on approaches to development and licensure of Zika vaccine candidates. *Vaccine*. febbraio 2019;37(6):863–8.
29. Tabata T, Petitt M, Puerta-Guardo H, Michlmayr D, Wang C, Fang-Hoover J, et al. Zika Virus Targets Different Primary Human Placental Cells, Suggesting Two Routes for Vertical Transmission. *Cell Host & Microbe*. 2016;1–12.
30. Bayer A, Lennemann NJ, Ouyang Y, Bramley JC, Morosky S, Torres E, et al. Type III Interferons Produced by Human Placental Trophoblasts Confer Protection Against Zika Virus Infection. *Cell Host Microbe*. 2017;19(5):705–12.

## **Chapter 2**

*Intended for publication*

# Host and viral lipids as determinants of Zika virus infectivity in full-term placenta

Eva Mazzetto<sup>1</sup>, Alessio Bortolami<sup>2</sup>, Alessandra Napolitan<sup>2</sup>, Elisa Mazzacan<sup>2</sup>, Maria Rosa Tran<sup>1</sup>, Giampiero Zamperin<sup>2</sup>, Adelaide Milani<sup>2</sup>, Andrea Fortin<sup>2</sup>, Davide Bovo<sup>3</sup>, Valentina Panzarin<sup>2</sup>, Michela Bigolaro<sup>4</sup>, Claudia Zanardello<sup>4</sup>, Isabella Monne<sup>2</sup>, Giuseppe Giordano<sup>1</sup>, Maria Teresa Gervasi<sup>3</sup>, Carlo Giaquinto<sup>1</sup>, Francesco Bonfante<sup>2</sup>.

<sup>1</sup>Department of Mother and Child Health, Università degli Studi di Padova, via Giustiniani, 3, 35122 Padova(PD)

<sup>2</sup>Department of Virology, Istituto Zooprofilattico Sperimentale delle Venezie, Viale dell'Università, Legnaro (PD)

<sup>3</sup>Department of Chemistry, Istituto Zooprofilattico Sperimentale delle Venezie, Viale dell'Università, Legnaro (PD)

<sup>4</sup>Department of Diagnostic Services, Histopathology, Parasitology, Istituto Zooprofilattico Sperimentale delle Venezie, Viale dell'Università, Legnaro (PD)

## Abstract

ZIKV is closely related to the other member of the Flaviviridae family and similarly to these viruses, it is transmitted to humans by arthropod-vectors causing clinical outcomes, which ranges from mild illness to a severe and life-threatening disease. Nevertheless, among flaviviruses, ZIKV is the only one officially recognized as a teratogenic agent, as consequence of its ability to infect and cross the placental barrier causing the impairment of fetal neuronal developments. Although, in the last years, many studies have revealed new insights in ZIKV pathogenesis, the viral mechanism used by ZIKV to hinder the fetal development during late stages of pregnancy is still unknown. In this study, we aimed to investigate the role of viral lipids as possible determinants of ZIKV pathogenesis at the level of the placenta. To reach this goal, ZIKV stocks were generated from replication of ZIKV strains respectively in mammalian and mosquito cell lines, and characterized by means of genetic and lipidomic analysis. Then, ZIKV stocks were compared for their replication, infectivity, binding and fusion capacity using *in-vitro* assays with immortalized placenta cell lines representative of both early and late gestational stages. Finally, ZIKV

stocks fitness was evaluated in full-term human placenta explants. Our results demonstrated that the envelope of ZIKV stocks derived from mammalian cells displayed an enrichment in phosphatidylcholine lipids, which conferred to these viruses higher infectivity in villous trophoblast cells compared to the ZIKV originating from mosquito cell lines. Moreover, irrespective of ZIKV strains, mammalian-derived viral stocks resulted having higher fitness in full-term placental explants. Collectively, our findings not only revealed a previously unexplored ZIKV pathogenic feature, pointing out to the importance of lipids in flavivirology, but also made available a model to study other viral diseases from a new perspective.

## **2.1 Introduction**

ZIKA virus (ZIKV), an arbovirus of the Flaviviridae family, has been recognized as the first TORCH agent to be transmitted by a mosquito vector (1). In pregnant women, ZIKV infection can cause adverse outcomes, ranging from fetal loss to the so-called congenital ZIKV syndrome (CZS), characterized by a combination of microcephaly, arthrogryposis, fetal growth reduction and other neurological and developmental disorders (2). Although experimental and clinical data have clearly proven ZIKV neurotropic tropism in the developing fetus, little is known about the ability of this virus to infect and traverse the placental barrier over the course of pregnancy (3). It has been demonstrated that, in the first trimester of pregnancy, several placental cells are highly susceptible to ZIKV infection, which is able to replicate in extravillous trophoblast (EVT), in villous cytotrophoblasts (CTB), fibroblast cells and Hofbauer macrophages (4). During the late stages of gestation, placenta become a full-developed barrier covered by an external layer of syncytiotrophoblasts (STBs), deriving from the underlying proliferative CTB cells (1). Beside the physical properties of the syncytium, STBs actively secrete type III interferon, a specific antiviral factors, constituting the primary defense of fetus from ZIKV and other

pathogens (5). Nevertheless, numerous longitudinal studies have pointed out impairments in the neuronal fetal development and sensory dysfunctions in children born from mothers infected by ZIKV during the second and third trimesters, suggesting that ZIKV can elude or compromise STBs barrier (6–8). To date, the lack of knowledge on the pathogenic mechanism exploited by ZIKV to evade the full-term placental defences hinders the application of effective prophylactic and post-exposure treatments for the control of ZIKV infection in pregnant women.

In the last few years, among omics sciences, lipidomic has been considered an additional tool in the study of flavivirology, describing, for the first time, a unique and intimate interplay between this viral family and the host cell lipids (9). Many lipidomic studies have principally explored the impact of viral replication on host cell metabolism, revealing how, post infection, ZIKV can severely affect the host-cell lipid machinery to create a favorable environment for viral multiplication (10,11). However, both viral and host lipids play fundamental roles also in the first stages of the flaviviruses replicative cycle, coordinating the viral attachment to the host cell receptors and the following membranes fusion during the uncoating phase inside the cell (12). Specifically, flaviviruses use the phospholipids on their envelope to mimic the signal of apoptotic cells, inducing the immune cells to their recognition and internalization by endocytosis. Moreover, Gollins et al. demonstrated that the lipid composition of both the viral envelope and endosome membranes drives the success of the uncoating process and allows the release of the viral genome into the host cell cytosol (13). Viral envelope lipids derive from membranes of host cell endoplasmic reticulum (ER), which, during viral replication, undergoes marked rearrangement required to recruit lipids necessary for virus's biogenesis (14). Scientific studies conducted on Dengue virus (DENV)'s assembly demonstrated that viral infection can modify up to 85% of the ER membrane lipids to complete its synthesis; however, it has been observed that

ER rearrangement and viral lipids recruitments strictly depend on the nature of the infected cell (15–17).

In this context, this study aimed to investigate the role of viral lipids as possible determinants of ZIKV pathogenesis at the level of the placenta. To reach this goal, two ZIKV stocks were generated from replication of a ZIKV strain belonging to the Asian lineage in mammalian and mosquito cell lines and characterized by means of genetic and lipidomic analysis. Once demonstrated the two viral stocks were genetically identical but different in the lipid composition of the envelope, their phenotypes were investigated in immortalized placental cell lines representative of placental tissues in both early and late gestational stages. In particular, the two ZIKV stocks were compared for their replication, infectivity, binding and fusion capacity using *in-vitro* assays. Our results showed that lipid composition of both viral and cell membranes affected ZIKV pathogenesis in cells present at the last stages of pregnancy. To further corroborated this finding, three ZIKV strains, two belonging to the Asian lineage and one to the African lineage, were replicated in mammalian and mosquito cell lines and the viral stocks obtained were compared for their replicative kinetic and infectivity in human full-term placental explants. Overall, this study provided unprecedented insights on viral lipids as driving factors of ZIKV pathogenesis during the last stages of human pregnancy.

## **2.2 Methods:**

### **2.2.1 Cell lines**

Vero African green monkey kidney cells (Vero, CCL-81™; ATCC®) were grown and maintained in Eagle Minimal Essential Medium (MEM; Gibco, Life Technology) supplemented with 10% of fetal calf serum (FCS; Corning, Sigma-Aldrich) at 37°C in 5% CO<sub>2</sub>. *Aedes albopictus* mosquito C6/36 cells (C6/36, CRL-1660, ATCC®) were grown and maintained in MEM supplemented with 1mM sodium pyruvate (Sigma-Aldrich), 1%, 100X

non-essential aminoacids (MP Biomedicals), 2mM L-glutamine (Gibco™, Life Technology), and 10% FCS, at 28°C in 5% CO<sub>2</sub>. Immortalized, human first-trimester extravillous trophoblast cells (HTR8/SVneo, CRL-3271™; ATCC®) were grown and maintained in RPMI 1640 medium (RPMI) supplemented with 5% FCS, at 37°C in 5% CO<sub>2</sub>. Human villous trophoblast BeWo cells (BeWo, CCL-98™; ATCC®) were grown and maintained in F12K Kaighn's modified medium supplemented with 10% FCS, at 37°C in 5% CO<sub>2</sub>. In this study, the growth and maintaining media were completed with penicillin 100 U/ml (Gibco, Life Technology) and streptomycin 100 µg/ml (Gibco, Life Technology) (1% P/S). All cells used tested negative for Mycoplasma sp.

### **2.2.2 BeWo cells syncytialization**

BeWo cells syncytialization was carried out by supplementing the maintaining medium of immortalized villous trophoblast cells with 10µM forskolin (Sigma-Aldrich) suspended in DMSO (Sigma-Aldrich), for 48 hours. To assess BeWo cells syncytialization, cells morphology was evaluated through an optic microscope and β human chorionic gonadotropin (β-hCG) level was measured in the supernatant of forskolin-treated cells at 0 and 48 hours post cells treatment, using a hCG+ β Elisa kit (IBL International). For the experimental procedures, syncytialized BeWo (Sync-BeWo) cells were plated on 24 or 96 well plates pre-coated with collagen type 1 solution (Sigma-Aldrich) diluted 1:3 in sterile water.

### **2.2.3 Full-term placenta explant cultures**

Normal human placenta tissues were obtained from full- term elective cesarean deliveries in cases of non-labor after 38 to 40 weeks of gestation (n = 3) at the Department of Women's and Children's Health, University of Padova (Padova, Italy), after approval from the national research ethics committee. Placentas were collected at the delivery, washed extensively with cold phosphate-buffered saline buffer (PBS) and transported in a RPMI

medium complemented with 2% FCS, 1% P/S, 10 $\mu$ M nystatin (Sigma-Aldrich) and 0.1 mg/ml gentamicin sulfate 10mg/mL (Euroclone) to the Istituto Zooprofilattico Sperimentale delle Venezie (Legnaro, Italy) laboratories. Under a class II biological safety cabinets flow, placentas were separated from decidual and amniotic tissue layers, dissected in three parts and abundantly washed with 1% P/S to remove blood clots. Explants were obtained by cutting squares of 30-mm<sup>3</sup> tissue from each placental section. Placental explants were singularly cultured in 24-wells plates with completed RPMI medium at 37°C, in a humidified atmosphere containing 5% CO<sub>2</sub>.

#### **2.2.4 Histology and Immunohistochemistry**

For each of the three placenta sampled, five placental explants were collected at 24 and 72 hours post cultivation and fixed with 10% formalin solution for 24 hours before embedding in paraffin. Placental tissues were routinely processed for histology by staining 4  $\mu$ m sections with hematoxylin and eosin (HE). Moreover, immunohistochemistry (IHC) was performed on 3  $\mu$ m sections of the placenta explants using the Roche automated immunostainer to detect  $\beta$ -hCG antigen. Briefly, the antigen retrieval was carried out using the pre-diluted ULTRA Cell Conditioning (ULTRA CC2) solution (Roche), at 91° C, and pH 6.0, for 44 minutes. The slides were incubated with the ready-to-use primary polyclonal  $\beta$ -hCG antibody (Leica) targeting the glycoprotein hormone synthesized by syncytiotrophoblast cells for 32 minutes at room temperature (RT). An ultraView Universal DAB Detection Kit (Roche) was used as detection system. Placental tissues collected immediately after the C-section were used as positive controls whereas the negative controls were obtained by omitting the primary antibody during the labelling steps to highlight the nonspecific bindings.

To detect the ZIKV antigen, placental explants were collected at 24, 48 and 72 hours post infection (HPI) and processed as previously reported. For each sample, 3  $\mu$ m section was obtained and antigen retrieval was performed through the commercial ready-to-use



Protease 2 (Roche), at 36°C, for 12 minutes. Then, the slides were incubated with primary recombinant monoclonal Flavivirus group antigen antibody, clone D1-4G2-4-15 (MyBiosource), at 1:50 dilution, for 80 minutes at RT. An ultraView Universal DAB Detection Kit (Roche) was used as detection system. The positive and negative controls consisted respectively of infected and mock-infected Vero cells.

## **2.2.5 Viruses propagation and titration**

This study included three different ZIKV strains. An African strain MR766 (ZK-MR; 001v-EVA143) isolated from a *Macaca mulatta* in Uganda in 1947, passaged on mouse brain and four times in Vero cells. Two Asian strains, H/PF/2013 (ZK-FP; 001V-EVA1545) isolated from a human serum in French Polynesia in 2013 and ZIKV/Homo sapiens/Honduras/R103451/2015 (ZK-HON; NR-50355) isolated from human placenta in Honduras in 2016; both viruses were passaged four times in Vero cells. ZK-MR and ZK-FP were purchased by the European Virus Archive goes Global (EVAg) platform, ZK-HON was provided by the Biodefense and Emerging Infections Research Resources Repository (BEI Resources-NIAID). ZIKV strains were propagated in Vero and in C6/36 cell lines at 70% confluence, using a multiplicity of infection (MOI) of 0.1 and 0.5 respectively. Each cell type were incubated with viral inoculum for 1 hour before maintaining medium addition. In Vero cells, the supernatant was harvested at 3 days post infection (DPI) when about 60% of cytopathic effect was observed, whereas, in C6/36 cells, the supernatant was collect at 5 DPI. The cell supernatants were clarified by centrifugation at 3000×g for 30 mins at 4°C to remove cell debris, divided in aliquots and stored at -80°C until use. Viral stocks obtained from ZK-FP, ZK-HON and ZK-MR propagation in Vero cells were respectively identified as HON-V, FP-V and MR-V, and the same strains propagated in C6/36 cell line were respectively reported a HON-C6, FP-C6 and MR-C6. Each viral stock was titrated in Vero cell line by focus forming unit (FFU) assays. Briefly, Vero cells were plated in 96-well plates at concentration of 135000 cell/cm<sup>2</sup> and cultured at 37°C, 5% CO<sub>2</sub>.

After 24 hours, cells were washed twice with warm PBS, and incubated with 50µl serial dilutions of viral samples diluted in RPMI with 2% FCS, at 37°C in 5% CO<sub>2</sub>. After 1 hour of incubation, a low viscosity overlay medium was added to the cells as described by Matrosovich et al. (18). At 48 HPI, inoculum and overlay medium were removed and cells were fixed with 10% formalin solution at 4°C. After 30 mins, cells were washed three times with cold PBS and permeabilized with a solution of 0.01% Triton X-100 (Sigma-Aldrich) in PBS for 10 mins at RT. Primary anti-flavivirus antibody 4G2 (Millipore Catalog No. MAB10216) were diluted at 1:10000 in a blocking buffer solution (BB) made with 0.1% Tween 20 (Sigma-Aldrich) and 1%w/v bovine albumin (Sigma-Aldrich) in PBS. After 1 hour of incubation, cell were washed three times with PBS containing 0.05 % Tween 20 (PBS-Tween) and incubated with peroxidase-conjugated goat anti-mouse IgG (H+L) antibody (Jackson Immuno Research Laboratories) diluted 1:1000 in BB, for 1 hour at RT. After five washed with PBS-Tween, revelation was performed incubating cells with True Blue™ (KPL) peroxidase substrate for 10 mins at RT. The reaction was stopped replacing true blue with distilled water. Virus titer was expressed as FFU/ml.

## **2.2.6 Lipidomic analysis**

To analyze the lipid composition of envelope of ZK-FP strain derived from mammalian (FP-V) and mosquito (FP-C6) cells, highly concentrated and purified ZK-FP stocks were respectively produced in Vero and C6/36 cell lines. Briefly, ZK-FP was propagated in VERO and C6/36 cells, as previously described, using ten 182.5 cm<sup>2</sup> T-flasks (CytoOne®). For each cell line, pooled supernatants were clarified at 3000×g for 30 mins at 4°C, and concentrated by ultracentrifugation in T-647.5 Fixed Angle Rotor (Thermo Scientific) at 150000×g for 2.5 hours, at 4°C. Supernatants were discharged and viral pellets were suspended in 0.5 ml of PBS and purified by ultracentrifugation through a discontinuous 10–60% sucrose gradient at 116,000×g for 1.5 h at 4 °C, using a TH-641 Swinging Bucket Rotor (Thermo Scientific). Visible viral fractions were collected and

dialyzed against PBS using Pur-A-Lyzer tubes (Sigma-Aldrich, USA) overnight, at 4°C. Dialyzed fractions were titrated by means of FFU assay, unified at the concentration of  $10^6$  FFU/ml for each viral stock and further concentrated by ultracentrifugation at  $150000\times g$  for 2.5 hours at 4°C. Then, the supernatants were discarded and highly concentrated and purified FP-V and FP-C6 viral pellets were suspended into 0.5 ml of ice-cold methanol (MeOH) and stored at -80°C until lipid extraction. In order to compare also the lipid profile of both Vero and C6/36 cells membranes,  $1\times 10^7$  Vero and C6/36 cells were respectively harvested, and centrifuged at  $5000\times g$ . After 20 mins, supernatants were discharged and cells pellets were suspended in 0.5 ml of ice-cold MeOH and stored at -80°C until lipid extraction. Lipids were extracted using a modified Folch/Matyash Extraction Method. Chloroform, Tert-Butyl Methyl Ether, methanol and water were added to samples for a final ratio of 2:2:2:3. Then, the samples were vortexed and chilled on ice for 5 mins, and then vortexed again before 1 hour of incubation at 4°C to allow phases separation. A saturated NaCl solution was added in order to obtain the phase inversion. The top layer containing organic lipids was removed, dried under nitrogen flow at 40 °C and stored at -20 ° C until analysis by LC-MS/MS-IMS. LC-MS/MS parameters and identifications were conducted as (outlined103). A Waters Aquity UPLC H class system interfaced with a SYNAPT XS High Resolution Mass Spectrometer Ion Mobility was used for LC-MS/MS-IMS analyses. Lipid extracts were dried under nitrogen flow, reconstituted in 50  $\mu$ l of Isopropanol for LCMS/acetonitrile for LCMS/water MilliQ 2:1:1, and injected onto a reverse-phase Waters CSH column (2.1mm  $\times$  100mm  $\times$  1.7 $\mu$ m particle size) and lipids were separated over a 34min gradient (mobile phase A: ACN/H<sub>2</sub>O (60:40) containing 10 mM ammonium formate, 0,1% formic acid; mobile phase B: IPA/ACN/H<sub>2</sub>O (90:8,9:1,1) containing 10mM ammonium acetate, 0,1% formic acid) at a flow rate of 250  $\mu$ l/min. Samples were analyzed in both positive and negative ionization modes using higher energy collision dissociation and collision-induced dissociation to obtain high coverage of

the lipidome. The fragment ions used for lipid identifications were used as previously outlined<sup>103</sup>. The LC–MS/MS raw data files were analyzed using LIQUID whereupon all identifications were manually validated by examining the fragmentation spectra for diagnostic and fragment ions corresponding to the acyl chains. In addition, the precursor mass isotopic profile and mass ppm error, extracted ion chromatograph, and retention time for each identification was examined. To facilitate quantification of lipids, a reference database for lipids identified from the MS/MS data was created, and features from each analysis were then aligned to the reference database based on their identification, m/z, and retention time using MZmine 2<sup>104</sup>. Aligned features were manually verified, and peak apex-intensity values were exported for statistical analysis

### **2.2.7 Next-generation sequencing**

Total RNA of an aliquot of each ZIKV stock propagated either in Vero cells or in C6/36 cells was extracted using a QIAamp Viral RNA mini kit (Qiagen) according to the manufacturer's instructions. Whole ZIKA genome was amplified using primers showed in S1 Table and overlapping fragments obtained with SuperScript III one-step reverse transcription-PCR (RT-PCR) system with Platinum Taq polymerase High Fidelity (Invitrogen). The thermal amplification profile was set at: 55°C for 30 mins, 94°C for 2 mins, 40 cycles at 94°C for 15 sec, 55°C for 30 sec and 68°C for 6 mins. Amplicons were purified using Agencourt AMPure XP (Beckman Coulter™), quantified with Qubit™ DNA HS Assay, diluted and mixed in equimolar proportion. Library preparation was performed using the Nextera XT DNA sample preparation kit and processed on an Illumina MiSeq platform with the MiSeq reagent kit V3 (300-bp paired-end [PE] mode; Illumina, San Diego, CA, USA). Raw data were filtered by removing: a) reads with more than 10% of undetermined ("N") bases; b) reads with more than 100 bases with Q score below 7; c) duplicated paired-end reads. Remaining reads were clipped from Illumina adaptors Nextera XT with scythe v0.991 (<https://github.com/vsbuffalo/scythe>), cleaned from PCR

primers with trimmomatic v0.32 (19) and finally trimmed with sickle v1.33 (<https://github.com/najoshi/sickle>). Reads shorter than 80 bases or unpaired after previous filters were discarded. High quality reads were aligned against corresponding reference sequence downloaded from Genbank (accession number KX262887.1 for ZK-HON strain, KJ776791.2 for ZK-FP strain, DQ859059.1 for ZK-MR strain) using BWA v0.7.12 (20) and standard parameters. Alignments were processed with SAMtools v1.6 (21) to convert them in BAM format e sort them by position. SNPs were called using LoFreq v2.1.2 (22) According to LoFreq usage recommendations, the alignment was first processed with Picard-tools v2.1.0 (<http://picard.sourceforge.net>) and GATK v3.5 (23–25) in order to correct potential errors, realign reads around indels and recalibrate base quality. LoFreq was then run on fixed alignment with option “--call-indels” to produce a vcf files containing both SNPs and indels. From the final set of variants, indels were discarded and SNPs with a frequency lower than 1% or supported by less than 10 reads were filtered out. Using standard genetic code, nucleotide variants falling into coding regions were transformed into aminoacid changes; nucleotide variants within the same codon where manually checked by visual inspection of alignment with IGV (26,27) in order to confirm their independence or, in case, correct their aminoacid change.

### **2.2.8 Growth curves of ZIKV strains in immortalized placenta cell lines**

Growth curve experiment was performed to study the replicative kinetic of FP-V and FP-C6 in immortalized placental cell lines. HTR-8 and BeWo cells were plated in 24-well plates at 135000 cell/cm<sup>2</sup>, and Sync-BeWo cells were plated at 140000 cell/cm<sup>2</sup>. After 24 hours, cell monolayers were washed in PBS and incubated with 1 MOI of FP-V and FP-C6, at 37°C in 5%CO<sub>2</sub>. After 1 hour, the inoculum was removed and cells were washed three times and replenished with 0.5 ml maintaining medium. Cell supernatants were collected at 0, 6, 24, 48 and 72 HPI, and subsequently store at -80°C. Collected samples

were titrated by means of FFU assays. The experiment was performed three times using four replicates per condition.

### **2.2.9 ZIKV strains infectivity and binding capacity in immortalized placenta cell lines**

To compare the infectivity between mammalian and mosquito cells-derived ZIKV stocks, the mean viral dose necessary to infect the 50% of immortalized placental cell lines ( $MID_{50}$ ) was defined for both FP-V and FP-C6 as follow. After plating HTR-8 and BeWo cells in 96-well plates at 135000 cell/cm<sup>2</sup>, and Sync-BeWo at 140000 cell/cm<sup>2</sup>, cells were incubated with the maintaining medium at 37°C in 5% CO<sub>2</sub>. Viral inoculum was prepared using FP-V and FP-C6 at the concentration of 2×10<sup>5</sup>FFU/50µl. After 24 hours post seeding, cells were washed with warm PBS and incubated with 5-fold dilutions of FP-V and FP-C6 viral inoculum at 37°C in 5%CO<sub>2</sub>. After 1 hour, maintaining medium was added, and cell cultures were incubated for five days at 37°C with 5% CO<sub>2</sub>. Infected cells were fixed and stained, as previously described in the FFU assay method.  $MID_{50}$  was calculated using the Reed and Muench method (28). To investigate how  $MID_{50}$  of FP-V and FP-C6 was affected by viral binding capacity, immortalized placental cell lines were plated and infected as reported for  $MID_{50}$  assay with the difference that cells were incubated with serial dilutions of viral inoculum for 5, 15 and 30 mins. Then, cell cultures were washed twice with warm PBS and maintaining medium was added. Each experiment was performed three times, using from 6 to 12 replicates for each condition.

### **2.2.10 ZIKV strains fusion efficiency in immortalized placenta cell lines**

To study the fusion capacity between ZIKV viral stocks and the cell endosomes after viral internalization in immortalized placental cells, FP-V and FP-C6 envelopes were labelled with a lipophilic probe able to release fluorescence during lipid mixing. Briefly, concentration and purification of FP-V and FP-C6 viral stocks were carried out as previously performed for lipidomic analysis. After sucrose gradient ultracentrifugation,

visible viral fractions were collected, dialyzed against PBS, and titrated by FFU assay. Moreover, each viral fraction was analyzed for ZIKV envelope protein content using a commercial enzyme-linked immunosorbent assay (ELISA, KIT40543; Sino Biological Inc.). Then, FP-V and FP-C6 purified fractions were inactivated by ultraviolet light (UV) of a laminar flow for 60 mins as reported by J. Müller et al. (29) resulting in UV-FP-V and UV-FP-C6 stocks. To label the viral envelope of UV-FP-V and UV-FP-C6 stocks, Octadecyl rhodamine B (R18; Thermo Fisher Scientific), a self-quenching lipophilic probe, was dissolved in ethanol at 10 mg/ml and further diluted 1:10000 in HB buffer containing 20mM Hepes and 150mM NaCl (pH 7.2) to produce a 1µg/ml stock solution. UV-FP-V and UV-FP-C6 were respectively incubated with R18 stock solution considering a ratio of 1:100 between the viral protein and the lipid probe (i.e. 2 ng of viral protein with 200 ng of R18) for 2 hours at 4°C, on a rocker. R18-labelled UV-FP-V and UV-FP-C6 were prepared freshly for each fusion experiment. In fusion assay, HTR-8 and BeWo cells were previously seeded in 96-well plates at 135000 cell/cm<sup>2</sup>, washed once with cold PBS and incubated with 5X10<sup>4</sup> FFU/ml of R18-labelled UV-FP-V and UV-FP-C6. The incubation between viruses and cells was conducted at 4°C to prevent viral internalization during cell-virus attachment. After 1 hour of incubation, viral inoculum was removed and cells washed twice with cold PBS to remove unbound virus. To initiate viral internalization and fusion, cells were rinsed with pre-warm medium and incubated for 12 mins at 37°C into a VICTOR Nivo Multimode Microplate Reader spectrofluorometer (Perkin-Elmer; USA). R18 fluorescence was monitored in 1 min intervals setting the spectrofluorometer at 530/30 nm excitation and 570/10 nm emission. Supernatant stocks of mock-infected Vero and C6/36 cells were processed as described for UV-FP-V and UV-FP-C6 stocks and used as assay controls. Data were visualized as relative fluorescence units (RFU) and corrected for background fluorescence by subtracting values derived from controls. The experiment was conducted twice.

### **2.2.11 ZIKV replication in human placental explants**

Human placenta explants were used to compare the replicative kinetic of ZIKV stocks originated from mammalian (FP-V, HON-V, MR-V) and mosquito (FP-C6, HON-C6, MR-C6) cell lines in the full-term placenta. Briefly, placental explants were washed twice with warm PBS and incubated with 0.5 ml complete RPMI medium containing  $10^5$  FFU of each ZIKV viral stock, at 37 °C in 5% CO<sub>2</sub>. After 12 hours of incubation, explants were washed four times with warm PBS and covered with 1.6 ml of complete RPMI medium containing 10% FCS, 1% P/S, 0.1 mg/ml gentamycin. At 24, 48, 72 HPI, 150 µl of explants supernatant was collected and stored at -80°C until viral detection by qualitative real-time RT-PCR (rRT-PCR). Moreover, ZIKV stocks infectivity in full-term placenta was investigated by determining the mean infectious dose necessary to infect the 50% of placental explants (PID<sub>50</sub>). To define PID<sub>50</sub>, placental explants were washed twice and subsequently incubated with 0.5 ml of 10-fold serial dilutions ( $1 \times 10^5$  FFU/0.5 ml -  $1 \times 10^1$  FFU/0.5 ml) of each viral stock, for 12 hours at 37 °C with 5% CO<sub>2</sub>. Then, explants were washed four times with warm PBS and covered with 1.6 ml of complete RPMI medium. Explants supernatants were collected at 0 and 72 HPI and stored at -80°C until viral detection by quantitative rRT-PCR. The PID<sub>50</sub> was calculated using the Spearman-Kärber method. The same experimental setting was applied for all placental tissues collected (n=3).

### **2.2.12 Molecular testing by real-time RT-PCR**

To determine ZIKV PID<sub>50</sub> and replication fitness in placental human explants, tissue culture supernatants were subject to rRT-PCR and qRT-PCR, respectively, according to Lanciotti et al. (30) (primers and probe set 1086/1162c/1107-FAM). Briefly, nucleic acids were isolated from 50µl suspension using the QIAAsymphony DSP Virus/Pathogen Midi Kit on a QIAAsymphony SP instrument (Qiagen). The amplification reaction was assembled



with the QuantiTect Probe RT-PCR Kit (Qiagen), 600 nM each primer, 400 nM probe, 5  $\mu$ l template and nuclease-free water up to 25  $\mu$ l. Thermal cycling was carried out on a CFX96 Real-time System (Biorad) as follows: 50°C for 30 min, 95°C for 15 min, followed by 40 cycles at 94°C for 15 sec and 55°C for 60 sec.

For viral genome quantification, standard curves consisting of 10-fold serially diluted in vitro transcribed RNA

were included in each run. Standard RNA was prepared in house using the MEGAscript T7 Transcription Kit and the MEGAclear Kit (Ambion) according to the manufacturer's instructions. The limit of quantification (LoQ) of the assay was preliminarily assessed (10 GC/ $\mu$ l with 43% CV). Viral load in explant supernatants was determined by interpolation with the calibration curves and expressed as log<sub>10</sub> genome copies (GC) per  $\mu$ l RNA.

### **2.2.13 Statistical analysis**

The statistical analyses and figure were performed using Prism 9.0 (Graph Pad) and Origin Pro (Origin Lab) software. Ratio paired t-test was used for comparison between two groups of normal or log-normal distributed data. The interval of confidence applied in ratio paired t-test ranged from 90 to 99%, depending on the data set analyzed. Contingency data were analyzed by Fisher's exact test considering significant  $p$  values  $\leq 0.05$ .

## **2.3 Results**

### **2.3.1 Genetic analysis of viral stocks generated from ZIKV replication in mammalian and insect-cell lines**

The three ZIKV strains ZK-FP, ZK-HON and ZK-MR were replicated in both mammalian Vero and mosquito C6-36 cells, resulting in viral stocks identified as FP-V, HON-V, MR-V and FP-C6, HON-C6 and MR-C6 respectively. Subsequently, ZIKV stocks were deep sequencing analyzed to reveal aminoacidic changes eventually occurred due to a different

cell environment (S2 Table). In FP-V and FP-C6 stocks were detected a total of 29 single amino acid polymorphisms (SAPs), of which 7 were exclusive of one of the two viral stocks with a maximum frequency of 3.2%, and 22 in common FP-V and FP-C6 stocks with an average of frequency difference of 0.9%. Similarly, HON-V and HOV-C6 displayed 16 SAPs, of which 6 viral stock-specific with a maximum frequency of 2.4% and 10 shared within both viruses with an average of frequency difference of 1.4%. Lastly, in MR-V and MR-C6, higher number of SAPs (n=45) were observed compared to the previous viruses. However, the 25 viral stock specific SAPs reached a maximum frequency of 5%, and the remaining 20 SAP in common displayed an average of frequency difference of 3.5%. Overall, these results supported the hypothesis that viruses belonging to the same strain and originated from different cell lines did not have any relevant difference in terms of aminoacidic composition. The sequencing data generated in this study is available from SRA under accession number PRJNA729665

### **2.3.2 Lipidomic analysis of the envelope of ZIKV strains originated from replication in mammalian or in insect-cell lines**

Vero and C6/36 are the mammalian and insect cell lines from which FP-V and FP-C6 stocks respectively originated. The lipidomic analysis on the cell membranes showed a great difference between lipid profile of Vero and C6/36 cell lines, confirming the importance of tissue and host origin in defining the lipid architecture of the cell membranes (S1 Fig.). This difference was also reflected in the lipid composition of the FP-V and FP-C6 envelopes. In Figure 1, the chromatograms of FP-V (in blue) and FP-C6 (in red) showed the viral lipid fractions expressed as peaks along the retention time on the x axis. Comparing the two chromatograms, the differences in terms of lipid fractions between FP-V and FP-C6 were determined as the classes of lipids mutually exclusive for each viral stock (Tab. 1). FP-V displayed nine specific lipid fractions, seven of which belonged to the phosphatidylcholine (PC) class, and two to the phosphoethanolamines (PEs). Whereas,

FP-C6 resulted in three lipid fractions unique to its lipid profile, two of them referred to the PEs and one to the phosphatidylglycerols (PGs). This finding suggested that the lipid structure of ZIKV envelope could greatly vary depending on the host cell of origin.

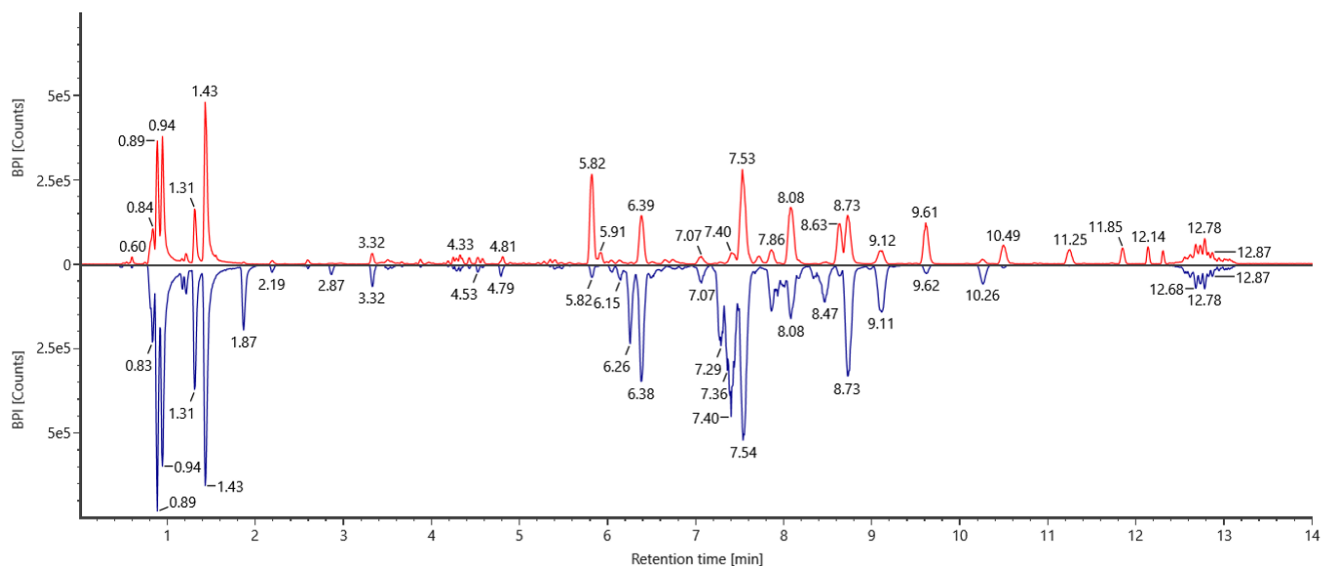


**Fig 1. Chromatograms of lipid fractions expressed in ZIKV strains envelope.** In red the chromatogram of lipid fractions expressed in FP-C6 ZIKV stock derived from C6/36 mosquito cells (FP-C6); in blue, the chromatogram of FP-V ZIKV stock originated from Vero mammalian cell line.

ZIKV stock	Lipid class	Retention time	Molecule	Chemical structure
FP-V	Phosphatidylcholine	1.79	PC (O-14:0_2:0)	Saturated
		6.38	PC (16:0_16:1)	Unsaturated
		7.29	PC (16:0_18:3)	Unsaturated
		7.42	PC (16:0_18:1)	Unsaturated
		7.57	PC (18:0_22:4)	Unsaturated
		8.47	PC (18:0_18:1)	Unsaturated
		9.10	PC (O-18:0_18:1)	Unsaturated
FP-V	Phosphoethanolamines	6,26	PE (18:3_20:0)	Unsaturated
		8,76	PE (18:0_18:1)	Unsaturated
FP-C6	Phosphoglycerols	8.64	PG (16:0_18:0)	Saturated
	Phosphoethanolamines	6,26	PE (12:0_20:2)	Unsaturated
		9.7	PE (16:1_22:0)	Unsaturated

**Tab 1. Lipid fractions of viral stocks envelope.** The table reported the lipid fraction unique of viral envelope of mammalian-derived FP-V and mosquito-derived FP-C6 viral stocks.

### 2.3.3 Replication of ZIKV strains originated from mammalian and mosquito cells in placental immortalized cell lines

To assess how a different lipid composition of ZIKV envelope could affect replication capacity in immortalized placental cell lines, the replicative kinetic of FP-V and FP-C6 viral stocks were studied in HTR-8 cells as a model of invasive extra-villous trophoblast and in

BeWo cells representative of villous cytotrophoblast cells. Moreover, BeWo cells were treated with forskolin to induce the syncytialization and establish an in vitro model of villous syncytiotrophoblast (Sync-BeWo) cells (S2 Fig.). Growth curves showed that all placental cell lines supported FP-V and FP-C6 replication; however, Sync-BeWo cells resulted in lower susceptibility to ZIKV strains infection compared to HTR-8 and BeWo cells (Fig 2). At 72 HPI, in HTR-8 and BeWo cells, FP-V and FP-C6 recorded mean viral titers above 7.00 Log<sub>10</sub> FFU/ml and 6.5 Log<sub>10</sub> FFU/ml respectively; whereas in Sync-BeWo, FP-V and FP-C6 reached mean viral titers of 6.3 Log<sub>10</sub> FFU/ml and 5.4 Log<sub>10</sub> FFU/ml respectively. The overall FP-V and FP-C6 replicative fitness was compared through the calculation of the area under the curve (AUC) in the three placental cell lines. The results showed that FP-C6 had a significantly lower replication efficiency in villous trophoblast BeWo and Sync-BeWo cells compared to FP-V. In contrast, no significant difference was observed for FP-V and FP-C6 AUCs in HTR-8. Taken together these data indicate that first-trimester extravillous trophoblasts are highly permissive to ZIKV irrespective from its cellular derivation, while full-term trophoblasts sustain a more efficient replication for mammalian-derived FP-V.

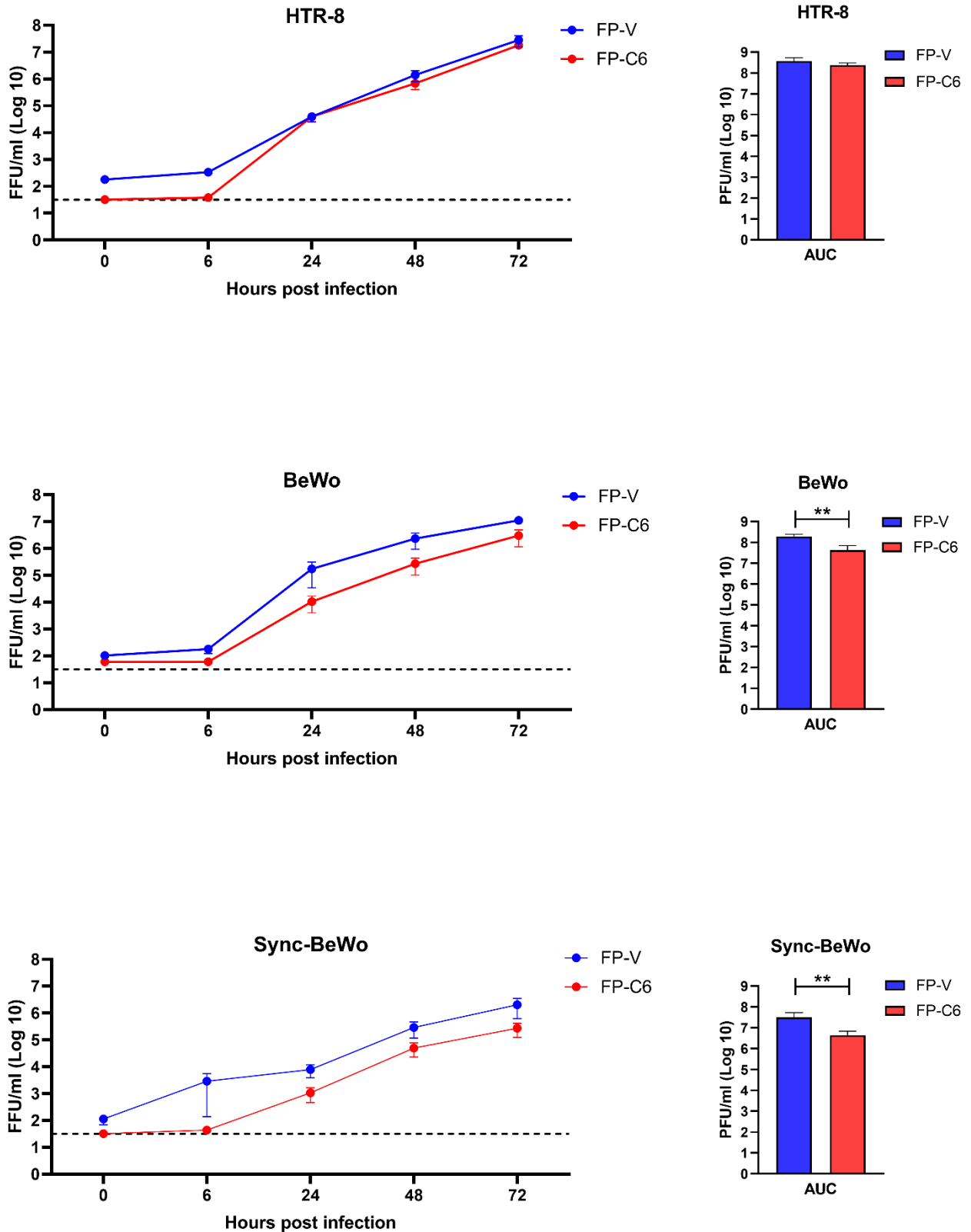


**Fig 2. Growth curves and area under the curve of ZIKV strains derived from mammalian and mosquito cell lines in immortalized placental cell lines.** On the left, the graphs of growth curves (GC) of ZIKV derived from mammalian Vero cell lines (FP-V) in blue, and ZIKV originated from mosquito C6/36 cell lines (FP-C6) in red, on immortalized extravillous trophoblast (HTR-8) cell lines, villous trophoblast (BeWo) and syncytiotrophoblast (Sync-BeWo) cell line. On the right, the area under the curve (AUC) of FP-V and FP-

C6 in the same cell lines. GC and AUC results were presented as means with standard error (SEM) from at least three independent experiments. Statistical significance was calculated using a ratio paired t test with 99% interval of confidence with \*,  $p \leq 0.01$ ; \*\*,  $p \leq 0.001$ ; \*\*\*,  $p \leq 0.0001$ .

### **2.3.4 Infectivity of ZIKV strains originated from mammalian and mosquito cells in placental immortalized cell lines**

To investigate the higher viral fitness of mammalian-derived virus in villous trophoblast cells, FP-V and FP-C6  $MID_{50}$  was determined in immortalized placental cell line. In BeWo and Sync-BeWo, FP-V  $MID_{50}$  (38.06 and 3025.79 FFU/50 $\mu$ l) resulted significantly lower compared to FP-C6  $MID_{50}$  (339.13 and 327470.78 FFU/50 $\mu$ l) showing how ZIKV strain derived from mammalian cells required a lower dose to infect villous trophoblasts compared to the viral strain originated from mosquito cell line. In the HTR-8 cells, FP-V and FP-C6 displayed a similar replicative fitness and consistently, no significant difference was observed between their  $MID_{50}$  (FP-V  $MID_{50}$  379.95 FFU/50 $\mu$ l and FP-C6  $MID_{50}$  513.48 FFU/50 $\mu$ l). ZIKV infectivity in the first phase of viral replicative cycle is determined by three main factors: binding affinity, entry and uncoating capacity (12). In binding assay, both attachment and entry capacity of FP-V and FP-C6 were investigated as determinants of ZIKV strains infectivity on immortalized placental cell lines. The Fig 3 showed that time of incubation did not change the ratio between FP-V and FP-C6  $MID_{50}$  (Figs 3b,c,d): in BeWo and Sync-BeWo, the difference in  $MID_{50}$  observed after 5 days of virus-cell incubation is the same reducing the time of infection to 5 mins (Figs 3c,d). Similarly, in the HTR-8 cells the  $MID_{50}$  of FP-V and FP-C6 did not differ irrespective of the incubation time. This data showed that a reduction in the time of interaction between ZIKV viral stocks and placental cells did not significantly affect the difference in infectivity efficiency between FP-V and FP-C6, which maintained a constant  $MID_{50}$  ratio along the incubation time.

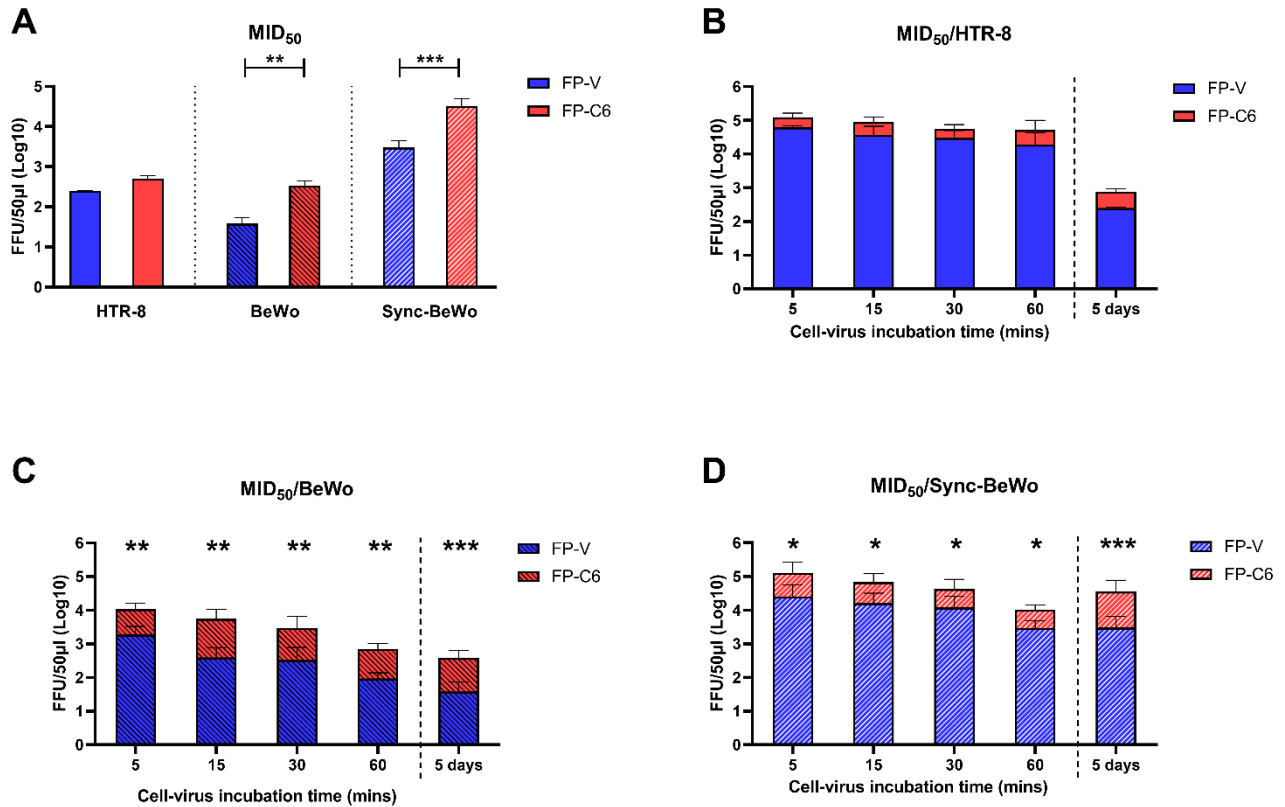


**Fig 3. Mean infectious dose 50 (MID<sub>50</sub>) and binding capacity of ZIKV strains derived from mammalian and mosquito cell lines in immortalized placental cell lines.** (A) MID<sub>50</sub> of ZIKV derived from mammalian VERO cell lines (FP-V) in blue, and ZIKV originated from mosquito C6/36 cell lines (FP-C6) in red on immortalized extravillous trophoblast (HTR-8) cell lines, villous trophoblast (BeWo) and syncytiotrophoblast (Sync-BeWo) cell line, presented as means with standard error (SEM) from at least five independent experiments. Statistical significance was calculated after data log-normalization using a ratio paired t test with 99% interval of confidence with \*,  $p \leq 0.01$ ; \*\*,  $p \leq 0.001$ ; \*\*\*,  $p \leq 0.0001$ . (B) (C) (D) Binding assay results was reported as MID<sub>50</sub> values of FP-V and FP-C6 at different time point of virus-cell incubation (5, 15, 30 and 60 mins) in HTR-8, in BeWo and Sync-BeWo respectively. In binding assay, MID<sub>50</sub> results were presented as means with standard error (SEM) from at least three independent experiments. Statistical significance was calculated after data log-normalization using a ratio paired t test with 90% interval of confidence with \*,  $p \leq 0.1$ ; \*\*,  $p \leq 0.01$ ; \*\*\*,  $p \leq 0.001$ .

### 2.3.5 ZIKV strains fusion efficiency in immortalized placenta cell lines

ZIKV strains derived from mammalian cell lines displayed a higher infectivity in villous trophoblast cells, resulting in a lower MID<sub>50</sub> compared to ZIKV originating from mosquito cells. Limited binding conditions did not affect the difference in the infectivity of FP-V and FP-C6, pointing to other factors as responsible of this gap. Among these factors, the role of viral uncoating mechanism in determining the ZIKV strain infectivity was investigated through an *in-vitro* fusion assay. The capacity of FP-V and FP-C6 to fuse with endosome membrane of HTR-8 and BeWo placental cells was explored by labelling UV-inactivated

ZIKV envelope with R18, a self-quenching lyophilic fluorophore R18. The fusion of the labelled viral envelope with cell endosome membranes, resulted in dilution of R18 cause lipid mixing, which was accompanied by increasing in fluorescence detectable as RFU with a fluorimeter. In HTR-8 cells, the fluorescence spectrum was similar between the two ZIKV viral stocks: UV-FP-V displayed the highest RFU value at 1 min of incubation and UV-FP-C6 reached the fluorescence peak 1 min delay. Differently, in BeWo cells, UV-FP-V arrived to the peak between 1-2 mins after incubation, whereas UV-FP-C6 reached the highest emission peak 6 mins later. Moreover, irrespective of the cell line type, UV-FP-V showed a greater fluorescence levels compared to UV-FP-C6. However, ZIKV stocks fusion capacity was exclusively evaluated on the fluorescence spectrum pattern rather than the fluorescence intensity levels, since these levels could be affected by the efficiency of R18 labelling. In fact, the different lipid composition of viral stocks' envelope combined with the heterogeneity of Flavivirus membrane appearance could have determined a degree in lipophilic R18 dye inclusion leading to the use of a FP-V stock with a higher amount of labelled lipids (46). Although this limitation was not verified in this study, it was taken into account comparing UV-FP-V and FP-C6-UV fusion ability in immortalized placental cell lines. However, the fusion kinetic clearly pointed out the peak of fusion events for each viral stocks in both HTR-8 and BeWo cells, showing that in BeWo cells, UV-FP-C6 fusion capacity was impaired in either emission intensity or timing of fusion, suggesting a less uncoating efficiency for ZIKV strains derived from mosquito cells than ZIKV originating from mammalian cells.



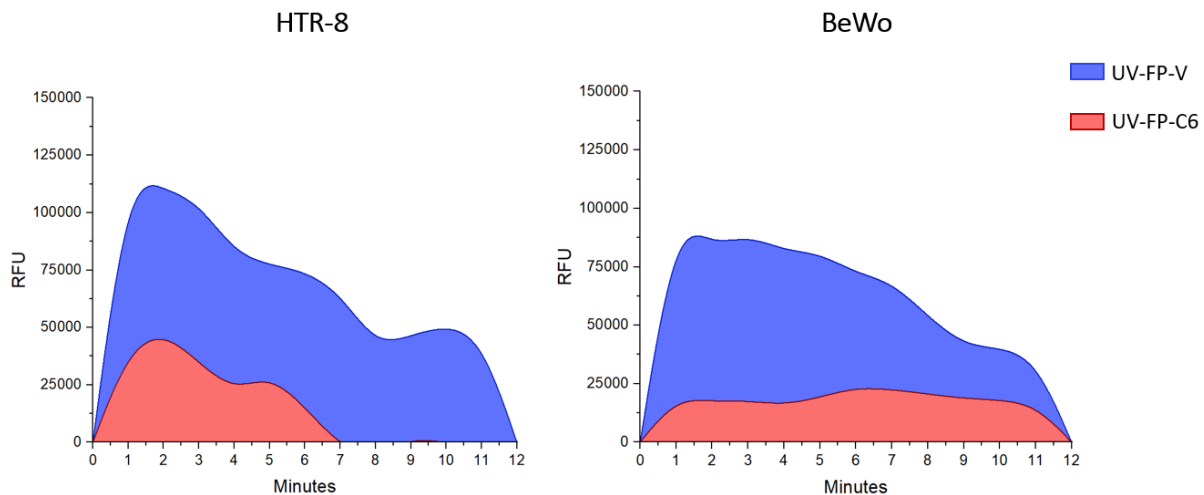


**Fig 4. Fusion efficiency of ZIKV strains derived from mammalian and mosquito cell lines in immortalized placental cell lines.** The lipid envelope of UV-inactivated ZIKV derived from mammalian VERO cell lines (UV-FP-V) in blue, and ZIKV originated from mosquito C6/36 cell lines (UV-FP-C6) in red, were labelled with Octadecyl rhodamine B (R18) a lipophilic, self-quenching fluorophore. Immortalized extravillous trophoblast (HTR-8), and villous trophoblast (BeWo) cells were incubated for 1 hours at 4°C with R18 labelled ZIKV strains using a MOI of 0.01. After two washes to remove viral inoculum, cells were incubated with pre-warmed medium in a fluorimeter set at 37°C. The fusion of labelled envelope of UV-FP-V and UV-FP-C6 with placental cell endosomes, caused R18 self-quenching, which was detectable as fluorescence spectrum by fluorimeter. Fluorescence of both UV-FP-V (left y axes) and UV-FP-C6 (right y axes) was expressed as relative fluorescence units (RFU) and presented as median of two experiments. For each time point, RFU were calculated subtracting background fluorescence of non-infected cells from fluorescence of cells incubated with UV ZIKV strains.

### 2.3.6 Infectivity and replication kinetic of ZIKV stocks derived from mammalian and mosquito cell lines in human full-term placental explants

To confirm the hypothesis of a higher infectivity of Vero-derived ZIKV strains in villous trophoblasts at late pregnancy, full-term placenta explants were inoculated with three different ZIKV strains produced in mammalian (FP-V, HN-V, MR-V) and mosquito (FP-C6, HN-C6, MR-C6) cells lines. Before infection, explanted villi displayed a histologically unaltered tissue with the syncytiotrophoblast cells tightly adherent to a dense stroma enrich in vessels and capillaries. Moreover, the viability of *ex-vivo* placental cultures was confirmed by the cytoplasmic positivity for the  $\beta$ -hCG signal of syncytiotrophoblast cells, indicating an active secretion of this hormone 72 hours post cultivation (S3 Fig). All ZIKV viruses rapidly replicated in full-term placenta explants reaching mean viral titer higher than 3Log<sub>10</sub> genome copies/ $\mu$ l by 24 HPI (Fig.5). Interestingly, in the Asian-lineage ZIKV

strains, values of mean viral titers between Vero and C6/36-derived viral stocks did not significantly differ and overall the two ZIKV strains reported a similar viral replication in placental explants successfully infected. On the contrary, in ZK-MR strain, belonging to the Africa lineage, was observed the major difference in replicative kinetic between the two ZIKV viral stocks. Moreover, MR-V, reached the highest mean viral titer in the ex-vivo cultures compared to other viruses used in this assay. Notably, irrespective of ZIKV lineage, at 72 hpi viruses derived from Vero cells successfully infected all placental explants. In contrast, C6/36-derived strains infected a significantly lower percentage of explants (25-50%), further corroborating evidence of lesser fitness of these viruses in this tissue. Accordingly, all ZIKV strains of mammalian derivation resulted in a significantly lower  $PID_{50}$  in full-term placental explants (Fig. 6), suggesting a common higher infectivity of these viral stocks in placental tissues collected in the third trimester of pregnancy. None IHC positivity was detected in infected placental explants collected at 24-48-72 HPI.

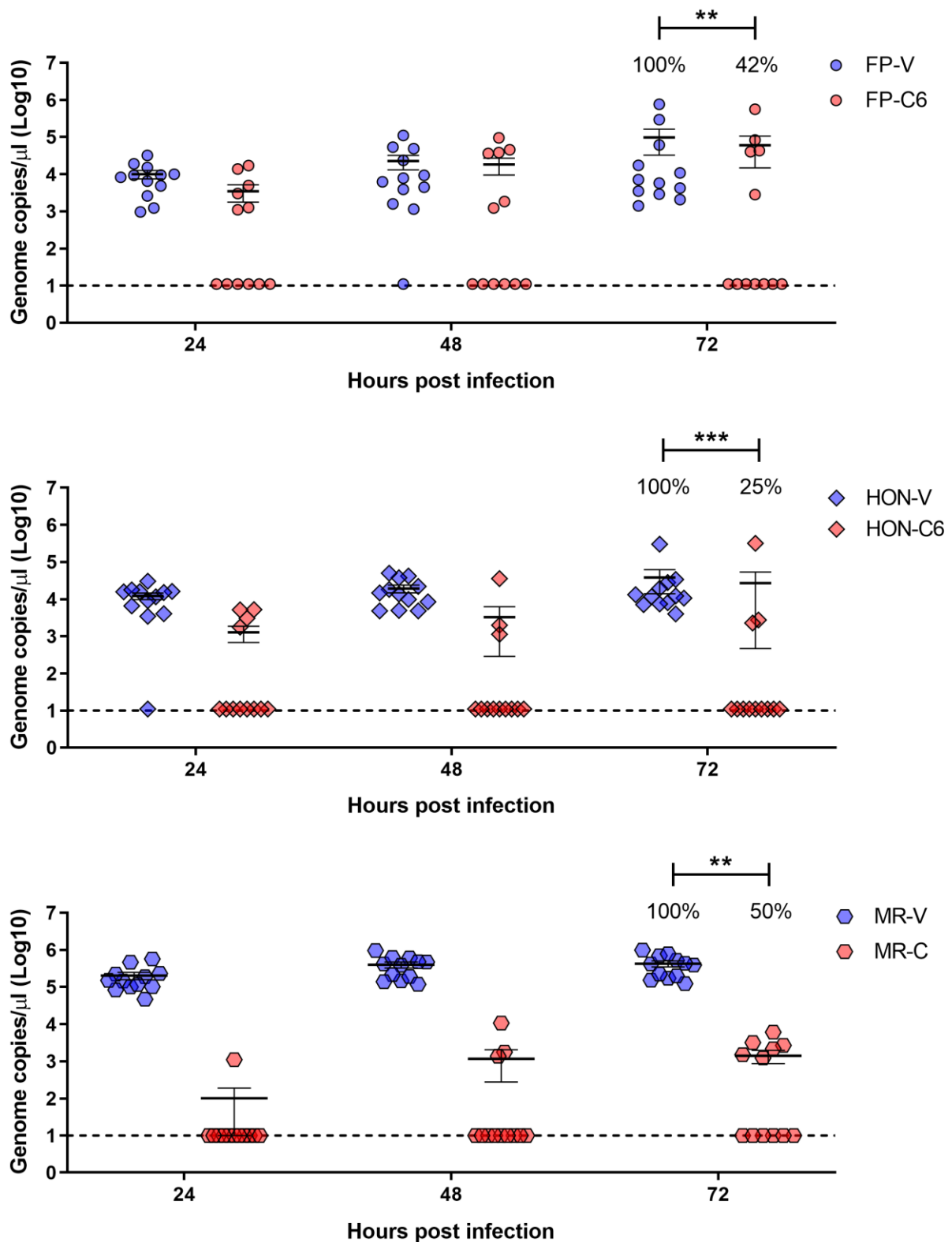


**Fig 5. Replicative kinetic of ZIKV strains derived from mammalian and mosquito cell lines in human full-term placenta explants.** Replicative kinetic of ZIKV derived from mammalian Vero cell lines (FP-V, HN-V, MR-V) in blue, and ZIKV originated from mosquito C6/36 cell lines (FP-C6, HN-C6, MR-C6) in red, on placenta explants from full-term elective cesarean deliveries. Results were presented as mean with standard error (SEM) from three independent experiments. At 72 HPI statistical significance was calculated using a Fisher's exact test considering \*,  $p \leq 0.05$ ; \*\*,  $p \leq 0.001$ ; \*\*\*,  $p \leq 0.0001$ .

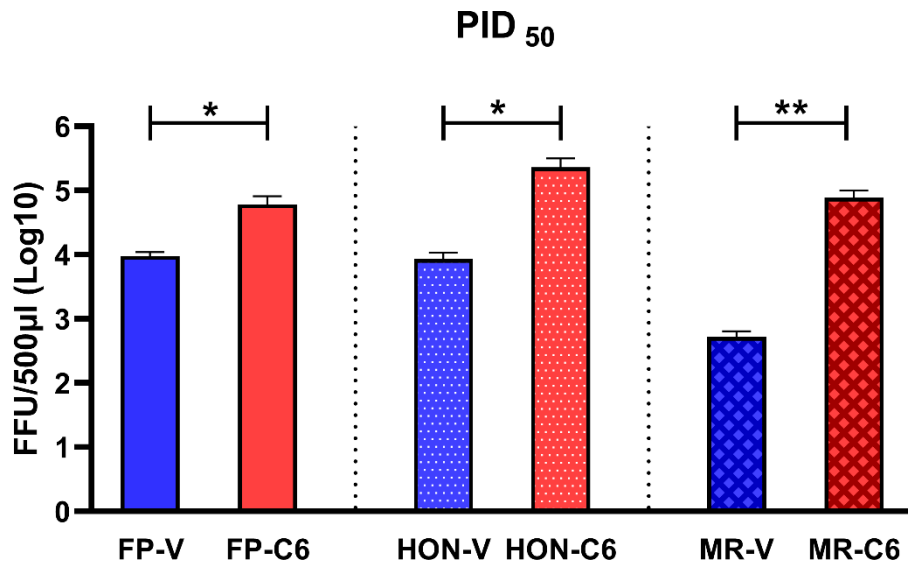


**Fig 6. Placenta mean infectious dose 50 (PID<sub>50</sub>) of ZIKV strains derived from mammalian and mosquito cell lines.** PID<sub>50</sub> of ZIKV derived from mammalian VERO cell lines (FP-V, HN-V, MR-V) in blue, and ZIKV originated from mosquito C6/36 cell lines (FP-C6, HN-C6, MR-C6) in red, in placenta explants from full-term elective cesarean deliveries. Results were presented as means with standard error (SEM) from at least three independent experiments. Statistical significance was calculated using a ratio paired t test with 90% interval of confidence with \*,  $p \leq 0.1$ ; \*\*,  $p \leq 0.01$ ; \*\*\*,  $p \leq 0.001$ .

## 2.4 Discussion

ZIKV is closely related to the other member of the Flaviviridae family, such as DENV, West Nile virus (WNV) and yellow fever virus (YFV); and similarly to these viruses, it is transmitted to humans by arthropod-vectors causing clinical outcomes which ranges from mild illness to a severe and life-threatening disease (31). Nevertheless, among flaviviruses, ZIKV is the only one officially recognized as a teratogenic agent, as consequence of its ability to infect and cross the placental barrier causing the impairment of fetal neuronal developments (32). It has been documented that in pregnant women ZIKV infection can cause vary fetal and neonatal complications, including fetal losses, growth restriction, fetal and neonatal developmental defects (33). The term ZIKV congenital syndrome describes the unique pattern of birth defects and disabilities correlated to ZIKV infection during pregnancy, and it is manly associates to microcephaly, brain calcifications; eye damage, congenital contractures; and marked muscle hypertonia restricting body movement soon after birth (34). Importantly, the CZS rate is not steady during the gestational period, and it

depends on the trimester of exposure to ZIKV infection since women infected by ZIKV in the first trimester of pregnancy reported a higher CZS rate than mothers affected by ZIKV in the second and third trimester (2). Although the placental cells, especially STB, increase their resistance to ZIKV infection during the course of pregnancy, this virus still able to directly or indirectly impair fetal development causing infant abnormalities (35). Numerous study have tried to explore alternative pathogenic mechanisms that ZIKV could use to bypass a full-developed placental barrier suggesting an antibody enhancement effect, paracellular route and transcytosis pathway but none of those hypothesis have considered the role of viral and host lipids (3).

In this study, according to Martín-Acebes and colleagues, viral lipids were recognized as a potential determinant of flavivirus pathogenesis by investigating their impact on ZIKV infection of the human placenta (12). From this perspective, ZIKV stocks, genetically identical but different in the lipid composition of the viral envelope were compared *in-vitro* and *ex-vivo* for their infectivity in placental tissues. To obtain viral stocks with these characteristics, ZIKV strains were replicated in mammalian Vero and mosquito C6/36 cell lines, considering that although ZIKV adapt lipid composition of host cell ER membrane, the insect cells do not synthesize sterols thus ensuring a different range of lipid substrates (36). The lipidomic analysis performed in this study, confirmed the high variability in the lipid composition between mammalian and insect cell membranes, and this difference was reflected on the two viral stocks respectively generated from each cell lines. Interestingly, comparing the lipid composition of viral envelopes, ZIKV derived from mammalian displayed a higher enrichment in lipids, of which PCs were predominant. PC is the most abundant plasma membrane phospholipid and its fatty acids composition regulates the physical properties of membranes, increasing or limiting the fluidity (37). In particular, most of PCs identified as specific for the mammalian-derived viral stock were constituted at least by an unsaturated chain, which was recognized a feature for maintaining the

membrane curvature and increasing the lipid raft fluidity (38). Moreover, in flaviviruses pathogenesis, PCs are considered markers of viral infection since a greater amount of these lipids were detected in infected cells than mock-infected group (10,38,39). Once obtained two ZIKV stocks different in the lipid composition of the viral envelope, the genomic of these viruses was analyzed to exclude the acquisition of any genetic change able to affect viral pathogenesis. Generally, the genome of Flavivirus is considered less subjected to a rapid mutations rate comparing to other RNA viruses family, such as influenza viruses or coronaviruses; nevertheless, viral replication in specific host and tissues can determine ZIKV acquisition of adaptive mutations (40,41). However the NGS data generated by this study did not report any relevant differences in term of genetic and consequently aminoacidic composition between viruses belonging to the same strain but originated from different cell lines.

Among ZIKV stocks generated from mammalian and insect cell lines in this study, FP-V and FP-C6 viral stocks derived from ZK-FP strain were selected to investigate the viral phenotype in immortalized placental cell lines. The reason was that ZK-FP strain is the progenitor of the Asian lineage which cause the first and larger ZIKV epidemic in Asian and American territories and it was considered the most representative of ZIKV strains circulated till now (42). FP-V and FP-C6 were compared for their viral growth in HTR-8 and BeWo cell lines used respectively as model of invasive trophoblasts and villous cytotrophoblasts. Moreover, to mimic villous syncytiotrophoblast, the major line of defense of mature placental tissues, BeWo cell were induced to syncytialization through a forskolin treatment (Sync-BeWo) (43). Sync-BeWo cells, as physiologic villous syncytiotrophoblasts, were characterized by fused and multinucleated cells, the hCG secretion, and other placenta-specific proteins, but differently from an *in-vivo* condition these cells did not express INF stimulated genes resulting susceptible to ZIKV infection (5). Data reported in Fig 2 showed that all placental cell lines resulted susceptible to both

ZIKV stocks, which rapidly replicated starting from 24 HPI to reach the highest viral titer at 72 HPI. However, ZIKV derived from mosquito cells displayed an overall lower viral fitness in BeWo and Sync-BeWo villous trophoblasts over time, which corresponded to a significant decrease in the total amount of viral replication expressed as AUCs. This divergence between FP-C and FP-V phenotype was attributed to the different infectivity of this two viral stock through the determination of the MID<sub>50</sub>. In this *in-vitro* assay, FP-V reported a significant lower MID<sub>50</sub> in BeWo and Sync-BeWo cells, suggesting that ZIKV derived from mammalian cells required a minor content of viral particles to infect the 50% of villous trophoblasts cells compared to mosquito-origin ZIKV. Consistently, in HTR-8 cell, where no difference was detected between the FP-V and FP-C6 viral replicative capacity, the two viral stocks resulted having a comparable MID<sub>50</sub>. Together these evidences indicated that the higher content of PCs on the envelope of mammalian-derived viruses guaranteed an infectivity advantage for ZIKV in placental cells of the advanced gestational stages. Considering that phospholipids of Flavivirus envelope drive the viral attachment and entry into the host cells, the infectivity of FP-V and FP-C6 were evaluated limiting the incubation time of viral particles to placental cell lines. As expected, the results of the binding assay showed an increase of viral dose necessary to infect the 50% of cell tissues proportional to the decrease of the incubation time; nevertheless, the ratio between FP-V and FP-C6 MID<sub>50</sub> remained the same irrespective of the incubation time applied and cell lines evaluated. This data demonstrated as the difference in ZIKV stocks infectivity and replication were not determined by a higher or lower binding and entry capacity, suggesting the lipid composition of FP-V and FP-C envelope affected other aspects of the viral replication cycle. Beside the viral internalization, lipids play an important role in the uncoating process by which the virus, entrapped in the host-cell endosome vesicle, fuses its envelope with the endosome membrane to release the genome into the cell cytoplasm (44). The fusion activity of FP-V and FP-C in immortalized placental cell lines were

investigated by purification, UV-inactivation and labelling of ZIKV viral stocks using a R18 fluorophore. R18 works as a self-quenching molecule, releasing fluorescence when the concentrated dye on viral envelope was diluted with the host membrane lipids at the fusion event (45). Notably, in HTR-8 cells, both UV-FP-V and UV-FP-C6 reached the fluorescence peak around 1 and 2 minutes after the incubation at 37°C. Similarly, in BeWo cells, UV-FP-V displayed an initial and rapid increase of the fusion events by the min 2, whereas UV-FP-C6 arrived to the peak of the emissions at 6-7 mins post incubation. These data were consistent with the cell entry pathways of other Flavivirus, which displayed a rapid viral internalization, the beginning of fusion events around 3-5 mins post entry and their finalization in the following 10 mins (45,47). Fusion assay results revealed that ZIKV envelope lipids can drive the viral uncoating efficiency, confirming the importance of lipid molecules especially in this stage of the virus replicative cycle. Particularly, unsaturated PCs identified in mammalian-derived ZIKV could have contributed to accelerate UV-FP-V fusion events in BeWo cells, through their physical-chemical properties in modeling membranes curvatures and fluidity(48). Interestingly, the difference in lipid composition determined an advantage for FP-V exclusively in villous trophoblast, indicating that a faster or slower fusion kinetic is the combination of both host and viral lipids interaction. Together these results suggested that depending on the stage of pregnancy and the susceptibility of placental cells, ZIKV could put in place different pathogenic strategies to overcome host defenses.

To corroborate this finding, the replicative fitness of mammalian and mosquito-derived ZIKV stocks were compared in explants of full-term placental villous. In this study, explanted villous resulted susceptible to all ZIKV strains tested (ZK-FP, ZK-HON, ZK-MR) and viral titration of explants supernatants showed a progressive increase in the ZIKV RNA load as early as 24 HPI, with genome copies ranging from 3 to 6 Log<sub>10</sub>. However, the infectivity of explants supernatants was not determined because the PFU assay was



prevented by the active interferon secretion of syncytiotrophoblast cells (5). Consequently, the results of this study probably overestimated the amount of infective viral particles detected in placental explants, explaining the lack of cells positivity in IHC assay. Comparing the replicative kinetic of ZIKV stocks with different cell origins, ZIKV strains derived from mammalian Vero cell lines displayed significant higher infectivity in placental explants. On the contrary, ZIKV strains derived from mosquito cell lines never infected the totality of explants showing an infection rate between 25 and 50%. The calculation of PID50 further confirmed that irrespective of the strain used, mammalian-like ZIKV viruses have a higher infectivity in placental villous explants than mosquito-derived viruses.

This study demonstrated that lipid composition of the viral envelope affected ZIKV infectivity in fully-developed placental tissues, probably by changing the viral uncoating efficiency during the first stages of the virus replicative cycle into the villous trophoblast cell. Importantly, the experiments conducted in this work did not provide further aspects on the role of each lipid class identified on viral envelope in determining ZIKV pathogenesis because the viral stocks generated from Vero and C6/36 cells were used as a proof-of-concept and did not represent the lipid structure of real ZIKV virions circulating in human tissues. Although, ZIKV replicates in mosquito cell lines during its vector-cycle, when the virus arrives to the placental barrier, it has already replicated in several different human cell type (49). However, our data suggested that ZIKV host cell lipid heritages could potentially increase or impair viral replication in the placental tissues. For example, Duggal et al. described that ZIKV derived from seminal fluid and sexually transmitted enhanced the viral dissemination to the female reproductive tract in a mouse model (50). Seminal fluid derived from cells of the male reproductive tract, namely Leydig cells, Sertoli cells, and germ cells, which resulted highly susceptible to ZIKV infection, harboring viral up for 6 months after acute viremic phase in humans (51). It has been demonstrated that those cells displayed an active lipid metabolism to ensure the correct lipids supply to sperm

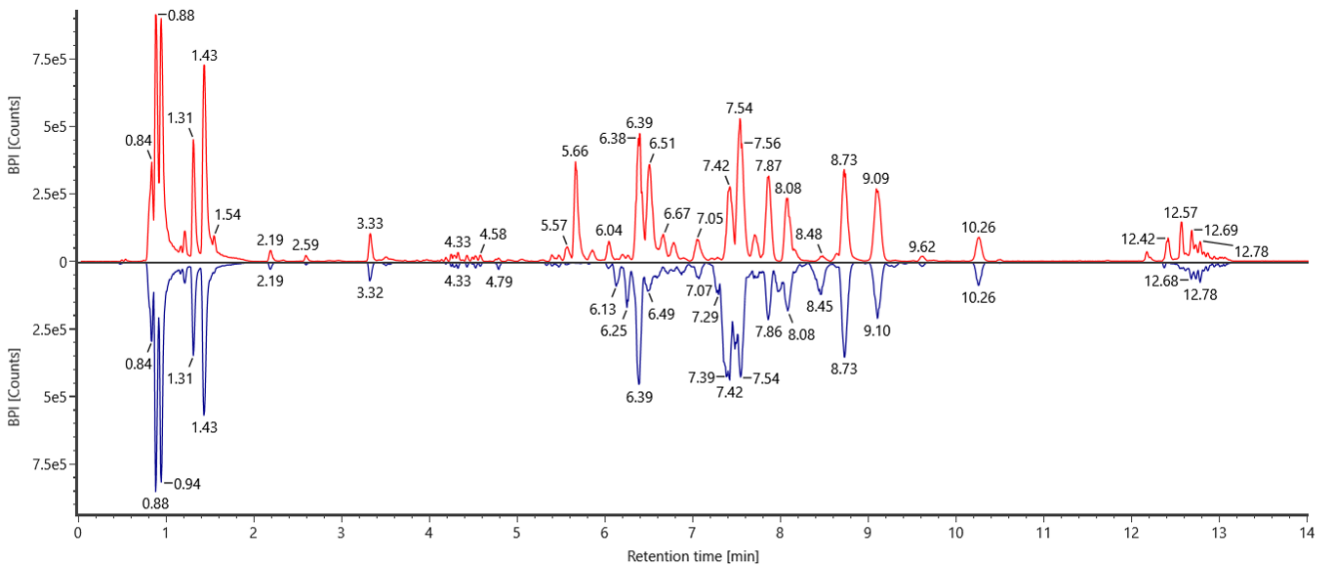
plasm membrane assembling during the spermatogenesis process. Interestingly, germ cells mainly provide sperm membranes of Diacylglycerophospholipd constituted by PC and PE, which modulate many sperm functions necessary to drive the fertilization process (52,53). Although the impact of ZIKV replication on lipid metabolism of the male reproductive cells is still unknown, ZIKV, as demonstrated for other tissues, could exploit lipids of germ cells to specifically constitute the viral envelope and consequently improve its infectivity at the level of the female reproductive tract (11). This hypothesis is also supported by the recent possibility to use the sperm lipid profile as biomarkers for identifying ZIKV infection (51,54). Another interesting aspect pointed out in this work is the different impact of viral lipid composition depending on the gestational phase. In the current study, lipids of viral envelope conferred an infective advantage to ZIKV only in the in-vitro and ex-vivo model of placental villous trophoblasts present in the late stages of pregnancy. Probably, a more successful interaction between viral and host lipids could be part of a neglected pathogenic mechanism that ZIKV use to overcome an hostile environment such as mature placental barrier secreting type III interferons (3). This perspective calls for more studies on viral and host lipids interplay focused on the characterization of lipid components in viral envelopes at the different stages of ZIKV transmission and their capacity to increase or decrease viral fitness in human tissues. Collectively, these further data could allow the development of new lipid-related antiviral drugs and alternative strategies to fight ZIKV but also other pathogens, as flaviviruses, that use similar pathogenic mechanisms (55). However, the implementation of antiviral molecules could represent a limited solution to solve ZIKV infection in pregnant women, for which the use of most drugs remains restricted (56). For this reason, since the ZIKV epidemic, research and public health organizations have dedicated many efforts to developing prophylactic actions such as vaccine therapy and vector bite prevention (57,58). To date, several vaccine candidates are in Phase 1 and 2 clinical trials, but the

waning incidence of ZIKV after the pandemic has hampered their testing in Phase 3, delaying the entire process to evaluate their effectiveness in the field. In terms of preventive strategies, the study conducted by Barbeito-Andrés et al., which investigated the relationship between protein malnutrition in pregnant women and the development of CZS, highlighted the potential role of diet in ZIKV pathogenesis. Although nutrition has not been commonly associated with infectious disease, many nutritional factors can influence susceptibility and severity of disease in the host affected by flaviviruses infection (59). The current study observed the role of both host cell membrane and viral envelope lipids in ZIKV pathogenesis, pointing out how the success of placental host cell infection, strictly depends on the type of viral and cell lipids and their reciprocal interactions. In vivo, ZIKV envelope lipids derive directly from the infected host cell membranes, and host cells, as placental cells, mainly derive their lipids from dietary fat (60). From this perspective, dietary lipids intake could be considered one of the risk factors associated to ZIKV infection in pregnant women and its modulation could be represent another possible strategy of prevention.

In conclusion, this work demonstrated for the first time the lipid composition of both viral and host membrane affected ZIKV infectivity in placental tissues during the late stages of pregnancy. However, further lipidomic analyses will be necessary to investigate the actual impact of each lipid class in determining ZIKV pathogenesis in the placenta and other tissues susceptible to ZIKV infection. Moreover, considering the complexity of lipid physiology and metabolism in living beings, it will be necessary to use an in-vivo model to corroborate the role of lipids during ZIKV transmission. Finally, our study not only revealed a previously unexplored ZIKV pathogenic feature but also made available a model to study from a new perspective other viral diseases.

## 2.5 Supplementary contents

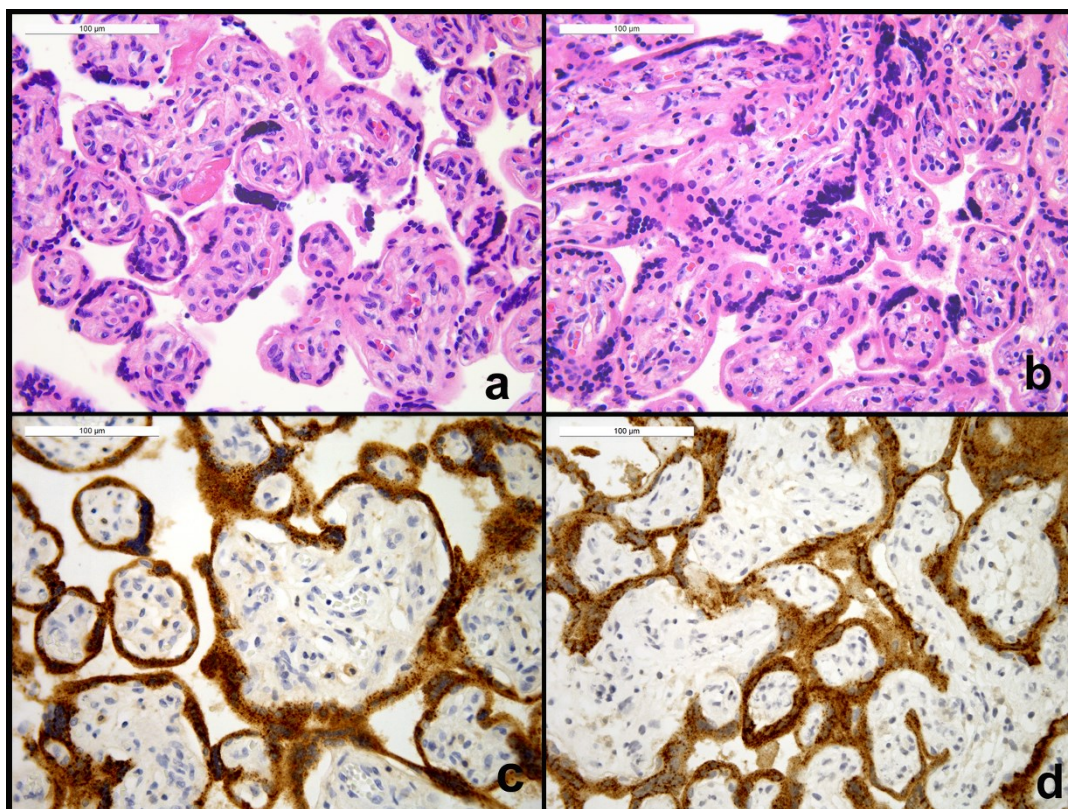
Item name: CELL\_CSH\_POS\_06  
Channel name: 1: TOF MS<sup>+</sup> BPI (20-1200) 4eV, 2eV ESI+



**S1 Fig. Chromatograms of lipid fractions expressed in mosquito and mammalian cell lines.** (A) In red the chromatogram of lipid fractions expressed in C6/36 mosquito cells; in blue, the chromatogram of lipids derived from Vero mammalian cell line.



**S2 Fig.  $\beta$  -hCG level in DMSO and Forskolin treated BeWo cell lines.** Levels of  $\beta$ -hCG hormone was measured in BeWo cell lines at 24 and 48 hours post treatment with DMSO and Forskolin substance.



**S3 Fig. Histological and immunohistochemistry of human full-term placental explant tissues.** (a, b) Placental villous explant hematoxylin–eosin (H&E) at respectively 24 and 72 hours post tissue collection (HPC). At 24 HPC, the stroma of the villi was hypercellular with abundant vessels and numerous syncytiotrophoblast cells were visible on the villi external surface. At 72 HPC villi stroma was dense and vessels were still detected. The integrity of syncytiotrophoblast layer was indicative of a well-preserved tissue (40X magnification). (c,d) At 24 HPC Placental villous explant showed a strong and diffuse positivity of the syncytiotrophoblast cells cytoplasm for hCG hormones which was maintained over the time and detected at 72 HPC (40X magnification).

Method	Viruses	Primer Name	Sequence (5'-3')	Size	Reference	
NGS seq.	FP-V	400_1_out_L	GACAGTTCGAGTTTGAAGCGAAAG	3470	Grubaugh et al., 2019	
		400_11_out_R	CCTGGGCCTTATCTCCATTCCA			
	FP-C6	400_10_out_L	ACGGTCGTTGTGGGATCTGTAA	2860		
		400_18_out_R	TGGTGAGTTGGAGTCCGGAAT			
	HON-V	400_18_out_L	CTGTTGAGTGCTTCGAGCCTTC	3180		
		HON-C6	400_27_out_R			ATGTGTAGAGTTGCGGGAGAGT
				400_26_out_L		ACTGGAACTCCTCTACAGCCAC
			400_35_out_R	ACCACTAGTCCCTCTTCTGGAG		
	MR-V	400_1_out_L	GACAGTTCGAGTTTGAAGCGAAAG	3760		Grubaugh et al., 2019
		MR-C6	400_12_out_R			TACTAATGCCAAGTGAGCTACG

	400_11_out_L	CAGCCGTCATAGGAACAGCTGT	3750	This study
	400_22_out_R	ATTCTGGCTGGTTCGATTTCTG		This study
	400_21_out_L	GGAGACTGATGAAGACCATGCA	4350	This study
	400_34_out_R	TGACTAGCAGGCCTGACAACAT		Grubaugh et al., 2019

**S1 Table: List of primer sets used during ZIKV next-generation sequencing**

<b>Protein</b>	<b>AA change</b>	<b>Type</b>	<b>FP-C6</b>	<b>FP-V</b>
polyprotein	H243Y	missense	7,6%	17,7%
polyprotein	F252L	missense	29,3%	40,6%
polyprotein	F257L	missense	1,4%	0,0%
polyprotein	M635I	missense	41,1%	25,9%
polyprotein	V681I	missense	1,2%	1,3%
polyprotein	H691Y	missense	3,2%	2,8%
polyprotein	S745L	missense	0,0%	2,3%
polyprotein	A791T	missense	4,8%	16,5%
polyprotein	W892R	missense	41,4%	27,7%
polyprotein	P895L	missense	0,0%	1,4%
polyprotein	T933I	missense	8,6%	19,9%
polyprotein	L939H	missense	1,0%	0,0%
polyprotein	L939P	missense	26,5%	34,4%
polyprotein	M1014I	missense	2,2%	1,8%
polyprotein	M1014T	missense	3,2%	0,0%
polyprotein	K1021E	missense	0,0%	1,1%
polyprotein	K1059A	missense	0,2%	0,1%
polyprotein	K1059E	missense	1,8%	1,7%
polyprotein	K1059I	missense	8,0%	3,5%
polyprotein	K1059T	missense	4,4%	3,3%
polyprotein	K1059V	missense	0,2%	0,1%
polyprotein	A1263V	missense	15,1%	16,6%
polyprotein	A1396V	missense	7,9%	20,3%
polyprotein	E1399Q	missense	9,0%	4,0%
polyprotein	M1404I	missense	23,7%	30,6%
polyprotein	M1404V	missense	39,0%	27,7%
polyprotein	N2800D	missense	3,1%	2,6%
polyprotein	Q3034P	missense	1,0%	0,0%
polyprotein	E3146V	missense	3,1%	1,1%
<b>Protein</b>	<b>AA change</b>	<b>Type</b>	<b>HON-C6</b>	<b>HON-V</b>
polyprotein	I80T	missense	1,2%	1,5%
polyprotein	H205R	missense	8,7%	8,9%

polyprotein	F252L	missense	7,5%	6,5%
polyprotein	A562S	missense	1,0%	0,0%
polyprotein	T605I	missense	12,9%	7,5%
polyprotein	H691Y	missense	46,3%	56,0%
polyprotein	K733R	missense	15,1%	7,4%
polyprotein	S745I	missense	0,0%	0,2%
polyprotein	S745L	missense	2,5%	12,8%
polyprotein	S745T	missense	0,0%	2,4%
polyprotein	F1241L	missense	2,2%	8,9%
polyprotein	A1263V	missense	3,1%	2,5%
polyprotein	A1428V	missense	0,0%	1,2%
polyprotein	M1836T	missense	1,1%	0,0%
polyprotein	E3146V	missense	1,3%	0,0%
polyprotein	T3220I	missense	3,7%	5,5%
<b>Protein</b>	<b>AA change</b>	<b>Type</b>	<b>MR-C6</b>	<b>MR-V</b>
polyprotein	A263T	missense	0,0%	2,0%
polyprotein	S270G	missense	0,0%	1,0%
polyprotein	R448S	missense	2,6%	0,0%
polyprotein	F482L	missense	2,6%	0,0%
polyprotein	L660M	missense	2,4%	0,0%
polyprotein	A706V	missense	0,0%	3,1%
polyprotein	S739L	missense	0,0%	3,4%
polyprotein	D996A	missense	1,1%	0,0%
polyprotein	A1257V	missense	0,0%	3,1%
polyprotein	I1258T	missense	0,0%	2,6%
polyprotein	I1258V	missense	2,0%	0,0%
polyprotein	A1297V	missense	1,2%	0,0%
polyprotein	E1393G	missense	1,9%	0,0%
polyprotein	E1393K	missense	1,9%	0,0%
polyprotein	E1393R	missense	0,7%	0,0%
polyprotein	E1393T	missense	0,0%	0,0%
polyprotein	R1603K	missense	1,1%	0,0%
polyprotein	K1962T	missense	1,7%	0,0%
polyprotein	I2050T	missense	2,0%	0,0%
polyprotein	T2062I	missense	1,0%	0,0%
polyprotein	K2083T	missense	0,0%	5,0%
polyprotein	I2305V	missense	0,0%	1,6%
polyprotein	A2351T	missense	1,2%	0,0%
polyprotein	V2892A	missense	1,1%	0,0%
polyprotein	E3074G	missense	0,0%	2,2%
polyprotein	F252L	missense	1,5%	6,8%
polyprotein	S341N	missense	2,1%	1,4%

polyprotein	K418R	missense	4,3%	9,5%
polyprotein	G440E	missense	4,6%	8,8%
polyprotein	K450E	missense	5,9%	9,9%
polyprotein	P455A	missense	1,4%	10,2%
polyprotein	H685Y	missense	3,3%	9,3%
polyprotein	A735V	missense	2,5%	3,9%
polyprotein	L933F	missense	1,6%	1,5%
polyprotein	D1391G	missense	5,0%	8,9%
polyprotein	E1393A	missense	1,3%	1,1%
polyprotein	M1398I	missense	2,4%	4,5%
polyprotein	I1405V	missense	6,1%	5,7%
polyprotein	V1518L	missense	1,9%	5,0%
polyprotein	S1852F	missense	10,2%	17,6%
polyprotein	S1852Y	missense	3,0%	12,6%
polyprotein	K1962N	missense	8,9%	11,4%
polyprotein	K1962R	missense	7,0%	11,5%
polyprotein	K1962S	missense	0,1%	0,1%
polyprotein	K2543R	missense	1,6%	5,0%

**S2 Table: Aminoacidic changes between ZIKV viral stocks derived from mammalian and mosquito cell lines and identified by next-generation sequencing**

## References

1. Arora N, Sadovsky Y, Dermody TS, Coyne CB. Microbial vertical transmission during human pregnancy. *2016;20(4):412–26.*
2. Ades AE, Soriano-Arandes A, Alarcon A, Bonfante F, Thorne C, Peckham CS, et al. Vertical transmission of Zika virus and its outcomes: a Bayesian synthesis of prospective studies. *The Lancet Infectious Diseases. 2021;21(4):537–45.*
3. Villalobos-Sánchez E, Burciaga-Flores M, Zapata-Cuellar L, Camacho-Villegas TA, Elizondo-Quiroga DE. Possible Routes for Zika Virus Vertical Transmission in Human Placenta: A Comprehensive Review. *Viral Immunology. 1 luglio 2022;35(6):392–403.*
4. Tabata T, Petitt M, Puerta-Guardo H, Michlmayr D, Wang C, Fang-Hoover J, et al. Zika Virus Targets Different Primary Human Placental Cells, Suggesting Two Routes for Vertical Transmission. *Cell Host and Microbe. 2016;20(2):155–66.*
5. Bayer A, Lennemann NJ, Ouyang Y, Bramley JC, Morosky S, Torres E, et al. Type III Interferons Produced by Human Placental Trophoblasts Confer Protection Against Zika Virus Infection. *Cell Host Microbe. 2017;19(5):705–12.*
6. Brasil P, Vasconcelos Z, Kerin T, Gabaglia CR, Ribeiro IP, Bonaldo MC, et al. Zika virus vertical transmission in children with confirmed antenatal exposure. *Nat Commun. dicembre 2020;11(1):3510.*
7. Einspieler C, Utsch F, Brasil P, Panvequio Aizawa CY, Peyton C, Hydee Hasue R, et al. Association of Infants Exposed to Prenatal Zika Virus Infection With Their Clinical, Neurologic, and Developmental Status Evaluated via the General Movement Assessment Tool. *JAMA Netw Open. 18 gennaio 2019;2(1):e187235.*



8. Noronha L de, Zanluca C, Burger M, Suzukawa AA, Azevedo M, Rebutini PZ, et al. Zika Virus Infection at Different Pregnancy Stages: Anatomopathological Findings, Target Cells and Viral Persistence in Placental Tissues. *Frontiers in Microbiology*. 2018;9(September):1–11.
9. Leier HC, Messer WB, Tafesse FG. Lipids and pathogenic flaviviruses: An intimate union. *PLoS Pathogens*. 2018;14(5):1–7.
10. Melo CFOR, De Oliveira DN, De Oliveira Lima E, Guerreiro TM, Esteves CZ, Beck RM, et al. A lipidomics approach in the characterization of zika-infected mosquito cells: Potential targets for breaking the transmission cycle. *PLoS ONE*. 2016;11(10):1–15.
11. Leier HC, Weinstein JB, Kyle JE, Lee JY, Bramer LM, Stratton KG, et al. A global lipid map defines a network essential for Zika virus replication. *Nature Communications*. 2020;11(1):1–15.
12. Martín-Acebes MA, Vázquez-Calvo Á, Saiz JC. Lipids and flaviviruses, present and future perspectives for the control of dengue, Zika, and West Nile viruses. *Progress in Lipid Research*. 2016;64:123–37.
13. Gollins SW, Porterfield JS. PH-dependent Fusion between the Flavivirus West Nile and Liposomal Model Membranes. *Journal of General Virology*. 1 gennaio 1986;67(1):157–66.
14. Peña J, Harris E. Early Dengue Virus Protein Synthesis Induces Extensive Rearrangement of the Endoplasmic Reticulum Independent of the UPR and SREBP-2 Pathway. Jin DY, curatore. *PLoS ONE*. 4 giugno 2012;7(6):e38202.
15. Biswas HH, Gordon A, Nuñez A, Perez MA, Balmaseda A, Harris E. Lower Low-Density Lipoprotein Cholesterol Levels Are Associated with Severe Dengue Outcome. *PLoS Neglected Tropical Diseases*. 2015;9(9):1–19.
16. Welsch S, Miller S, Romero-Brey I, Merz A, Bleck CKE, Walther P, et al. Composition and Three-Dimensional Architecture of the Dengue Virus Replication and Assembly Sites. *Cell Host & Microbe*. aprile 2009;5(4):365–75.
17. Junjhon J, Pennington JG, Edwards TJ, Perera R, Lanman J, Kuhn RJ. Ultrastructural Characterization and Three-Dimensional Architecture of Replication Sites in Dengue Virus-Infected Mosquito Cells. Doms RW, curatore. *J Virol*. maggio 2014;88(9):4687–97.
18. Matrosovich M, Matrosovich T, Garten W, Klenk D. New low-viscosity overlay medium for viral plaque assays. 2006;7:1–7.
19. Bolger AM, Lohse M, Usadel B. Trimmomatic: a flexible trimmer for Illumina sequence data. *Bioinformatics*. 1 agosto 2014;30(15):2114–20.
20. Li H, Durbin R. Fast and accurate long-read alignment with Burrows–Wheeler transform. *Bioinformatics*. 1 marzo 2010;26(5):589–95.
21. Li H, Handsaker B, Wysoker A, Fennell T, Ruan J, Homer N, et al. The Sequence Alignment/Map format and SAMtools. *Bioinformatics*. 15 agosto 2009;25(16):2078–9.
22. Wilm A, Aw PPK, Bertrand D, Yeo GHT, Ong SH, Wong CH, et al. LoFreq: a sequence-quality aware, ultra-sensitive variant caller for uncovering cell-population heterogeneity from high-throughput sequencing datasets. *Nucleic Acids Research*. 1 dicembre 2012;40(22):11189–201.

23. McKenna A, Hanna M, Banks E, Sivachenko A, Cibulskis K, Kernytsky A, et al. The Genome Analysis Toolkit: a MapReduce framework for analyzing next-generation DNA sequencing data. *Genome research*. 2010;
24. Depristo MA, Banks E, Poplin R, Garimella KV, Maguire JR, Hartl C, et al. A framework for variation discovery and genotyping using next-generation DNA sequencing data. *Nature Genetics*. 2011;
25. Van der Auwera GA, Carneiro MO, Hartl C, Poplin R, del Angel G, Levy-Moonshine A, et al. From fastQ data to high-confidence variant calls: The genome analysis toolkit best practices pipeline. *Current Protocols in Bioinformatics*. 2013;
26. Robinson KA, Akinyede O, Dutta T, Sawin VI, Li T, Spencer MR, et al. Framework for Determining Research Gaps During Systematic Review: Evaluation [Internet]. Rockville (MD): Agency for Healthcare Research and Quality (US); 2013 [citato 3 settembre 2022]. (AHRQ Methods for Effective Health Care). Disponibile su: <http://www.ncbi.nlm.nih.gov/books/NBK126708/>
27. Thorvaldsdottir H, Robinson JT, Mesirov JP. Integrative Genomics Viewer (IGV): high-performance genomics data visualization and exploration. *Briefings in Bioinformatics*. 1 marzo 2013;14(2):178–92.
28. Reed LJ, Muench H. A simple method of estimating fifty per cent endpoints. *American Journal of Epidemiology*. 1938;
29. Müller JA, Harms M, Schubert A, Jansen S, Michel D, Mertens T, et al. Inactivation and Environmental Stability of Zika Virus. *Emerg Infect Dis*. settembre 2016;22(9):1685–7.
30. Lanciotti RS, Kosoy OL, Laven JJ, Velez JO, Lambert AJ, Johnson AJ, et al. Genetic and Serologic Properties of Zika Virus Associated with an Epidemic, Yap State, Micronesia, 2007. *Emerg Infect Dis*. agosto 2008;14(8):1232–9.
31. Pierson TC, Diamond MS. The continued threat of emerging flaviviruses. *Nature Microbiology*. 2020;5(6):796–812.
32. Coyne CB, Lazear HM. Zika virus — reigniting the TORCH. *Nat Rev Microbiol*. novembre 2016;14(11):707–15.
33. Charlier C, Beaudoin MC, Couderc T, Lortholary O, Lecuit M. Arboviruses and pregnancy: maternal, fetal, and neonatal effects. *The Lancet Child and Adolescent Health*. 2017;1(2):134–46.
34. Frota LM da CP, Sampaio RF, Miranda JL, Brasil RMC, Gontijo APB, Mambrini JV de M, et al. Children with congenital Zika syndrome: symptoms, comorbidities and gross motor development at 24 months of age. *Heliyon*. giugno 2020;6(6):e04130.
35. Nielsen-Saines K, Brasil P, Kerin T, Vasconcelos Z, Gabaglia CR, Damasceno L, et al. Delayed childhood neurodevelopment and neurosensory alterations in the second year of life in a prospective cohort of ZIKV-exposed children. *Nat Med*. agosto 2019;25(8):1213–7.
36. Hafer A, Whittlesey R, Brown DT, Hernandez R. Differential Incorporation of Cholesterol by Sindbis Virus Grown in Mammalian or Insect Cells. *Journal of Virology*. 2009;83(18):9113–21.

37. Kanno K, Wu MK, Scapa EF, Roderick SL, Cohen DE. Structure and function of phosphatidylcholine transfer protein (PC-TP)/StarD2. *Biochimica et Biophysica Acta (BBA) - Molecular and Cell Biology of Lipids*. giugno 2007;1771(6):654–62.
38. Perera R, Riley C, Isaac G, Hopf-Jannasch AS, Moore RJ, Weitz KW, et al. Dengue Virus Infection Perturbs Lipid Homeostasis in Infected Mosquito Cells. *PLoS Pathogens*. 2012;8(3).
39. Zhang J, Zhang Z, Chukkapalli V, Nchoutmboube JA, Li J, Randall G, et al. Positive-strand RNA viruses stimulate host phosphatidylcholine synthesis at viral replication sites. *Proc Natl Acad Sci USA* [Internet]. 23 febbraio 2016 [citato 3 settembre 2022];113(8). Disponibile su: <https://pnas.org/doi/full/10.1073/pnas.1519730113>
40. Hung SJ, Huang SW. Contributions of Genetic Evolution to Zika Virus Emergence. *Front Microbiol*. 6 maggio 2021;12:655065.
41. Grubaugh ND, Weger-Lucarelli J, Murrieta RA, Fauver JR, Garcia-Luna SM, Prasad AN, et al. Genetic Drift during Systemic Arbovirus Infection of Mosquito Vectors Leads to Decreased Relative Fitness during Host Switching. *Cell Host & Microbe*. aprile 2016;19(4):481–92.
42. Hu T, Li J, Carr MJ, Duchêne S, Shi W. The Asian Lineage of Zika Virus: Transmission and Evolution in Asia and the Americas. *Virol Sin*. febbraio 2019;34(1):1–8.
43. Szklanna PB, Wynne K, Nolan M, Egan K, Áinle FN, Maguire PB. Comparative proteomic analysis of trophoblast cell models reveals their differential phenotypes, potential uses, and limitations. *Proteomics*. maggio 2017;17(10):1700037.
44. Carro AC, Damonte EB. Requirement of cholesterol in the viral envelope for dengue virus infection. *Virus Research*. 2013;174(1–2):78–87.
45. Nour AM, Li Y, Wolenski J, Modis Y. Viral Membrane Fusion and Nucleocapsid Delivery into the Cytoplasm are Distinct Events in Some Flaviviruses. Pierson TC, curatore. *PLoS Pathogens*. 5 settembre 2013;9(9):e1003585.
46. Rey FA, Stiasny K, Heinz FX. Flavivirus structural heterogeneity: implications for cell entry. *Current Opinion in Virology*. giugno 2017;24:132–9.
47. van der Schaar HM, Rust MJ, Chen C, van der Ende-Metselaar H, Wilschut J, Zhuang X, et al. Dissecting the Cell Entry Pathway of Dengue Virus by Single-Particle Tracking in Living Cells. Farzan M, curatore. *PLoS Pathog*. 19 dicembre 2008;4(12):e1000244.
48. Byrd-Leotis L, Cummings RD, Steinhauer DA. The interplay between the host receptor and influenza virus hemagglutinin and neuraminidase. *International Journal of Molecular Sciences*. 2017;18(7).
49. Khaiboullina SF, Ribeiro FM, Uppal T, Martynova EV, Rizvanov AA, Verma SC. Zika Virus Transmission Through Blood Tissue Barriers. *Frontiers in Microbiology*. 2019;10(July):1–13.
50. Duggal NK, McDonald EM, Ritter JM, Brault AC. Sexual transmission of Zika virus enhances in utero transmission in a mouse model. *Scientific Reports*. 2018;8(1):1–8.
51. Borges ED, Vireque AA, Berteli TS, Ferreira CR, Silva AS, Navarro PA. An update on the aspects of Zika virus infection on male reproductive system. *J Assist Reprod Genet*. luglio 2019;36(7):1339–49.

52. Masson D. Human seminal plasma displays significant phospholipid transfer activity due to the presence of active phospholipid transfer protein. *Molecular Human Reproduction*. 1 agosto 2003;9(8):457–64.
53. Gautier C, Aurich C. “Fine feathers make fine birds” – The mammalian sperm plasma membrane lipid composition and effects on assisted reproduction. *Animal Reproduction Science*. novembre 2021;106884.
54. Queiroz A, Pinto IFD, Lima M, Giovanetti M, de Jesus JG, Xavier J, et al. Lipidomic Analysis Reveals Serum Alteration of Plasmalogens in Patients Infected With ZIKA Virus. *Frontiers in Microbiology*. 2019;10(April):1–10.
55. Mart MA, Jim N. Lipid Metabolism as a Source of Druggable Targets for Antiviral Discovery against Zika and Other Flaviviruses. 2019;
56. Marbán-Castro E, Goncé A, Fumadó V, Romero-Acevedo L, Bardají A. Zika virus infection in pregnant women and their children: A review. *European Journal of Obstetrics & Gynecology and Reproductive Biology*. ottobre 2021;265:162–8.
57. Musso D, Ko AI, Baud D. Zika Virus Infection — After the Pandemic. Longo DL, curatore. *N Engl J Med*. 10 ottobre 2019;381(15):1444–57.
58. Vannice KS, Cassetti MC, Eisinger RW, Hombach J, Knezevic I, Marston HD, et al. Demonstrating vaccine effectiveness during a waning epidemic: A WHO/NIH meeting report on approaches to development and licensure of Zika vaccine candidates. *Vaccine*. febbraio 2019;37(6):863–8.
59. Weger-Lucarelli J, Auerswald H, Vignuzzi M, Dussart P, Karlsson EA. Taking a bite out of nutrition and arbovirus infection. *PLoS Neglected Tropical Diseases*. 2018;12(3):1–25.
60. Levental KR, Malmberg E, Symons JL, Fan YY, Chapkin RS, Ernst R, et al. Lipidomic and biophysical homeostasis of mammalian membranes counteracts dietary lipid perturbations to maintain cellular fitness. *Nat Commun*. dicembre 2020;11(1):1339.

## **Chapter 3**

*Intended for publication*

# Maternal dietary lipids as risk factor of Zika virus vertical transmission in a rodent model

Eva Mazzetto<sup>1</sup>, Matteo Pagliari<sup>2</sup>, Lisa Baraldo<sup>2</sup>, Davide Bovo<sup>3</sup>, Giada Morelli<sup>4</sup>, Diletta Fornasiero<sup>5</sup>, Matteo Stocchero<sup>1</sup>, Michela Bigolaro<sup>6</sup>, Elisa Mazzacan<sup>2</sup>, Andrea Fortin<sup>2</sup>, Valentina Panzarin<sup>2</sup>, Paolo Mulatti<sup>5</sup>, Claudia Zanardello<sup>6</sup>, Annalisa Stefani<sup>4</sup>, Giuseppe Giordano<sup>1</sup>, Carlo Giaquinto<sup>1</sup>, Francesco Bonfante<sup>2</sup>.

<sup>1</sup>Department of Mother and Child Health, Università degli Studi di Padova, via Giustiniani, 3, 35122 Padova(PD)

<sup>2</sup>Department of Virology, Istituto Zooprofilattico Sperimentale delle Venezie, Viale dell'Università, Legnaro (PD)

<sup>3</sup>Department of Chemistry, Istituto Zooprofilattico Sperimentale delle Venezie, Viale dell'Università, Legnaro (PD)

<sup>4</sup>Department of Animal Medicine, Production and Health, Università degli Studi di Padova, Viale dell'Università 16, 35020 Legnaro (PD)

<sup>5</sup>Department of Epidemiology, Istituto Zooprofilattico Sperimentale delle Venezie, Viale dell'Università, Legnaro (PD)

<sup>6</sup>Department of Diagnostic Services, Histopathology, Parasitology, Istituto Zooprofilattico Sperimentale delle Venezie, Viale dell'Università, Legnaro (PD)

## Abstract

Zika virus (ZIKV) is a member of the Flaviviridae family mainly transmitted among human populations by mosquito vectors. In pregnant women, ZIKV is able to replicate and cross the placenta barrier causing adverse consequences to the fetus ranging from miscarriages to fetal malformations called congenital ZIKV syndrome (CZS). It has been demonstrated that the placental susceptibility to ZIKV infection decreases during pregnancy; nevertheless, ZIKV can impair fetal development throughout the entire pregnancy, supporting the hypothesis that, depending on the gestational phase, ZIKV could use different unknown pathogenic mechanisms to undermine the placenta barrier. Recent works underlined the important role of both host cell membrane and viral envelope lipids in Flavivirus pathogenesis, pointing out how the success of host cell infection strictly

depends on the type of viral and cell lipids and their reciprocal interactions. ZIKV envelope lipids derive directly from the infected host cell membranes, and host cells, as placental cells, mainly derive their lipids from dietary fat. From this perspective, we decided to investigate whether dietary lipids could affect ZIKV pathogenesis at the level of placenta in pregnant women by performing a translational *in-vivo* study in immuno-competent mice.

To test our hypothesis, we fed mice with different diets that reproduce the lipid content of the main human dietary patterns, namely: a) diets with a high content of either saturated or unsaturated fatty acids to mimic a Western and a Mediterranean diet, respectively; b) diets with a low content of saturated or unsaturated fatty acids to represent an African or an Asian diet, respectively. Six-week-old female C57BL/6J mice were divided into four groups and each group was fed with one of the four experimental feeds. After four weeks of feeding, females were mated and successively checked for vaginal plugs to define the gestation time. For each diet group, ten female mice were sacrificed at 15 days of gestation to perform biochemical and lipidomic analyses on serum, liver and placental tissues; ten females were intraperitoneally infected with French Polynesia ZIKV strain at gestational day 12 and subsequently sacrificed at 6 days post-infection to collect lung, spleen, placentas and fetal brains for virological analyses.

Biochemical parameters of pregnant mice resulted comparable among the four diet-groups demonstrating that, despite the different lipid content, the four feed formulations represented diverse but healthy diets suitable for sustaining a normal pregnancy. On the contrary, the lipidomic analysis revealed that the lipid composition of placentas significantly differed among the four diet-groups. This result demonstrated for the first time how the lipid composition of placental tissues can be severely modified by the quality and quantity of dietary lipids. Virological analyses identified the placenta as the main tissue target of ZIKV and most importantly revealed a lower susceptibility to infection in animals fed with a low content of saturated fatty acids, recording a significantly lower number of

infected placentas in mice fed with Mediterranean and African diets compared to mice fed with a Western and Asian diet.

To date, due to the lack of ZIKV vaccines and effective antiviral drugs, prevention of infection mainly relies on chemical and biological vector control. For the first time, our study has unveiled maternal diet as a fundamental determinant of ZIKV pathogenesis in a pre-clinical animal model of placental infection.

### **3.1 Introduction**

Zika virus (ZIKV) is transmitted among humans by mosquito bite, causing, in most cases, an asymptomatic or self-limited disease (1). However, in 2013-16, its diffusion in the naïve population has corresponded with a significantly higher incidence of congenital malformation in the fetuses of women infected by ZIKV during pregnancy. This peculiar ability of ZIKV to cross the placental barrier has included this virus among TORCH agents and, nowadays, the term "congenital ZIKV syndrome" (CZS) is used to describe the spectrum of fetal impairments caused by ZIKV infection (2,3). In the last decades, many researchers and international scientific consortia have investigated ZIKV pathogenesis during pregnancy trying to find an effective therapeutic or prophylactic approach against this infectious disease (4). However, to date, no vaccine or antiviral drugs are available, and the clinical management of acute ZIKV infection is limited to supportive care (1). The delay in identifying a combat strategy to protect or cure pregnant women from ZIKV infection is probably due to the lack of a complete picture of ZIKV diffusion and replication during pregnancy. Several studies demonstrated the high susceptibility of placental cells during the first stages of placenta development, explaining how ZIKV impairs fetal development in the first trimester of pregnancy (5). On the contrary, few pieces of evidence discussed ZIKV infection in the fully-formed placental barrier in the second and third trimester. In this period, the secretion of antiviral factors by villous trophoblast cells



makes the placental tissues more resistant to ZIKV infection, which displays a lower vertical transmission rate compared to the first weeks of gestation (6). However, it has been demonstrated that ZIKV infection can still cause relevant damage to fetal development and the health of the newborn in the late stages of pregnancy (7). These data suggest high versatility of the pathogenic mechanisms exploited by ZIKV to hinder the placental defences and consequently they explain the difficulty in establishing an effective approach to tackle this infectious disease.

In the study reported in Chapter 2, we demonstrated how host and viral lipids could determine ZIKV infectivity in a fully-developed placenta. In particular, we reported that ZIKV virions with a viral envelope rich in phosphatidylcholine lipids displayed high infectivity in villous trophoblast cells thanks to the efficient interaction between the viral envelope and the membranes of host cells. Lipids of the ZIKV envelope derive from the rearrangement of infected-cells intracellular membranes, hence the lipid composition of ZIKV virus strictly depends on the lipids supplied by the host cell (8). The host cells, in turn, derive their lipids from dietary nutrients, such as animal and plants fatty acids, or from the oversupply of carbohydrates, which are physiologically converted into triglycerides. From this perspective, we decided to investigate whether maternal dietary intake could determine the lipid composition of the placental tissues and, consequently, the viral envelope, affecting ZIKV pathogenesis in pregnant women. To achieve this goal, in the Chapter 3, we performed a translational *in-vivo* study using a rodent model. Firstly, we designed four experimental diets to mimic the lipid content of the main human dietary patterns. Then, we determined whether nutritional regimens, different in terms of lipid quantity and quality, were capable of redefining the structure of the cellular membrane of placental tissues. Secondly, we assessed whether the changes in lipid composition of placental tissues could influence the susceptibility of pregnant mice and their fetuses to ZIKV infection.

## **3.2 Methods**

### **3.2.1 Animals and husbandry**

Four to six-week-old immunocompetent C57BL/6J mice were obtained from Charles River Laboratories Italia, in accordance with the Ministry of Health authorization n. 1066/2020-PR, released on November 4th, 2020. Animals were housed in BCU1000-42B cages (Allentown, NJ), equipped with Certified HEPA filtration, negative pressure and unidirectional single-pass consistent airflow. Female mice were housed in groups of 4, while male mice were individually housed. They were maintained at a temperature of 22°C and kept in a controlled environment with a 14:10 light-dark cycle. All animals underwent a minimum acclimation period of 1 week. Identification was obtained through ear punching, after the application of a local anaesthetic. To obtain pregnant mice, the female's estrous cycle was daily checked through vaginal cytology (S1\_Fig) as reported by Cora et al. to identify the proestrus or estrous stage, during which the mating was carried out (9). Female mice were moved to male mice's cages to mate for 24 hours, and successively checked for the presence of a vaginal copulatory plug to confirm the successful mating and define the embryonic age (E) as 0.5. Animals' treatment and care was carried out according to the decisions of the Animal Welfare Body of the Istituto Zooprofilattico Sperimentale delle Venezie (IZSVe), under the guidelines established in the Legislative Decree DLGS no. 26 dated 4 March, 2014.

### **3.2.2 Diets**

From literature, we defined the most important fatty acids constituting human placental tissue which are obtained from the physiological transformation of dietary fats (10). However, the Worldwide dietary fats differ for quality and content depending on many factors including food viability, dietary habits and social condition (11). In our study, we considered the lipids supplied by the most diffuse human diets identifying four main

patterns: a Western diet with high level of saturated fatty acids (SFA), a Mediterranean diet with a high content of unsaturated fatty acids (UFA), an Asiatic diet with a low content of lipids of which the SFA were predominant and an African diet with a general low level of fatty acids mostly unsaturated. We worked together with Research Diet Inc.® (20 Jules Lane New Brunswick, NJ 08901 USA) to tailor human dietary nutrients to mouse metabolism creating four translational experimental diets. Diets 1 and 2 were isocaloric (3.91Kcal/g) and characterized by a high content of lipids (20%Kcal) but differed for the saturated and unsaturated fatty acids (SFA/UFA) ratio which is 3:1 for Diet 1 and inversely 1:3 in Diet 2. At the same way, Diet 3 and Diet 4 were isocaloric (3.71Kcal/g) with a lower lipid content (10%Kcal) comparing Diet 1 and 2. Finally Diet 3 presented a saturated and unsaturated fatty acids ratio of 3:1 and conversely Diet 4 had a SFA/UFA ratio of 1:3. All experimental diet detail comprehensive of ingredients, energy supply, cholesterol content, SFA/UFA ratio and fatty acids profile were reported in Supplementary table 1 and 2.

### **3.2.3 Viruses**

The ZIKV strain H/PF/2013 (ZK-FP; 001V-EVA1545), purchased from the European Virus Archive goes Global (EVAg) platform, was isolated from a human serum in French Polynesia in 2013 and passaged four times in Vero cells. For our study, ZIKV was propagated in Vero cells (Vero, CCL-81™; ATCC®) at 70% confluence, using a multiplicity of infection (MOI) of 0.1. Briefly, Vero cells were incubated with viral inoculum diluted in RPMI 1640 medium (RPMI) supplemented with 2% FCS, penicillin 100 U/ml (Gibco, Life Technology) and streptomycin 100 µg/ml (Gibco, Life Technology) for 1 hour before maintaining medium addition. The supernatant (270 ml) was harvested at 3 days post infection (DPI) when about 60% of cytopathic effect was observed and clarified by centrifugation at 3000×g for 30 mins at 4°C to remove cell debris. The clarified supernatant was concentrated by ultracentrifugation in T-647.5 Fixed Angle Rotor (Thermo Scientific) at 150000×g for 2.5 hours, at 4°C. The supernatant was discharged

and viral pellet was suspended in 10 ml PBS, divided in aliquots and stored at -80°C until use. The titration of the viral stock obtained was performed in Vero cell line by means of focus forming unit (FFU) assays. Vero cells were plated in 96-well plates at concentration of 135000 cell/cm<sup>2</sup> and cultured at 37°C, 5% CO<sub>2</sub>. After 24 hours, cells were washed twice with warm PBS, and incubated with 50µl serial dilutions of viral samples diluted in RPMI with 2% FCS, at 37°C in 5% CO<sub>2</sub>. After 1 hour of incubation, a low viscosity overlay medium was added to the cells as described by Matrosovich et al (12). At 48 HPI, inoculum and overlay medium were removed and cells were fixed with 10% formalin solution at 4°C. After 30 mins, cells were washed three times with cold PBS and permeabilized with a solution of 0.01% Triton X-100 (Sigma-Aldrich) in PBS for 10 mins at RT. Primary anti-flavivirus antibody 4G2 (Millipore Catalog No. MAB10216) were diluted at 1:10000 in a blocking buffer solution (BB) made with 0.1% Tween 20 (Sigma-Aldrich) and 1%w/v bovine albumin (Sigma-Aldrich) in PBS. After 1 hour of incubation, cell were washed three times with PBS containing 0.05 % Tween 20 (PBS-Tween) and incubated with peroxidase-conjugated goat anti-mouse IgG (H+L) antibody (Jackson Immuno Research Laboratories) diluted 1:1000 in BB, for 1 hour at RT. After five washed with PBS-Tween, revelation was performed incubating cells with True Blue™ (KPL) peroxidase substrate for 10 mins at RT. The reaction was stopped replacing true blue with distilled water. Virus titer was expressed as FFU/ml.

### **3.2.4 Experimental design: diet administration and ZIKV infection**

To assess the ZIKV dose and the time points to collect infected organs from pregnant female mice, a pre-trial was assessed as follow. We infected 18 six-weeks-old mice at E12 with a ZIKV dose of 1X10<sup>8</sup> FFU/0.1ml suspended in phosphate-buffered saline (PBS buffer) by intraperitoneal route. Successively infected pregnant mice were sacrificed at 3, 5, 6, 7, 8 and 9 days post infection (DPI) to collect serum, lung, spleen, placentas, fetal brain and miscarriages. After the 6 DPI, (7-9 DPI) females gave birth and placentas were

available anymore, for this reasons at those time points the collection of this tissue was substituted with the entire uterus. Each collected organ was divided in two parts: one part was used to identify ZIKV genome by biology molecular (qRT-PCR) assay; the second part was sampled to detect ZIKV antigenic by means of immunohistochemistry (IHC) assay. Number of fetuses and miscarriages for each sacrificed pregnant mouse were recorded. These animals were fed with a standard diet for mice in reproduction (Mucedola s.r.l.).

Once ZIKV pathogenesis was established in this mouse model, 72 female mice were used to assess the impact of dietary lipid intake in ZIKV maternal infection. Four-weeks-old females were divided into four cohorts of 18 animals and each cohort was fed with one of four experimental diets for at least a month prior to mating and then throughout the entire reproductive and gestation period. During diet administration period body weight gain and feed consumption recorded weekly. In each diet-group, at 12E of gestation, 8 animals were mock-infected using PBS buffer and 10 animals were infected with a ZIKV dose of  $1 \times 10^8$  FFU/0.1ml by intraperitoneal route. The mock-infected mice were sacrificed at 15E after 6 hours fast and serum, liver, placentas and fetus were collected to perform biochemical and lipidomic analysis. Differently, the ZIKV infected mice were sacrificed at 6 DPI and serum, lung, placentas, miscarriages and fetuses were collected to define ZIKV host tissue tropism by IHC and quantify ZIKV genome in the collected organs through qRT-PCR. Moreover, number of fetuses was recorded and for infected-mice, the size of collected fetuses were measured by means of a caliber (S2\_Fig.)

### **3.2.5 Biochemical parameters and hormones**

The serum of pregnant mice fed with the four experimental diets and sacrificed at 15E was analysed for glucose, non-esterified fatty acids (NEFA), triglycerides, total cholesterol, HDL-cholesterol, LDL-cholesterol using a clinical chemistry analyzer (Cobas C501, Roche Diagnostics GmbH, Mannheim, Germany). Moreover, serum levels of leptin, insulin and

interleukin 6 (IL-6) in mock-infected mice were assessed by applying the manufactory protocols of the following ELISA kit: mouse leptin ELISA kit, mouse insulin ELISA kit and (Life Technologies Italy). To determine the cholesterol and triglycerides levels in mice liver, this organ was collected by dipping around 500mg of tissue in cold distillate water and mechanically homogenizing through a TissueLyser instrument (QIAGEN) at 4°C. Then, the homogenized organ was lyophilized and stored at -80°C until use. The content of liver cholesterol and triglycerides was determined using the clinical chemistry analyzer (Cobas C501, Roche Diagnostics GmbH, Mannheim, Germany) on 25 mg of powdered tissues previously suspended in distilled water with a ratio of 1:10.

### **3.2.6 Lipidomic analysis on placental tissues**

To conduct the lipidomic analysis on placental tissues of mice fed with the four experimental diets, the sampling was performed as followed. Briefly, for each sacrificed mouse placental tissues were pooled up to 100mg using instruments and plastic previously treated with MeOH solution. The collected tissues were snap-frozen liquid nitrogen and stored at -80°C until extraction. Frozen tissue samples were crushed with a FastPrep®-24 Instrument (MP Biomedical, Santa Ana, CA) in 1 mL HBSS (Invitrogen, 14170112). After 2 crush cycles (6.5 m/s, 30 s), 50 µL were withdrawn for protein quantification. Different classes of lipids were extracted according to the manufacturer's instructions. Signal intensity for specific lipid species was extracted according to the retention time. Samples with spiked internal standards were analysed by either gas/ liquid chromatography followed by mass spectrometry. The statistical analyses performed after lipidomic data extraction were reported in the results.

### **3.2.7 Viral detection by qRT-PCR**

To assess the effect of feed fat content on the susceptibility of pregnant mice to ZIKV infection, viral load was estimated by quantitative real-time RT-PCR (qRT-PCR) in

placenta, uterus, miscarriage, lung, spleen. To verify viral transmission to progeny, fetal brains were also tested. Approximately 0,1-0,01 g tissue for each sample was collected by storing the organ in 1 ml of RNAlater stabilize (Millipore-Sigma) for 24 hours at 4°C. Then, the solution was removed and samples were stored at -80°C until RNA extraction. For the RNA extraction, samples were thawed, dipped in 1 ml minimum essential medium (MEM) and homogenized at 30 Hz for 10 min with the TissueLyser (Qiagen). 200 µl supernatant were subject to nucleic acids isolation with the MagMAX CORE Nucleic Acid Purification Kit (Applied Biosystems) (Simple Workflow) on a KingFisher Flex Purification System (ThermoFisher Scientific). RNA concentration was determined with the Qubit RNA BR Assay Kit on a Qubit 4 Fluorometer (ThermoFisher Scientific) and subsequently diluted to 50 ng/ µl. Amplification reactions were assembled using the oligonucleotides set 1086/1162c/1107-FAM according to (13). In a separate reaction, host β-actin mRNA was amplified using oligos from Gigante et al. (2018) modified to match mouse target sequence (14). For both ZIKV and β-actin assays, a series of 10-fold dilutions of target-specific plasmids (Integrated DNA Technologies) was included in each run to determine RNA copy number per µl template (CN/ µl) and assess amplification efficiency. ZIKV qRT-PCR limit of detection (LoQ) was established as 10 CN/ µl). Viral load was expressed both as CNZIKV/ µl normalized to β-actin mRNA expression (CNβ-act/ µl) and as CNZIKV/ng RNA. Additional details on qRT-PCR protocols are provided in the Supplementary contents. Moreover, to determine the correlation between viral genome copies and ZIKV infectivity *in-vitro*, 100 samples (11 half-spleens, 11 half-lungs and 78 half-placentas) were processed as follows. At the collection each of these samples was directly stored to -80°C without using RNAlater solution to avoid any viral inactivation. Then, tissues were thawed and dipped in 1 ml MEM and homogenized at 30 Hz for 10 min with the TissueLyser. 200 µl supernatant were analysed for ZIKV genome content as previously reported, and 100 µl

supernatant was serial five-fold diluted and used to infected Vero cells plated in 96-well to determine sample viral infectivity by FFU assay.

### **3.2.8 Immunostaining**

Liver and placentas were collected from the sacrificed of mock-infected pregnant mice and fixed with 10% formalin solution for 24 hours before embedding in paraffin. Then, the embedded tissues were routinely processed for histology by staining 4 µm sections with hematoxylin and eosin (HE). The same method was applied to collect and store the lung, spleen, placentas, and fetal heads of ZIKV-infected mice. In addition to HE, these samples were analysed for the presence of ZIKV envelope antigen by immunohistochemistry (IHC) using the Roche automated immunostainer. Briefly, the antigen retrieval was carried out in 3 µm sections with a commercial ready-to-use Protease 2 (Roche), at 36°C, for 12 minutes. Then, the slides were incubated with primary recombinant monoclonal Flavivirus group antigen antibody, clone D1-4G2-4-15 (MyBioSource), at 1:50 dilution, for 80 minutes at RT. An Ultra-View Universal DAB Detection Kit (Roche) was used as the detection system. The positive and negative controls consisted respectively of infected and mock-infected Vero cells.

### **3.2.9 Statistical analyses**

Graphs of diets administration data, biochemical parameters, hormones levels and virological results were created by using Prism-GraphPad version 9.0 (GraphPad Software, Inc., San Diego, CA, USA). The same software was used to statistically compare the diets administration data, biochemical parameters and hormones levels among the four-diets groups. To define the correlation between genome copies and infectivity of infected mice tissues a ROC curve analysis was performed in association to the Youden index. Moreover, the effect of the different types of diets on the risk of placental infection was assessed through logistic regressions (LRs), which consider the



logarithm of the odds of the outcome (i.e. the placental infectious status) as a function of the diets compositions, that is, the predictor variable of interest. A preliminary LR was performed to assess the absence of any individual effect related to different individual susceptibility to infection. Then, two different LRs were performed separately considering as dependent variable the state of infection defined according to: i) the count of the genome copies (modelgc), and ii) the count of the plaque forming units (modelpfu). Finally, contrasts among estimated marginal means were computed to evaluate the significant differences among the four tested diets, considering a confidence level of 0.95. All data cleaning and preparation, and model building were conducted using R statistical software version 4.2.1 and the packages stats and emmeans.

### **3.3 Results**

#### **3.3.1 Dietary impact on mice metabolism**

Feed consumption among groups was monitored before the beginning of matings to guarantee the same numerosity and physiological condition to each diet-group. The Fig. 1A showed no difference in daily feed consumption (about 2.5g/day) among the four diet-groups indicating a comparable feed intake and diets' palatability. Moreover, the four experimental diets did not differ in daily mouse growth, showing a daily weight gain ranging from 0.045 to 0.098 g per mouse per diet (Fig.1B). To evaluate the impact of the experimental diets on pregnant mice metabolism, the female mice weights were recorded during the gestational period. The statistical comparison among the four diet-groups did not reveal any difference in weight gain of pregnant females (Fig.2). Assessing the hormones' levels, we observed that the experimental diets did not affect the release of the insulin and leptin, which results similar among groups (Fig 3). In the same way, the serum glucose, triglycerides, NEFA and LDL resulted comparable among groups (Fig 4). Interestingly, serum cholesterol and HDL levels were significantly higher in Diet 1 group

compared with levels of animals fed with Diet 4. Nevertheless, the four-diet groups displayed the same content of both cholesterol and triglycerides in the liver tissue (Fig 5). Finally, the number of fetuses and miscarriages did not statistically differ among the four groups, although, the diets characterized by a high content of lipids (Diet 1 and 2) showed a slight increase in the miscarriages' rate (Fig 6).

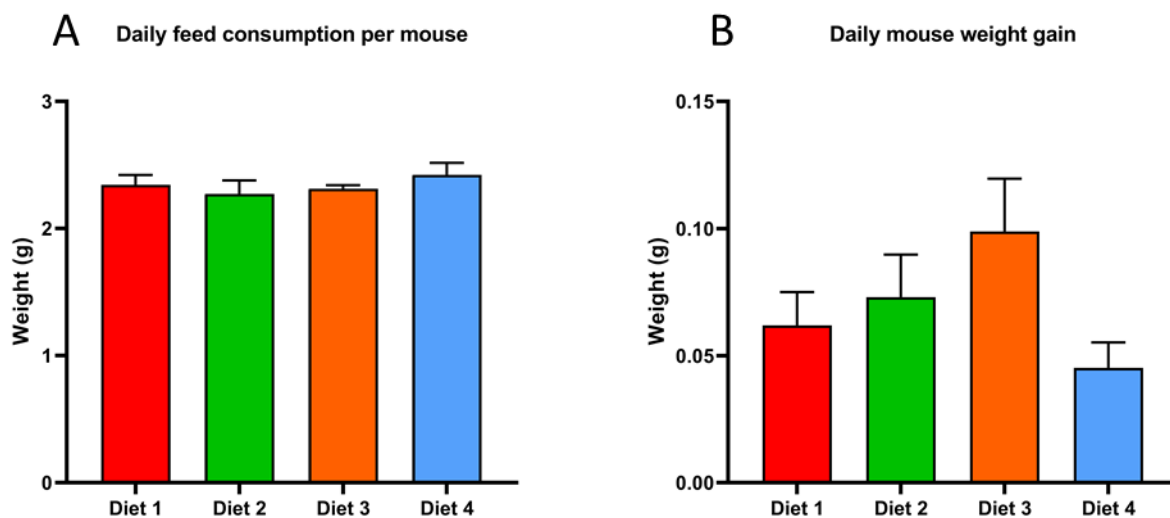


**Fig. 1 Feed parameters of the four experimental diets.** A) The mean feed weight consumed by a mouse per day, per diet considering a period of two weeks. B) The mean weight gain per mouse per diet considering a period of two weeks. Data were compared by parametric one-way ANOVA with Tukey post-test. P values less than 0.05 were considered significant.

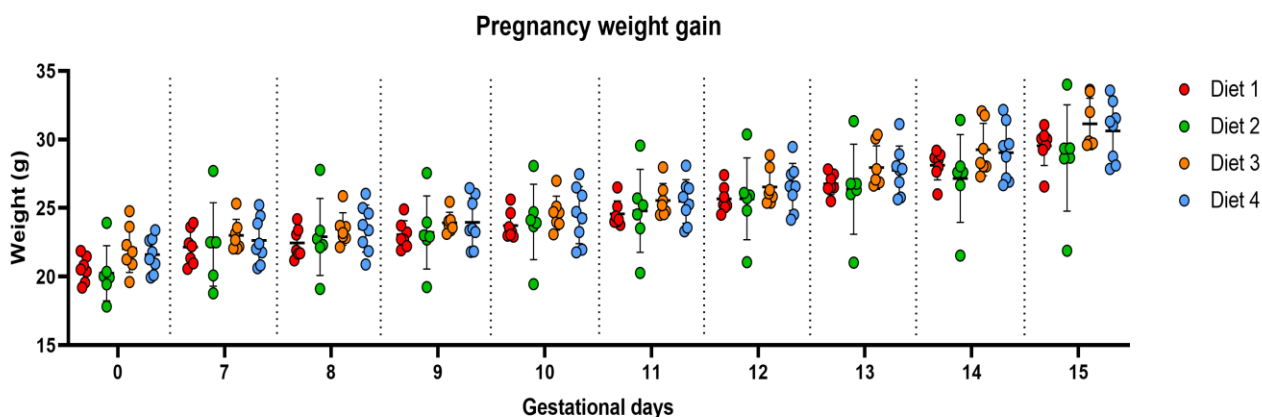


**Fig. 2 Pregnancy weight gain.** The weight of each mouse per diet was recorded during the gestational period which ranged from 7 to 15 days post-conception. The means of weights were compared among diet groups by parametric one-way ANOVA with Tukey post-test. P values less than 0.05 were considered significant.

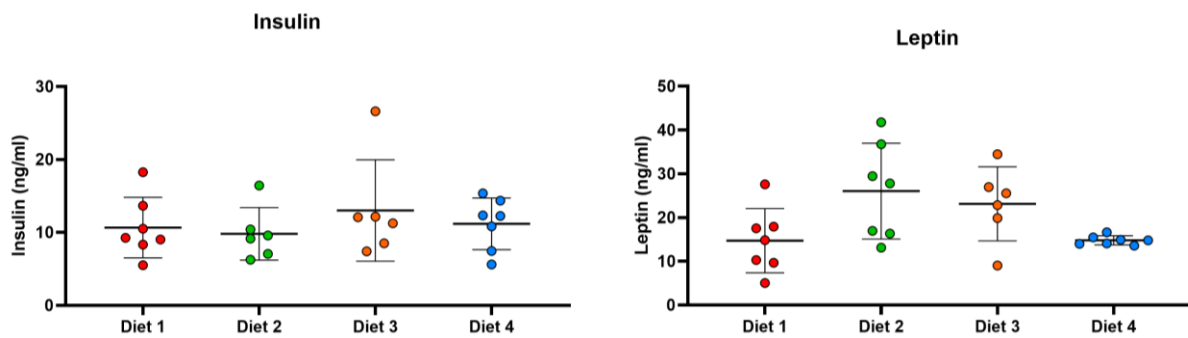


**Fig. 3 Serum hormones' levels.** Insulin and leptin hormone content was measured in serum of pregnant mice sacrificed at 15E. The hormones' mean level was compared among diet groups by parametric one-way ANOVA with Tukey post-test. P values less than 0.05 were considered significant.

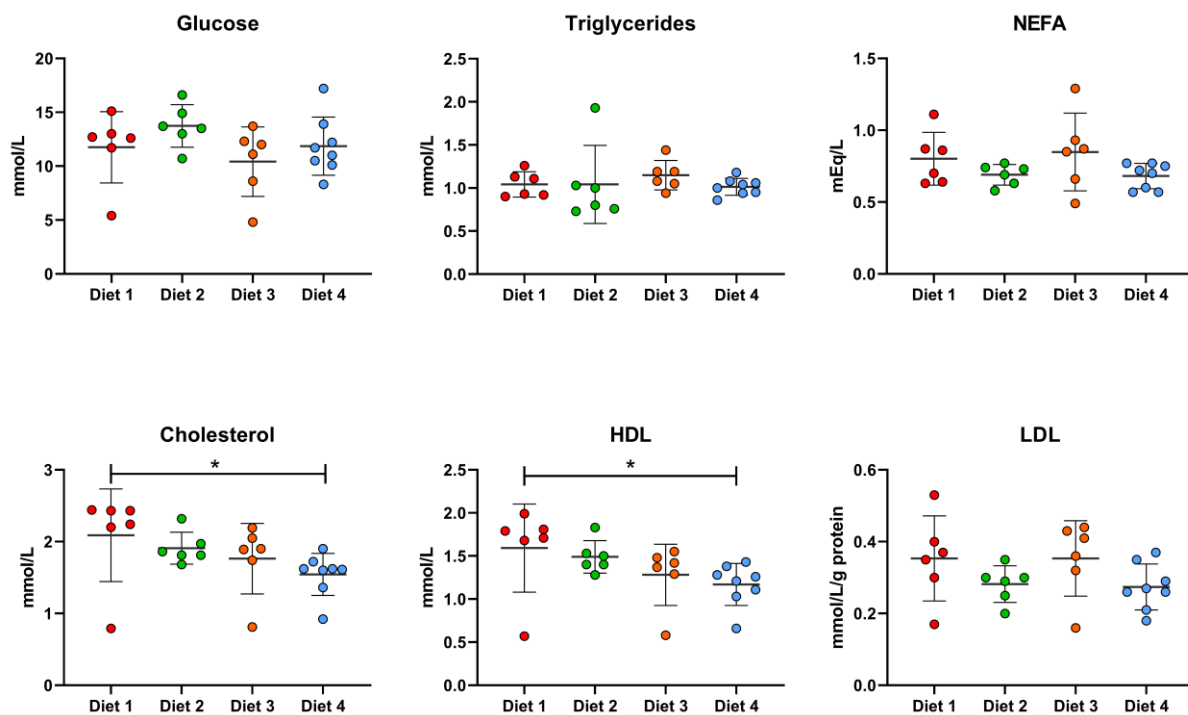


**Fig. 4 Biochemical parameters level in serum.** Glucose, triglycerides, NEFA, cholesterol, HDL and LDL content was measured in serum of pregnant mice sacrificed at 15E. The biochemical parameters' median content was compared among diet groups by non-parametric Kruskal Wallis with Dunn's multiple comparison post-test. P values less than 0.05 were considered significant.

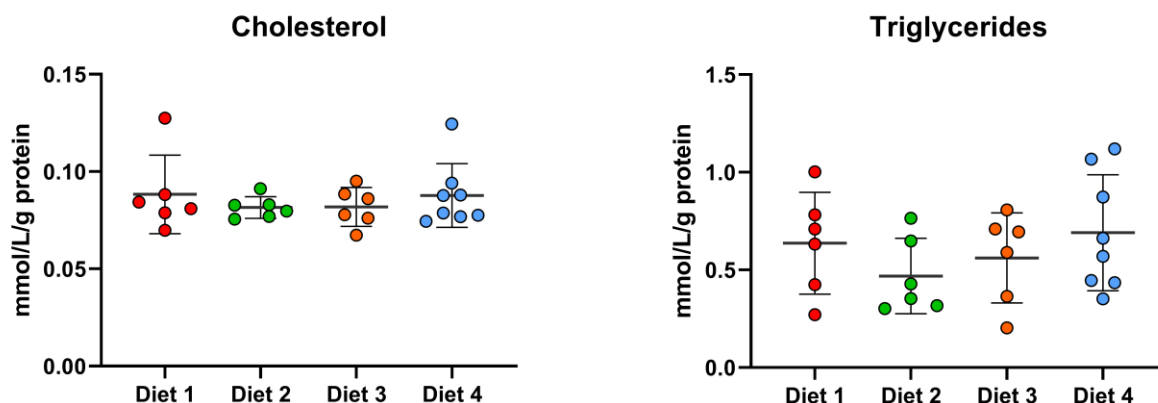


**Fig. 5 Cholesterol and triglycerides content in liver.** Cholesterol and triglycerides were measured in liver of pregnant mice sacrificed at 15E. The Cholesterol and triglycerides' median content was compared among diet groups by non-parametric Kruskal Wallis with Dunn's multiple comparison post-test. P values less than 0.05 were considered significant.

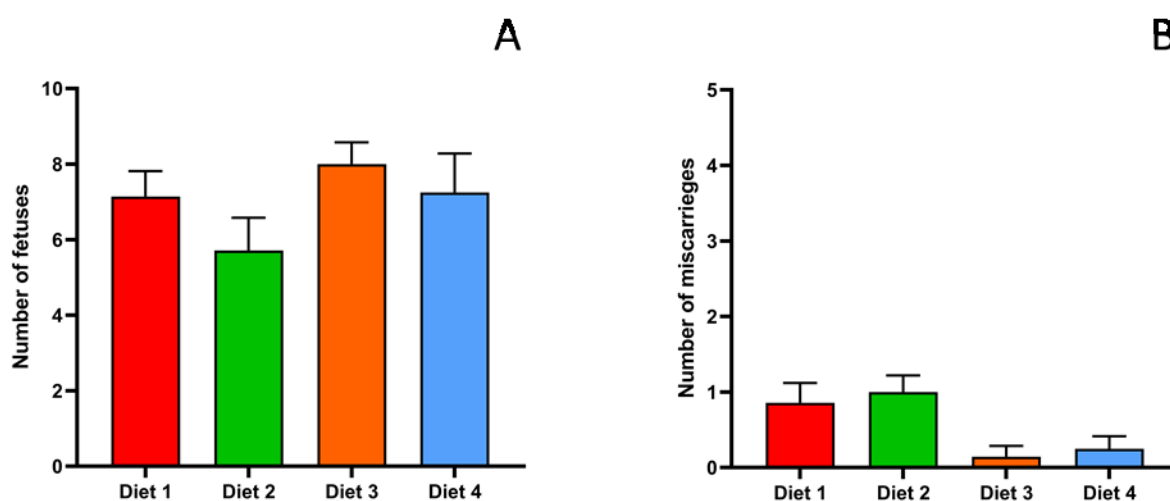


**Fig. 6 Mean number of fetuses and miscarriages per mouse per diet.** A) Mean number of fetuses recorded per mouse per diet. B) Mean number of miscarriages per mouse per diet. Data were compared among diet groups by non-parametric Kruskal Wallis with Dunn's multiple comparison post-test. P values less than 0.05 were considered significant.

### 3.3.2 Dietary impact on mice placental lipid composition

Lipidomic analysis investigated the lipid composition of placental tissues depending on the experimental diet administered before and during pregnancy. Principal component analysis (PCA) was performed on placental tissues collected from mock-infected pregnant mice sacrificed at 15E. PCA identified 180 lipid features responsible for an inter diet-groups variability of 75% ( $R^2=0.75$ ) with four main components: PC1 (42.9%), PC2 (20.2%), PC3

(7%) and PC4 (4.9%) (Fig. 7A). Importantly, PCA results clustered placental samples in four different group which corresponded to the four diets administrated. Therefore, this model supported the hypothesis that both quality and quantity dietary lipids can influence the lipid composition of placental cells. This finding was further corroborated by Partial least squares discriminant analysis (PLS2C), which identified a correlation coefficient  $r=0.8999$  between diet type and placental lipidomes (Fig. 7B).

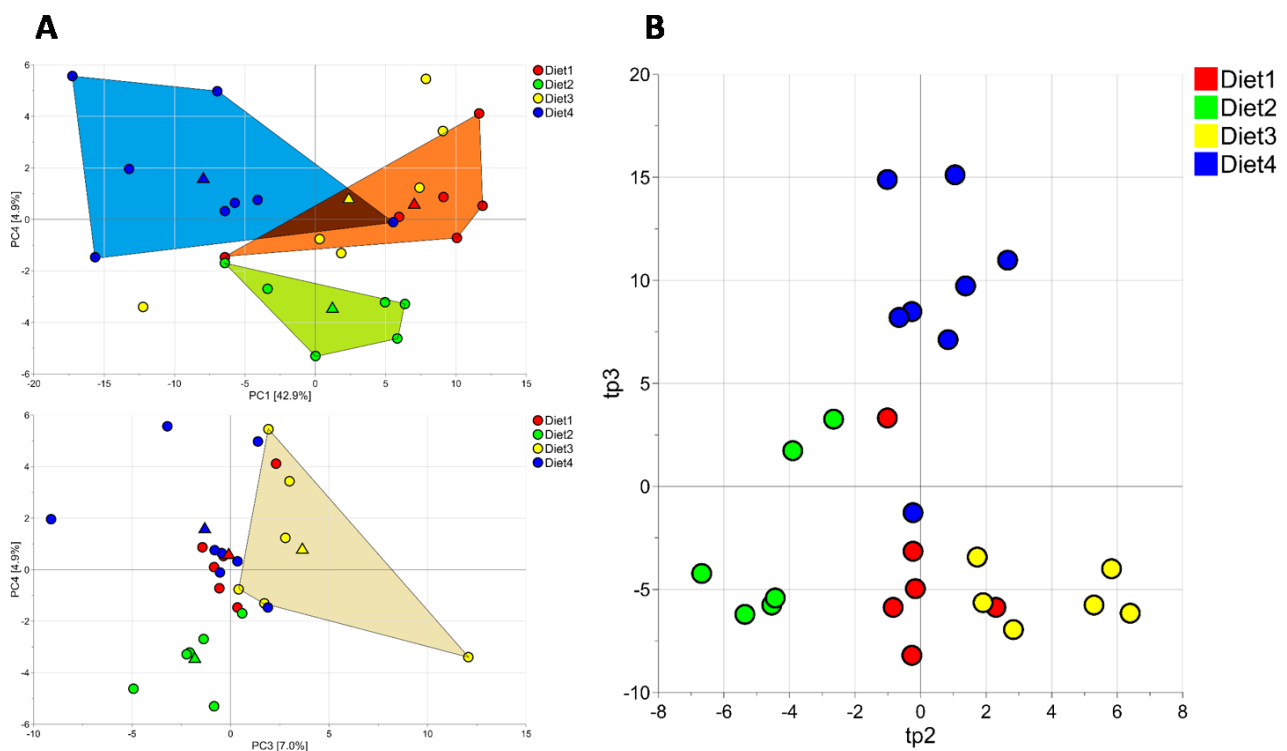


**Fig. 7 Principal component analysis (PCA) and Partial least squares discriminant analysis (PLS-2C) of the lipidomics dataset.** A) PC1, PC2, PC4 showed the differentiation in four different groups of the total placental samples analysed. B) Result of PLS-2C analysis showing the placental lipidomes clustered in four groups correlated to the diet type.

### 3.3.3 ZIKV pathogenesis in an immunocompetent mouse model

The C57BL/6J mouse strain was selected to assess ZIKV infection at the level of placenta. In our study, we used a high dose of ZIKV infection ( $10^8$ PFU/100 $\mu$ l) administrated via intraperitoneal route to overcome the innate immune system. Moreover, we collected organs at different time points to monitor the ZIKV kinetic of replication in this model. We collected spleen to detect ZIKV viremia since this organ is a blood cells'

collector (15). Then, we sampled uterus, placentas, fetuses and miscarriages, which represent the main ZIKV tissues target in pregnant model, whereas, lungs were collected as negative control tissues as ZIKV should not replicate in these organs. The Fig. 8 showed ZIKV replication started at 5DPI to reach its peak at 6DPI (18E), unfortunately it was impossible to monitor the replication over this time point because this mouse strains gave birth at 19-21E. In fact, at 7-9 DPI, the placentas tissues was substituted with the uterus sample and fetal head with new-born mice heads. Consistently with ZIKV tissue tropism, the placentas resulted ZIKV target organs, displaying the highest viral replication in terms of genome copies/ $\mu$ l. Based on these data, we selected 6 DPI as the time point to collect tissues from ZIKV-infected pregnant mice. Interestingly, fetal head collected during 5-6 DPI were completely embedded in ZIKV-positive placental tissues and liquids, which suggested that positivity in fetal head was probably determined by the placental genomic contamination. In fact, the heads of new-born mice did not display any ZIKV genomic positivity. For this reason, in the following pathogenic study, fetal head were exclusively collected for IHC analysis in order to detect ZIKV envelope antigen. Finally, we used ZIKV positive organs to determine the correlation between ZIKV genome copies and ZIKV infectivity in cells. Using a ROC analysis associated with a Youden Index, we established the genome copies threshold (cut-off 45900 genome copies/ $\mu$ l) above which ZIKV detected in organs could be considered infective. Positive placentas were also analysed by IHC. In the panel of Fig. 9, a specific ZIKV positivity was detected in the cytoplasm of several cells present in the junctional zone of mouse placental tissues. This result pointed out an active ZIKV replication in the first layers of placental tissue confirming the validity of this *in-vivo* model to study ZIKV pathogenesis at the placental barrier.

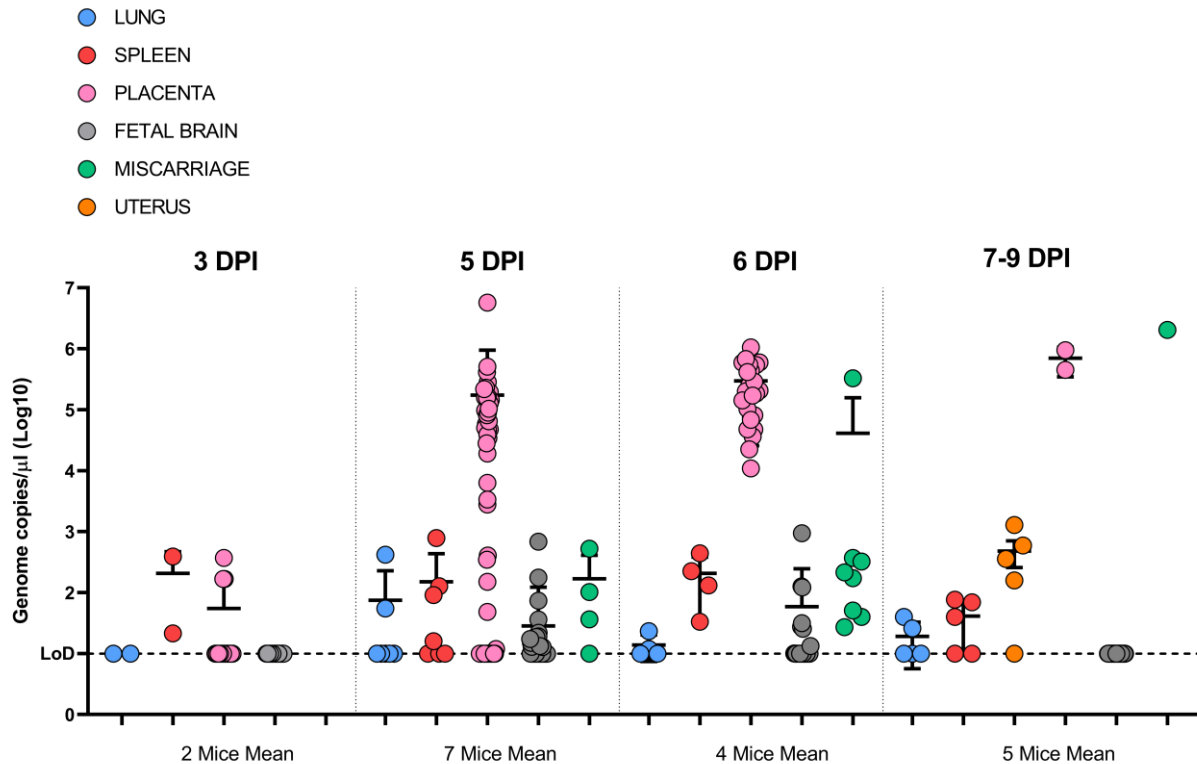


**Fig. 8 ZIKV genome copies in pregnant mice's organs collected at different time points.** ZIKV-infected pregnant mice fed with a standard diet for mice in reproduction (Mucedola s.r.l.) were sacrificed at 3-5-6-7-8-9 DPI. Lungs, spleen, placentas, fetal head, uterus and miscarriages were collected and analysed for viral genome content by qRT-PCR. Data were reported as genome copies/ $\mu$ l.

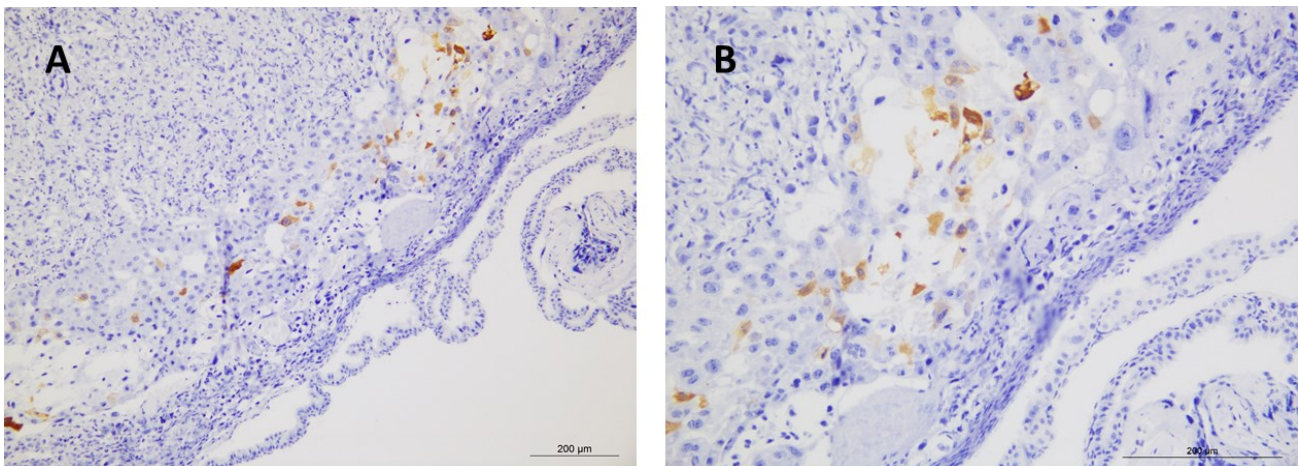


**Fig. 9 Immunohistochemistry analysis on ZIKV-infected mouse placental tissues.** A) Placental trophoblasts positive for ZIKV antigen in the junctional zone (in brownish) at 20X magnification. B) Cells referable to spongiotrophoblasts and glycogentrophoblasts of mouse placental junctional zone positive for ZIKV antigen (in brownish) at 40X magnification

### 3.3.4 Dietary impact on the placental susceptibility to ZIKV infection

Once defined the in-vivo model to study ZIKV infection using immunocompetent mice, and established that quality and quantity of dietary lipids can define the placental tissue lipidome, we infected pregnant mice fed with the four experimental diets at 12E using a

ZIKV dose of  $10^8$  FFU/100 $\mu$ l. To evaluate ZIKV tropism in this model, we collected the lung as a negative control, the spleen as a viremia indicator and the placentas as a ZIKV tissue target. Comparing these organs for ZIKV genome copies content, we considered that different organs can vary in the RNA extraction efficiency or for the presence of inhibitory factors, hence the viral genome copies could be the result of a higher or lower RNA availability in the tissues. For this reason, ZIKV detection was normalized on the  $\beta$ -actin gene expression and reported as fold-change (Fig. 10). As expected, ZIKV did not replicate in the lungs and no viremia was observed at 6DPI, whereas, irrespective of the diet group, ZIKV fold-change ranged from 0.2 to 3 in placental tissues. The four diet-groups were compared for ZIKV replication considering the content of ZIKV genome copies in each placenta collected. Fig 11 showed that placental tissues reached high ZIKV values that mostly ranged from  $10^4$  to  $10^7$  genome copies/ $\mu$ l irrespective of diet administered, reporting similar means of ZIKV genome copies in positive placentas among diet groups: Diet 1 group  $2.79 \times 10^5$ , Diet 2 group  $4.89 \times 10^5$ , Diet 3 group  $3.66 \times 10^5$ , Diet 4 group  $3 \times 10^5$ . Nevertheless, the diet groups significantly differed in the ZIKV infection rate, showing that the four tested diets were associated with a different risk of placental infection. The number of ZIKV-positive and ZIKV-negative placentas with the relative percentages were reported by considering as positivity threshold both genome copies LoD (Tab. 1) and infectivity cut-off (Tab. 2). Specifically, Diet 1, Diet 2 and Diet 3 were associated with a higher risk of placental infection, compared to diet Diet 4 (complete statistical analysis was reported in the supplementary contents). These results indicated that a diet characterized by a low percentage of fats and highly rich in unsaturated fatty acids offered higher levels of protection against ZIKV infection, compared with fatter diets with higher concentrations of saturated fats. No significant differences were observed among Diet 1, Diet 2 and Diet 3 comparisons. This can be interpreted as the fact that diets containing higher levels of fats (regardless of the fatty-acids composition) and lower-fat



diets characterized by higher percentages of saturated fats similarly affected the placental risk of infection. To evaluate the impact of dietary intake on ZIKV vertical transmission, we assessed the presence of ZIKV envelope antigen in all fetal heads by IHC assay. No ZIKV-positive cells were found in head tissues.

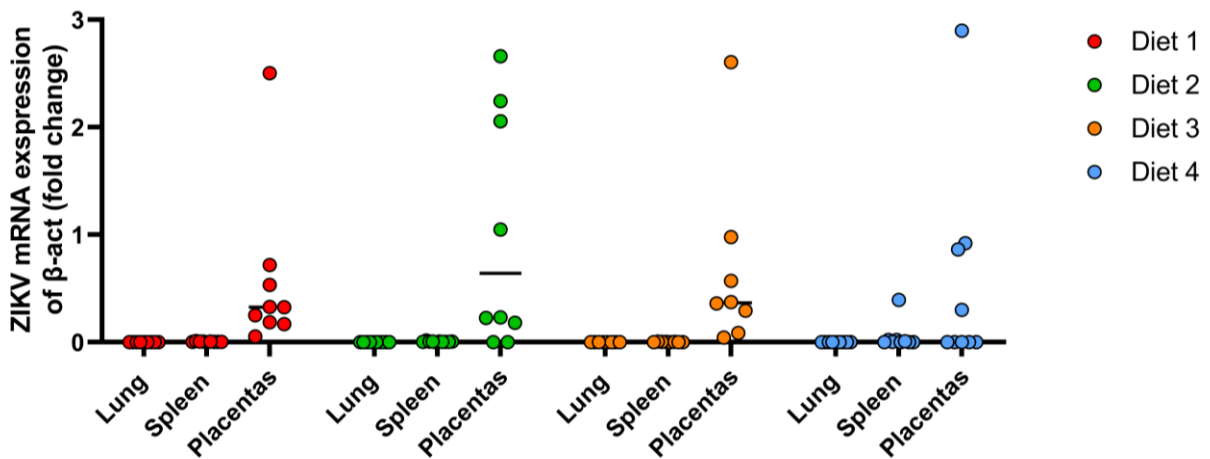


**Fig.10 ZIKV mRNA in infected-mouse organs.** ZIKV mRNA levels was reported as expression of  $\beta$ -actin gene in lung, spleen and placenta tissues. Placental value was reported as ZIKV mRNA expression mean of all placentas collected from each pregnant mouse.

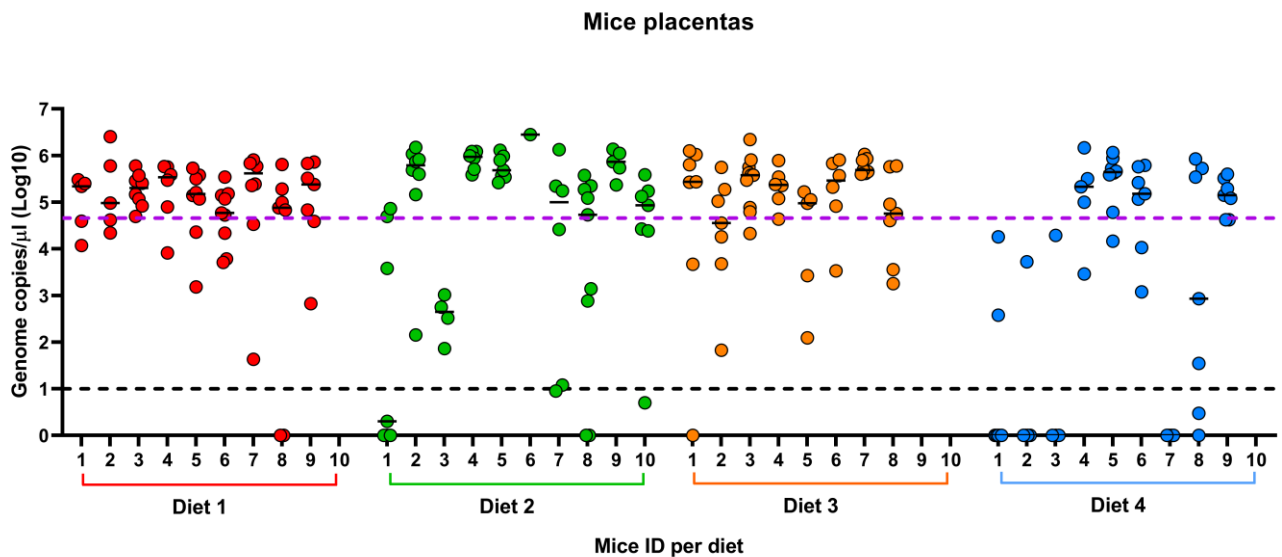


**Fig.11 ZIKV genome copies in placentas.** ZIKV genome copies in placentas of mice fed with the four experimental diets expressed as genome copies/ $\mu$ l. The numbers (ranged from 1 to 10) indicate the mouse ID for each diet (n=9 mice in Diet 1, n=10 mice in Diet 2, n=8 mice in Diet 3, n=9 mice in Diet 4). For each mouse, the plotted points represent its placentas. The black dashed-line indicate the qRT-PCR limited of detection and quantification (LoD and LoQ=10 genome copies). The purple dashed-line indicates the threshold of 45900 above which ZIKV detected in organs could be considered infective by FFU assay.

Placental positivity for genome copies content (LoD >10 genomes copies/ $\mu$ l)			
	Positive (%)	Negative (%)	Total

<b>Diet 1</b>	61 (96,8%)	2,0 (3,2%)	63
<b>Diet 2</b>	52 (86,7%)	8,0(13,3%)	60
<b>Diet 3</b>	54 (98,2%)	1 (1,8%)	55
<b>Diet 4</b>	36 (63,2%)	21 (36,8%)	57

**Tab. 1 ZIKV genome positivity rate in placentas of mouse groups fed with the four experimental diets.**

	<b>Placental positivity for viral infectivity (cut-off &gt;45900 genomes copies/μl)</b>		
	<b>Positive (%)</b>	<b>Negative (%)</b>	<b>Total</b>
<b>Diet 1</b>	47 (74,6%)	16 (25,4%)	63
<b>Diet 2</b>	40 (66,7%)	20 (33,3%)	60
<b>Diet 3</b>	41 (74,5%)	14 (25,5%)	55
<b>Diet 4</b>	24 (42,1%)	33 (57,9%)	57

**Tab. 2 ZIKV infective positivity rate in placentas of mouse groups fed with the four experimental diets.**

### **3.3.5 Correlation between placental lipids and ZIKV infection**

We determined that animals fed with Diet 4 displayed a significant higher protection to ZIKV infection compared to pregnant mice in Diet 1, 2, and 3-group. The correlation between placental lipids and ZIKV susceptibility was investigated by univariate and multivariate analyses. The univariate analysis performed an ordinal logistic regression among 180 independent lipid features and ZIKV placental susceptibility considering placenta tissues belonging to Diet 1 and 3 group highly susceptible, Diet 2 group moderately susceptible and Diet 4 lowly susceptible. The results were filtered with a false discovery rate method (FDR=0.15). Moreover, the entire lipidome of each single placental sample was correlated to the susceptibility to ZIKV using a PLS ordinal regression. Both statistical analyses identified 72 lipids, grouped in two main clusters which significantly affected ZIKV susceptibility (Fig. 12). The first cluster was characterized by the phosphatidylserines (PS), whereas, the second cluster was constituted by phosphatidylcholines (PC), Phosphatidylethanolamines (PE), sphingomyelins (SM) and phosphatidylinositol (PI). Importantly, in the placentas of animals fed with Diet 4, which resulted less susceptible to ZIKV infection, there was a higher expression of PS and a low expression of lipids belonging to the second cluster. On the contrary, in placental tissues

of Diet 1 and 3, it was observed a high expression of PC, PE, SM and PI and a low presence of PS. The lipid expression in placentas of animals fed with Diet 2 was in-between among Diet 1, 3 and diet 4 lipid expression.

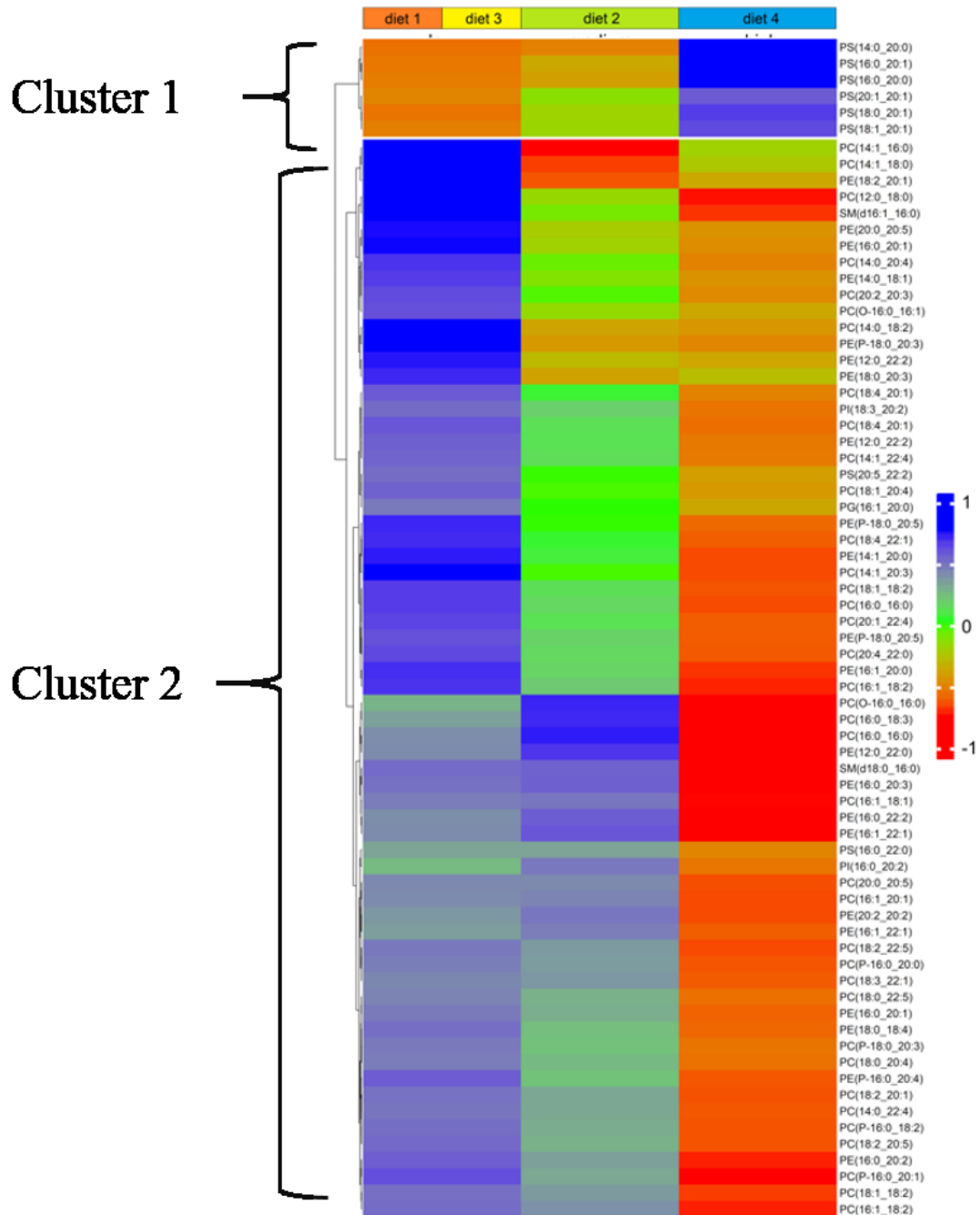


**Fig.12 Placental lipids correlated with ZIKV tissue susceptibility.** The heat maps showed the 72 lipids features (on the right) of four diet-groups' placentas (above) identified as significantly correlated to ZIKV tissue susceptibility by the univariate and multivariate analyses. The expression of a single lipid class ranged from a low expression (in red) to a high expression (in blue). The clusters grouped lipids for the expression behaviour in the different four diet-groups.

### 3.3.6 ZIKV vertical transmission

We evaluated ZIKV vertical transmission by performing IHC assays on fetal head tissue after formalin fixation. Moreover, we measured the size of fetuses to determine a decrease in head circumference and an overall impairment of fetal development. The IHC did not reveal any ZIKV antigen in the neuronal cells of fetuses' heads, although we selected fetuses enveloped by highly ZIKV-positive placental tissue. Moreover, comparing the body size of fetuses collected by mothers fed with the four experimental diets, no significant difference was detected (Fig. 13A). Finally, the number of fetuses and miscarriages was comparable among the four experimental groups, suggesting that dietary lipids did not influence ZIKV vertical transmission in this model (Fig. 13B-C).

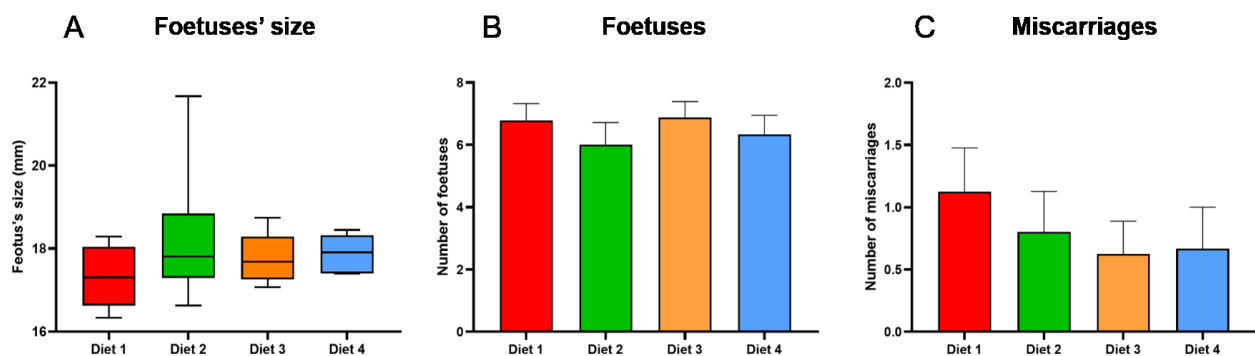


**Fig. 13 ZIKV vertical transmission data per diet. A) Mean fetuses size recorded per mouse per diet. B) Mean fetuses recorded per mouse per diet. C) Mean miscarriages per mouse per diet. Data were compared among diet groups by non-parametric Kruskal Wallis with Dunn's multiple comparison post-test. P values less than 0.05 were considered significant**

## 3.4 Discussions

The current work aimed to study the role of dietary lipids in ZIKV pathogenesis in fully-developed placental tissues. Several studies have demonstrated the fundamental role of nutrition in arbovirus disease (16). For example, critical condition's states, such as undernutrition, obesity, and micronutrient deficiencies were proved to negatively impact the immune function, consequently hindering the host defenses against viral infection (17). Moreover, it was reported that some food could alter individual body odors associated with

mosquitoes' attraction, increasing the host exposition to the viral vectors (18). A relevant study performed by Barbeito-Andrés et al. described the impact of mother undernutrition on the CZS, highlighting the importance of pregnant women's diet in determining ZIKV pathogenesis (19). Specifically, the authors suggested that maternal protein undernutrition could have compromised several innate and adaptive pathways of the immune system, increasing fetal microcephaly rate in ZIKV-infected mothers. Among dietary nutrients, in our previous work (Chapter 2), we demonstrated that lipids of viral and host membranes could affect ZIKV infectivity at the level of full-term placental tissue. Since viral envelope lipids derived from host cells membranes, such as villous trophoblasts, we decided to focus our attention on the role of placental cell lipids as ZIKV pathogenesis's determinants. In placental tissues, following proteins, lipids are most present nutrients and they are prevalently composed by 70.7% phospholipids, 12.2% sterols, 5.5 triglycerides and 2.9 % sterol esters (20,21). The analysis on fatty acids (FA) composition of placental phospholipids and triglycerides revealed a high content of palmitic (16:0) and arachidonic (20:4n-6) FA, followed by the stearic (18:0), oleic (18:1n-9), linoleic (18:2n-6) and docosahexaenoic (DHA) (22:6n-3) FA (10). However, this composition can fluctuate depending on pregnant women's FA daily intake. For example, it has been reported that the diet of Spanish women, which is characterized by a high intake of marine fish and olive oil, resulted in placental higher contents of oleic, eicosapentaenoic (EPA) and DHA acid, comparing to the FA in placental tissues of English and German women (10,22). Trying to identify the lipid content of pregnant women's diet worldwide, we synthesized the main human dietary patterns as follows: i) high total dietary lipids and high intake of saturated animal lipids typical of most countries in Europe, North America and Oceania; ii) high total dietary lipids with a low intake of animal lipids, which are characteristic of Mediterranean countries; iii) moderate total dietary lipids with a low to moderate animal lipids content, representative of intake in Near East and South America, iv) low total

dietary lipids intake and low levels of animal lipids, typical of countries in Africa and Far East (11). These patterns were simplified and mouse-adapted in order to obtain four diets easily comparable in terms of lipids quantity and quality. The resulting diets were reported as “Western diet or Diet 1” and “Mediterranean diet or Diet 2” with a high content of lipids and as “Asian diet or Diet 3” and “African diets or Diet 4” with a low lipid content. Moreover, the Western and Asian Diets lipids were predominantly characterized by SFA; on the contrary, Mediterranean and African diets displayed a higher percentage of UFA/PUFA. In tailoring these four diet patterns to mouse nutrition, we set the lipid content in a healthy range to avoid status of undernutrition or obesity, since they not only can predispose to higher severity of infectious disease, but they can also compromise the course of the gestation (23). Analyzing the parameters associated with diets’ consumption, we observed that the four experimental diets were comparable in terms of daily intake and, weight gain before and during the gestational period. Moreover, the sera and liver profiles of all diet group fell in the physiological range reported for pregnant mice (24). Only the total serum cholesterol and HDL were significantly higher in Diet 1 respect to Diet 4, however, it was expected since the two diets were opposite for SFA content (25). We also investigated hormone levels associated with high-fat intake and pregnancy, such as insulin, IL-6, and leptin hormone. The levels of leptin and insulin did not differ among diet-groups, whereas, IL-6 was not detected suggesting the lack of an inflammatory status (26). Interestingly, the experimental diet’s did not affect number of fetuses or miscarriages, even if, according to Akerele et al , the reabsorption events seemed less numerous in diets with a low fat content (27). Although the experimental diets determined similar biochemical and hormonal conditions in the four mouse groups, their impact on placental lipid composition was significant: through the lipidomic analysis conducted on the placental tissues of pregnant mice fed with the experimental diets, we proved that both quantity and quality of dietary lipids could affect the placental lipidome. Once we ensured

four different placental environments in terms of lipids, we infected the four diet groups of pregnant mice, using high viral dose of an Asian ZIKV strain, via intraperitoneal route at 12 E. In this way, we simulated ZIKV infection in healthy and immunocompetent women at the late stages of pregnancy. Firstly, the comparison of ratios between ZIKV genome and the internal  $\beta$ -actin gene expression in the organs collected confirmed the placenta as the main ZIKV tissue target, indicating that the applied *in-vivo* model well-represented ZIKV pathogenesis in pregnant women (28). Moreover, we demonstrated that ZIKV infectivity significantly differed among diet-groups: female mice fed with high content of SFA (Diet 1 and 3) reported significantly higher ZIKV infection rates compared to animals fed with a low fat content mostly characterized by PUFA (Diet 4). Interestingly, the ZIKV infectivity rate in mice fed with Diet 2, composed by high quantity of PUFA, was statistically comparable to the infection rate of animals' placentas in Diet 1 and 3 groups; however, the placental tissues of Diet 2 group seemed more resistant to the ZIKV replication, suggesting an overall positive influence of dietary PUFA. Successively, we interpolated the virological data with the placental lipidome profiles to identify the lipids that have affected the susceptibility of placental tissues to the ZIKV infection. Our data showed that placentas from animals fed with Diet 1 and 3 were characterized by a high expression of PC, PE, PI e SM; on the contrary, Diet 4's placentas resulted in an enrichment of PS lipid class. Consistently with the virological results, the lipid profile of placental tissues in Diet 2-group was in between those of Diets 1-3 and Diet 4. Our finding supported the evidence that the administration of a diet constituted by a low content of lipids with a predominant component of PUFA, can confer to the placental tissue a significant resistance to ZIKV infection. Specifically, this placental protection seemed to be ensured by the high expression of PS and a lower expression of other lipid classes. In this study, no vertical transmission was detected irrespective of the viral load of infected placental tissues. However, the absence of vertical transmission could be a limitation of the *in-vivo* model

used for this experiment. In immunocompetent mice, ZIKV NS5 is unable to bind the activator of transcription 2 (STAT2) and the resulting lack of inhibition of IFN responses could have determined an efficient control of viral replication and lack of overt disease (28). Moreover, in the mouse placenta, the fetal blood circulation is separated from the mother's circulation by three layers of trophoblasts compared to the single-layered syncytiotrophoblast in humans resulting in a more complex barrier to cross for ZIKV (29).

For the first time, our study showed the impact of different dietary patterns on placental lipid composition by means of *in-vivo* study. The experimental diets formulated in this experiment were similar in caloric intake and protein content, whereas differed in lipid quantity and quality suggesting these nutrients as the main responsible of lipids expression at the level of placental tissues. However, we considered that lipids do not derive exclusively from dietary fats, but they can also be physiologically supplied by conversion of carbohydrates. To limit the impact of carbohydrates in lipid metabolism of our mouse model, we ensured the same sugars sources in all diets and we did not vary the carbohydrates content in diets with the same caloric percentage of fat. Moreover, our work is one of the few that investigated the effect of healthy diets on pregnant women metabolism, respecting the recommended mice nutritional standards to avoid any metabolic syndrome (exceeding the limit of 25% of calories derived from fat meant mouse over-nutrition) (23). In fact, each diet administrated determined a specific lipid composition of placental tissues guaranteeing biochemical, hormonal and liver parameters within the physiological ranges for this species. This enforced the virological findings, highlighting how minimal changes in maternal dietary intake could affect placental susceptibility to ZIKV infection during pregnancy. Looking closer at ZIKV pathogenesis in this model, we observed that the difference among infected groups relied on ZIKV placental infectivity rate rather than on the viral replicative capacity in this tissue. This feature was already observed in our previous study (Chapter 2), where the structural lipids of viral and host

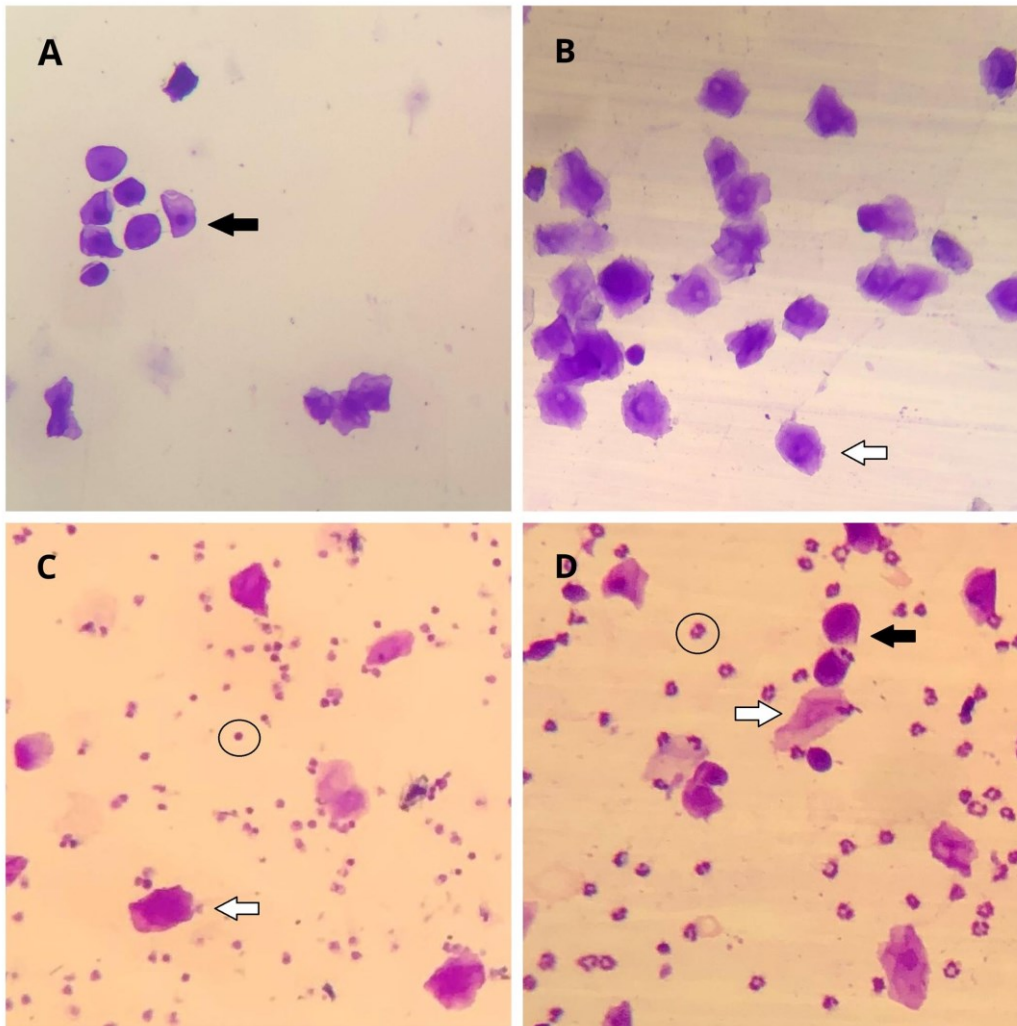


membranes affected ZIKV infectivity in the first stages of viral replicative cycle, leading to an efficient or abortive host-cell infection. Conversely, when ZIKV manages to infect the host cells, starting its replicative cycle, it modulates host lipid metabolism to promote viral replication and new progeny assembly. This evidence was supported also by the present work, in which, we showed that mouse placentas positive for ZIKV displayed the same viral titers in all four diet-groups. This finding confirmed the importance of cell lipids in determining ZIKV infectivity, and it demonstrated that once ZIKV overcomes host defenses the viral replicative capacity is maintained among tissues irrespective of lipid composition. In particular, the mouse group with placentas enriched with PS displayed significant resistance to ZIKV infection, reporting fewer ZIKV positive organs compared to other groups having placentas with a low expression of this lipid class. On the contrary, the placental tissues with cells enriched of PC lipids reported the highest rate of ZIKV infection. We hypothesized that the right balance between these lipid classes in host cell membranes can affect several factors involving ZIKV pathogenesis such as membranes curvatures, permeability and receptor protein arrangement (30). Moreover, PS is key to the recruitment and activation of numerous enzymes and structural components, and they signal important events such as the clearance of apoptotic cells, which is often mimicked by flaviviruses to begin the internalization into the host cells (8). Besides the lipid composition of placentas, in this study we neglected the role of dietary lipids, such as cholesterol, in modulating pregnant female's hormones (31). However, this aspect should be further investigated as well, since it has been demonstrated that ZIKV infection can be affected by the level of steroid hormones (32,33).

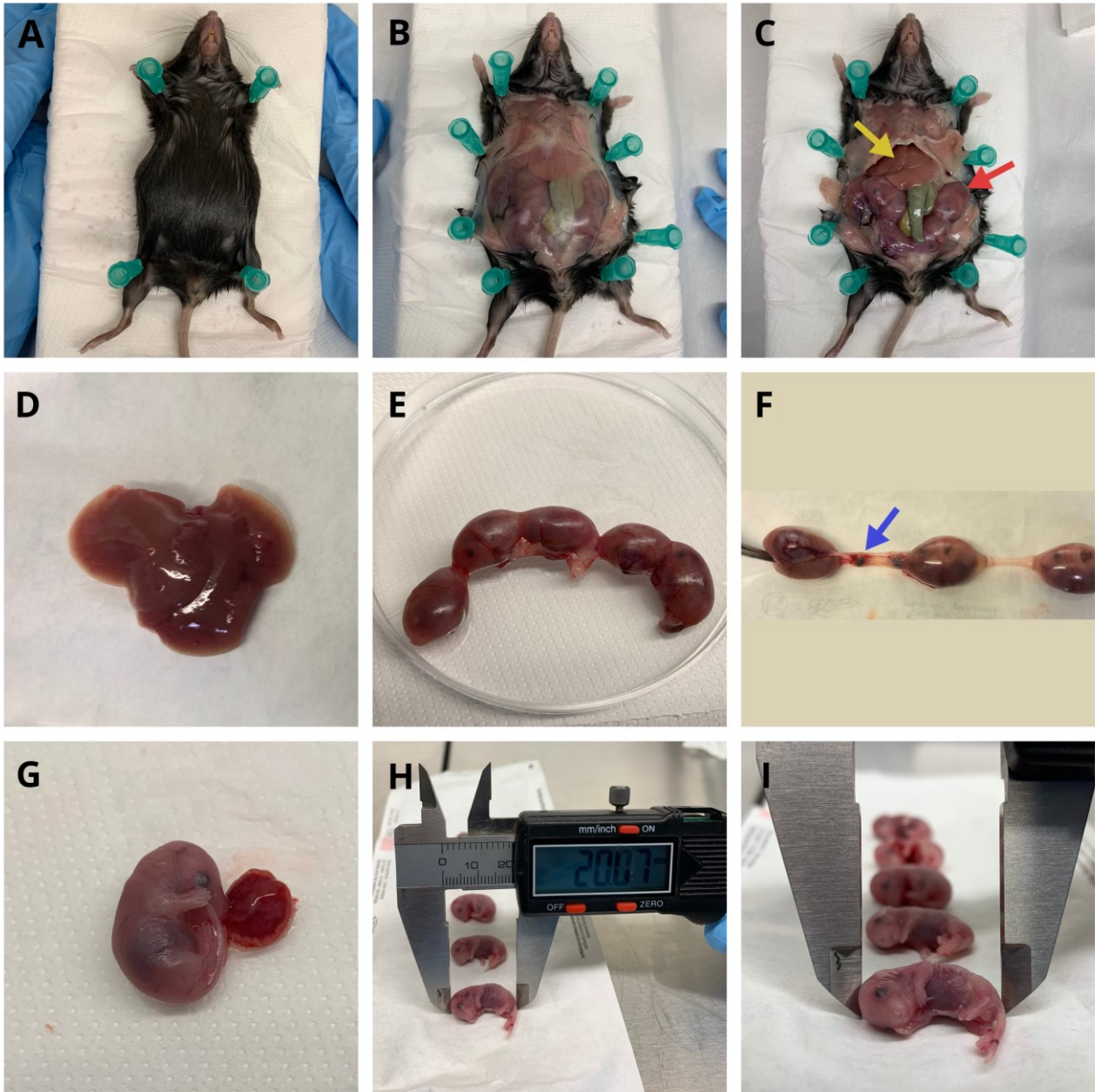
In conclusion, in the first part of this experiment, we revealed how minimal changes in the dietary pattern during pregnancy can affect placental lipidome. Besides the implication of these changes on ZIKV pathogenesis, it would be interesting to understand how the

correlation between diet and placental lipids could influence other aspects of fetal development and maternal health condition. For example, completing the lipidomic results with other omics data, such as transcriptomic and metabolic analysis, could allow to have the full picture of the dietary impact on the placenta's functions. Furthermore, for the first time, we established the role of dietary lipids as determinants of ZIKV infection in the fully-developed placenta, defining an unknown ZIKV pathogenesis feature in women at the late stages of pregnancy. The effect of diet on infectious disease has been often neglected and the correlation between lipidomic and flavivirology has been investigated only in recent years. For this reason, our study could be considered pioneering in this field. However, our findings need to be completed by further studies on the underlying mechanism by which placental lipids affected ZIKV infection. This information would allow the development of an effective approach to fight this virus, giving the unprecedented possibility to use the maternal diet as a new safe prophylactic tool to tackle ZIKV infection, and other similar pathogens, in pregnant women.

### 3.5 Supplementary contents



**S1\_Fig. Vaginal cytology representing each stage of the estrous cycle.** Three main cell types are detected: nucleated epithelial (black arrow), cornified squamous epithelial (white arrow), and leukocytes (circle). The ratio of these cell types present in the vaginal lavage can be used to identify the stage of the estrous cycle. Four stages are identified: Proestrus (A), Estrus (B), Metestrus (C), Diestrus (D).



**S2\_Fig. Necropsy of pregnant mouse for organ collection.** A) Euthanized mouse lies in dorsal recumbence with all limbs pinned down with a needle. Fur is dampened with alcohol solution B) Skin is incised the full length of the ventrum to expose abdominal wall C) Opening of the abdominal wall to expose abdominal viscera. Localization of liver (yellow arrow) and gravid uterus (red arrow) for organ collection D) Liver is removed in its entirety. Texture and color are assessed E) Gravid uterus is removed and positioned on a sterile petri dish. Fetuses are numbered from left to right F) Gravid uterus is pulled by the left and right ovaries with sterile forceps to expose the presence of any miscarriages (blue arrow). Number and position of miscarriages is recorded G) Each fetus is freed from the uterus and separated from its placenta for individual collection H) Each fetus is measured from crown to rump with a caliper.

	Diets							
	Diet 1		Diet 2		Diet 3		Diet 4	
	High Fat		High Fat		Low Fat		Low Fat	
	Sat : Unsat 3 to 1		Sat : Unsat 1 to 1		Sat : Unsat 3 to 1		Sat : Unsat 1 to 1	
	gm%	kcal%	gm%	kcal%	gm%	kcal%	gm%	kcal%
Protein	19,4	20	19,4	20	18,4	20	18,4	20
Carbohydrate	60,2	60	60,2	60	66,4	70	66,4	70
Fat	8,7	20	8,7	20	4,1	10	4,1	10
Total		100		100		100		100
kcal/gm	3,91		3,91		3,71		3,71	
<b>Ingredient</b>	<b>gm</b>	<b>kcal</b>	<b>gm</b>	<b>kcal</b>	<b>gm</b>	<b>kcal</b>	<b>gm</b>	<b>kcal</b>
Casein	200	800	200	800	200	800	200	800
L-Cystine	3	12	3	12	3	12	3	12
<b>Corn Starch</b>	<b>333,8</b>	<b>1335,2</b>	<b>333,8</b>	<b>1335,2</b>	<b>436,2</b>	<b>1744,8</b>	<b>436,2</b>	<b>1744,8</b>
Maltodextrin 10	110	440	110	440	110	440	110	440
Dextrose	150	600	150	600	150	600	150	600
Cellulose, BW200	75	0	75	0	75	0	75	0
Inulin	25	37,5	25	37,5	25	37,5	25	37,5
<b>Soybean Oil</b>	<b>5</b>	<b>45</b>	<b>10</b>	<b>90</b>	<b>2,5</b>	<b>23</b>	<b>5</b>	<b>45</b>
<b>Butter, Anhydrous</b>	<b>9</b>	<b>81</b>	<b>13,5</b>	<b>121,5</b>	<b>4,5</b>	<b>41</b>	<b>6,8</b>	<b>61</b>
<b>Coconut Oil, Hydrogenated</b>	<b>57</b>	<b>513</b>	<b>0</b>	<b>0</b>	<b>28,5</b>	<b>257</b>	<b>0</b>	<b>0</b>
<b>Corn Oil</b>	<b>9,5</b>	<b>85,5</b>	<b>17,5</b>	<b>157,5</b>	<b>4,7</b>	<b>42</b>	<b>8,7</b>	<b>78</b>
<b>Lard</b>	<b>9,5</b>	<b>85,5</b>	<b>7,5</b>	<b>67,5</b>	<b>4,8</b>	<b>43</b>	<b>3,8</b>	<b>34</b>
<b>Menhaden Oil (200 ppm tBHQ)</b>	<b>1</b>	<b>9</b>	<b>2,5</b>	<b>22,5</b>	<b>0,5</b>	<b>5</b>	<b>1,2</b>	<b>11</b>
<b>Olive Oil</b>	<b>0</b>	<b>0</b>	<b>40</b>	<b>360</b>	<b>0</b>	<b>0</b>	<b>20</b>	<b>180</b>
Mineral Mix S10026	10	0	10	0	10	0	10	0
Dicalcium Phosphate	13	0	13	0	13	0	13	0
Calcium Carbonate	5,5	0	5,5	0	5,5	0	5,5	0
Potassium Citrate, 1 H2O	16,5	0	16,5	0	16,5	0	16,5	0
Vitamin Mix V10001	10	40	10	40	10	40	10	40
Choline Bitartrate	2	0	2	0	2	0	2	0
Yellow Dye #5, FD&C	0	0	0	0	0,025	0	0,05	0
Red Dye #40, FD&C	0,05	0	0	0	0,025	0	0	0
Blue Dye #1, FD&C	0	0	0,05	0	0	0	0	0
<b>Total</b>	<b>1044,85</b>	<b>4084</b>	<b>1044,85</b>	<b>4084</b>	<b>1101,75</b>	<b>4084</b>	<b>1101,75</b>	<b>4084</b>
<b>Cholesterol (g)</b>	<b>0,08</b>		<b>0,10</b>		<b>0,06</b>		<b>0,07</b>	
<b>Cholesterol (%)</b>	<b>0,007</b>		<b>0,009</b>		<b>0,005</b>		<b>0,006</b>	
<b>tBHQ (mg)</b>	<b>0,2</b>		<b>0,5</b>		<b>0,1</b>		<b>0,24</b>	

S1\_Tab Experimental diets content.

	Diets			
	Diet 1	Diet 2	Diet 3	Diet 4
	High Fat	High Fat	LowFat	LowFat
	Sat : Unsat 3 to 1	Sat : Unsat 1 to 3	Sat : Unsat 3 to 1	Sat : Unsat 1 to 3
Ingredient	gm	gm	gm	gm
Butter, Anhydrous	9	13,5	4,5	6,8
Canola Oil (Rapeseed Oil)				
Cocoa Butter, Deodorized				
Coconut Oil, 101	57		28,5	
Com Oil	9,5	17,5	4,7	8,7
Flaxseed Oil				
Lard	9,5	7,5	4,8	3,8
Menhaden Oil, ARBP-F	1	2,5	0,5	1,2
Olive Oil		40		20
Palm Oil, RBD				
Soybean Oil	5	10	2,5	5
<b>Total</b>	<b>91,0</b>	<b>91,0</b>	<b>45,5</b>	<b>45,5</b>
C2, Acetic	0,0	0,0	0,0	0,0
C4, Butyric	0,3	0,4	0,1	0,2
C6, Caproic	0,5	0,3	0,3	0,1
C8, Caprylic	4,5	0,1	2,2	0,1
C10, Capric	3,6	0,3	1,8	0,2
C12, Lauric	27,4	0,4	13,7	0,2
C14, Myristic	11,3	1,6	5,7	0,8
C14:1, Myristoleic, n-9	0,1	0,2	0,1	0,1
C15	0,0	0,0	0,0	0,0
C16, Palmitic	10,9	12,9	5,4	6,5
C16:1, Palmitoleic, n-9	0,4	1,1	0,2	0,6
C16:2, n-4	0,0	0,0	0,0	0,0
C16:3, n-9	0,0	0,0	0,0	0,0
C16:4, n-4	0,0	0,0	0,0	0,0
C17	0,0	0,0	0,0	0,0
C17:1	0,0	0,0	0,0	0,0
C18, Stearic	8,5	4,1	4,3	2,1
C18:1, Oleic, n-9	9,4	41,0	4,7	20,5
C18:1, Elaidic, Trans	0,0	0,0	0,0	0,0
C18:1n7C, Vaccenic	0,0	0,0	0,0	0,0
C18:2, Linoleic	10,9	23,1	5,4	11,5
C18:2, Trans	0,0	0,0	0,0	0,0
C18:3, Linolenic	0,8	1,6	0,4	0,8
C18:3, n-6	0,0	0,0	0,0	0,0
C18:3, Trans	0,0	0,0	0,0	0,0
C18:4, Stearidonic	0,0	0,1	0,0	0,0
C19, Nonadecanoic	0,0	0,0	0,0	0,0
C20, Arachidic	0,1	0,3	0,1	0,2
C20:1	0,1	0,2	0,0	0,1
C20:2	0,1	0,1	0,0	0,0
C20:3, n-6	0,0	0,0	0,0	0,0
C20:3, n-3	0,0	0,0	0,0	0,0
C20:4, Arachidonic, n-6	0,048	0,074	0,024	0,036
C20:4, n-3	0,0	0,0	0,0	0,0
C20:5,	0,14	0,36	0,07	0,17
Eicosapentaenoic, n-3				
C21, Heneicosanoic	0,0	0,0	0,0	0,0
C21:5, n-3	0,0	0,0	0,0	0,0
C22, Behenic	0,0	0,0	0,0	0,0
C22:1, Erucic	0,0	0,0	0,0	0,0
C22:4, Clupanodonic, n-6	0,002	0,005	0,001	0,002
C22:5,	0,036	0,076	0,018	0,037
Docosapentaenoic, n-3				
C22:6,	0,103	0,257	0,051	0,123
Docosahexaenoic, n-3				
C24, Lignoceric	0,0	0,0	0,0	0,0
C24:1	0,0	0,0	0,0	0,0
<b>Total</b>	<b>89,5</b>	<b>88,9</b>	<b>44,7</b>	<b>44,4</b>
Saturated (g)	67,2	20,7	33,6	10,4
Monounsaturated (g)	10,1	42,5	5,1	21,3
Polyunsaturated (g)	12,1	25,7	6,1	12,8
Unsaturated (g)	22,3	68,2	11,1	34,1
Saturated (%)	75,1	23,3	75,2	23,3
Monounsaturated (%)	11,3	47,8	11,3	47,8
Polyunsaturated (%)	13,6	28,9	13,5	28,8
<b>Saturated:Unsaturated ratio</b>	<b>3,02</b>	<b>0,30</b>	<b>3,02</b>	<b>0,30</b>
n6 (g)	10,9	23,2	5,4	11,6
n3 (g)	1,1	2,3	0,5	1,1
<b>n6:n3 ratio</b>	<b>10,1</b>	<b>10,0</b>	<b>10,1</b>	<b>10,1</b>

## S2\_Tab Experimental diets fatty acids content.

### qRT-PCR

Amplification reaction were assembled with the AgPath-ID One-Step RT-PCR Reagents (Applied Biosystems), oligonucleotides according to Table S1, 5 µl template and molecular-grade water up to 25 µl. Thermal cycling was carried out on a CFX96 Touch Deep Well Real-time PCR Detection System (Biorad) following the specifications reported in S3\_Tab.

Assay	Oligonucleotide 5' □ 3'	Final conc.	Ref.	Thermal profile
ZIKV	ZIKV 1086: CCGCTGCCCAACACAAG	600 nM	Lanciotti	45°C for 10 min 95°C for 10 min 45 cycles: 95°C for 15 sec 55°C for 45 sec
	ZIKV 1162c: CCACTAACGTTCTTTTGCAGACAT			
	ZIKV 1107: FAM-AGCCTACCTTGACAAGCAGTCAGACACTCAA-BHQ1	400 nM		
β-actin	β-Actin_mouse_F: CCATGAAGATCAAGATCATTGC	400 nM	This study	50°C for 30 min 95°C for 10 min 45 cycles: 95°C for 15 sec 56°C for 30 sec
	β-Actin_mouse_R: AAGCACTTGCGGTGCAC			
	β-Actin Probe: FAM-TCCACCTTCCAGCAGATGTGGATCA-BHQ1	200 nM	Gigante	

**S3\_Tab. Oligonucleotides and amplification protocols of ZIKV and β-actin qRT-PCR assays.**

### Statistical analysis on ZIKV positivity rate in placentas of mice fed with the four experimental diets

No significant differences in the infection susceptibility were found among the 36 animals included in the study (data not shown), indicating that no random effect was required in the subsequent analysis to group the placentas belonging to the same individuals. S4 and S5 Tab. report the logistic regression coefficients in the log odds form and their 95% CIs. The four tested diets were associated with a different risk of placental infection. In general, a significantly lower risk was associated with diet D4 with respect to the reference level, i.e. diet D1, in both models (modelgc: Coef.=-2.879, S.E.=0.769, P<0.001; modelpfu: Coef.=-1.396, S.E.=0.395, P<0.001). To better evaluate the significant differences between the diets, pairwise contrasts were computed to obtain the odds ratios (S6 and S7 Tab). Three of the six pairwise comparisons of the tested diets showed statistically

significant differences: D1 vs D4, D2 vs D4 and D3 vs D4. Specifically, diets D1, D2 and D3 were associated with a higher risk of placental infection, compared to diet D4, and the results are consistent in both models (modelgc: ratioD1 vs D4=17.792, P=0.001; ratioD2 vs D4=3.792, P=0.023; ratioD3 vs D4=31.500, P=0.005; modelffu: ratioD1 vs D4=4.039, P=0.002; ratioD2 vs D4=2.750, P=0.041; ratioD3 vs D4=4.027, P=0.004).

	<b>Estimate</b>	<b>2.5%</b>	<b>97.5%</b>	<b>P</b>
Intercept (Diet1)	3.418	2.009	4.826	<0.0001
Diet 2	-1.546	-3.139	0.047	0.057
Diet 3	0.571	-1.857	2.999	0.645
Diet 4	-2.879	-4.386	-1.371	<0.001

**S4\_Tab ZIKV genome positivity (modelgc).** Coefficient estimates (logit form), 95% confidence intervals and statistical significance for the count of the genome copies. In red the significant p-value>0.05.

	<b>Estimate</b>	<b>2.5%</b>	<b>97.5%</b>	<b>P</b>
Intercept (Diet1)	1.078	0.510	1.645	<0.0001
Diet 2	-0.384	-1.165	0.397	0.335
Diet 3	-0.003	-0.834	0.828	0.994
Diet 4	-1.396	-2.170	-0.623	<0.001

**S5\_Tab ZIKV FFU infective positivity (modelffu).** Coefficient estimates (logit form), 95% confidence intervals and statistical significance for the count of the plaque forming units. In red the significant p-value>0.05.

<b>Contrasts</b>	<b>Odds ratio</b>	<b>S.E.</b>	<b>2.5%</b>	<b>97.5%</b>	<b>P</b>
D1 / D2	4.692	3.81	0.582	37.860	0.227
D1 / D3	0.565	0.70	0.023	13.620	0.968
D1 / D4	17.792	13.69	2.466	128.380	0.001
D2 / D3	0.120	0.13	0.008	1.920	0.202
D2 / D4	3.792	1.78	1.138	12.640	0.023
D3 / D4	31.500	32.94	2.145	462.500	0.005

**S6\_Tab ZIKV genome positivity (modelgc).** Contrasts between trapping device estimated marginal means after model fitting for the count of the genome copies, at a confidence level of 0.95; estimates are back-transformed from the log scale. D1, D2, D3 and D4 stood for Diet 1, Diet 2, Diet 3 and Diet 4. In red the significant p-value>0.05.

<b>Contrasts</b>	<b>Odds ratio</b>	<b>S.E.</b>	<b>2.5%</b>	<b>97.5%</b>	<b>P</b>
D1 / D2	1.469	0.585	0.528	4.090	0.770
D1 / D3	1.003	0.425	0.338	2.980	1.000
D1 / D4	4.039	1.594	1.465	11.130	0.002
D2 / D3	0.683	0.282	0.236	1.970	0.793
D2 / D4	2.750	1.054	1.027	7.360	0.041
D3 / D4	4.027	1.649	1.406	11.530	0.004

**S7\_Tab ZIKV FFU infective positivity (modelffu).** Contrasts between trapping device estimated marginal means after model fitting for the count of the plaque forming units at a confidence level of 0.95; estimates are back-transformed from the log scale. D1, D2, D3 and D4 stood for Diet 1, Diet 2, Diet 3 and Diet 4. In red the significant p-value>0.05.



## References

1. Musso D, Ko AI, Baud D. Zika Virus Infection — After the Pandemic. Longo DL, curatore. *N Engl J Med*. 10 ottobre 2019;381(15):1444–57.
2. Freitas DA, Souza-Santos R, Carvalho LMA, Barros WB, Neves LM, Brasil P, et al. Congenital Zika syndrome: A systematic review. Fujioka K, curatore. *PLOS ONE*. 15 dicembre 2020;15(12):e0242367.
3. Coyne CB, Lazear HM. Zika virus — reigniting the TORCH. *Nat Rev Microbiol*. novembre 2016;14(11):707–15.
4. Munjal A, Khandia R, Dhama K, Sachan S, Karthik K, Tiwari R, et al. Advances in Developing Therapies to Combat Zika Virus: Current Knowledge and Future Perspectives. *Front Microbiol*. 3 agosto 2017;8:1469.
5. Villalobos-Sánchez E, Burciaga-Flores M, Zapata-Cuellar L, Camacho-Villegas TA, Elizondo-Quiroga DE. Possible Routes for Zika Virus Vertical Transmission in Human Placenta: A Comprehensive Review. *Viral Immunol*. 1 luglio 2022;35(6):392–403.
6. Ades AE, Soriano-Arandes A, Alarcon A, Bonfante F, Thorne C, Peckham CS, et al. Vertical transmission of Zika virus and its outcomes: a Bayesian synthesis of prospective studies. *Lancet Infect Dis*. 2021;21(4):537–45.
7. Brasil P, Vasconcelos Z, Kerin T, Gabaglia CR, Ribeiro IP, Bonaldo MC, et al. Zika virus vertical transmission in children with confirmed antenatal exposure. *Nat Commun*. dicembre 2020;11(1):3510.
8. Martín-Acebes MA, Vázquez-Calvo Á, Saiz JC. Lipids and flaviviruses, present and future perspectives for the control of dengue, Zika, and West Nile viruses. *Prog Lipid Res*. 2016;64:123–37.
9. Cora MC, Kooistra L, Travlos G. Vaginal Cytology of the Laboratory Rat and Mouse: Review and Criteria for the Staging of the Estrous Cycle Using Stained Vaginal Smears. *Toxicol Pathol*. agosto 2015;43(6):776–93.
10. Klingler M, Demmelmair H, Larque E, Koletzko B. Analysis of FA contents in individual lipid fractions from human placental tissue. *Lipids*. maggio 2003;38(5):561–6.
11. Trichopoulou A, Lagiou P. Worldwide patterns of dietary lipids intake and health implications. *Am J Clin Nutr*. 1 ottobre 1997;66(4):961S-964S.
12. Matrosovich M, Matrosovich T, Garten W, Klenk D. New low-viscosity overlay medium for viral plaque assays. 2006;7:1–7.
13. Lanciotti RS, Kosoy OL, Laven JJ, Velez JO, Lambert AJ, Johnson AJ, et al. Genetic and Serologic Properties of Zika Virus Associated with an Epidemic, Yap State, Micronesia, 2007. *Emerg Infect Dis*. agosto 2008;14(8):1232–9.

14. Gigante CM, Dettinger L, Powell JW, Seiders M, Condori REC, Griesser R, et al. Multi-site evaluation of the LN34 pan-lyssavirus real-time RT-PCR assay for post-mortem rabies diagnostics. *Kalendar R, curatore. PLOS ONE.* 16 maggio 2018;13(5):e0197074.
15. Haese N, Hirsch AJ, Streblow DN. Isolation and Detection of Zika Virus-Infected Rhesus Macaques Lymph Node Cells and Splenocytes. In: Kobinger G, Racine T, curatori. *Zika Virus [Internet].* New York, NY: Springer US; 2020 [citato 19 settembre 2022]. pag. 197–213. (Methods in Molecular Biology; vol. 2142). Disponibile su: [http://link.springer.com/10.1007/978-1-0716-0581-3\\_16](http://link.springer.com/10.1007/978-1-0716-0581-3_16)
16. Weger-Lucarelli J, Auerswald H, Vignuzzi M, Dussart P, Karlsson EA. Taking a bite out of nutrition and arbovirus infection. *PLoS Negl Trop Dis.* 2018;12(3):1–25.
17. Farhadi S, Ovchinnikov R. The relationship between nutrition and infectious diseases: A review. *Biomed Biotechnol Res J BBRJ.* 2018;2(3):168.
18. Havlicek J, Lenochova P. Environmental Effects on Human Body Odour. In: Hurst JL, Beynon RJ, Roberts SC, Wyatt TD, curatori. *Chemical Signals in Vertebrates 11 [Internet].* New York, NY: Springer New York; 2008 [citato 19 settembre 2022]. pag. 199–210. Disponibile su: [http://link.springer.com/10.1007/978-0-387-73945-8\\_19](http://link.springer.com/10.1007/978-0-387-73945-8_19)
19. Barbeito-Andrés J, Pezzuto P, Higa LM, Dias AA, Vasconcelos JM, Santos TMP, et al. Congenital Zika syndrome is associated with maternal protein malnutrition. *Sci Adv.* 10 gennaio 2020;6(2).
20. Roux JF, Takeda Y, Grigorian A. Lipid concentration and composition in human fetal tissue during development. *Pediatrics.* ottobre 1971;48(4):540–6.
21. Chang S, Lodico L, Williams Z. Nutritional composition and heavy metal content of the human placenta. *Placenta.* dicembre 2017;60:100–2.
22. Lakin V, Haggarty P, Abramovich DR, Ashton J, Moffat CF, McNeill G, et al. Dietary intake and tissue concentration of fatty acids in omnivore, vegetarian and diabetic pregnancy. *Prostaglandins Leukot Essent Fatty Acids.* settembre 1998;59(3):209–20.
23. Williams L, Seki Y, Vuguin PM, Charron MJ. Animal models of in utero exposure to a high fat diet: A review. *Biochim Biophys Acta - Mol Basis Dis.* 2014;1842(3):507–19.
24. Borges Manna L, Papacleovoulou G, Flaviani F, Pataia V, Qadri A, Abu-Hayyeh S, et al. Ursodeoxycholic acid improves fetoplacental and offspring metabolic outcomes in hypercholanemic pregnancy. *Sci Rep.* dicembre 2020;10(1):10361.
25. Rosario FJ, Kanai Y, Powell TL, Jansson T. Increased placental nutrient transport in a novel mouse model of maternal obesity with fetal overgrowth: Maternal Obesity and Placental Nutrient Transport. *Obesity.* agosto 2015;23(8):1663–70.
26. Jones HN, Woollett LA, Barbour N, Prasad PD, Powell TL, Jansson T. High-fat diet before and during pregnancy causes marked up-regulation of placental nutrient transport and fetal overgrowth in C57/BL6 mice. *FASEB J.* gennaio 2009;23(1):271–8.

27. Akerele OA, Cheema SK. A low-fat diet enriched in fish oil increased lipogenesis and fetal outcome of C57BL/6 mice. *Reproduction*. agosto 2017;154(2):153–65.
28. Narasimhan H, Chudnovets A, Burd I, Pekosz A, Klein SL, Simanjuntak Y, et al. Animal models of congenital zika syndrome provide mechanistic insight into viral pathogenesis during pregnancy. *PLoS Negl Trop Dis*. 2020;14(10):1–20.
29. Georgiades P, Fergyson-Smith AC, Burton GJ. Comparative developmental anatomy of the murine and human definitive placentae. *Placenta*. 2002;23(1):3–19.
30. Leventis PA, Grinstein S. The Distribution and Function of Phosphatidylserine in Cellular Membranes. *Annu Rev Biophys*. 1 aprile 2010;39(1):407–27.
31. Kallen CB. Steroid hormone synthesis in pregnancy. *Obstet Gynecol Clin North Am*. dicembre 2004;31(4):795–816.
32. Caine EA, Scheaffer SM, Arora N, Zaitsev K, Artyomov MN, Coyne CB, et al. Interferon lambda protects the female reproductive tract against Zika virus infection. *Nat Commun*. 2019;10(1):280.
33. Tang WW, Young MP, Mamidi A, Regla-Nava JA, Kim K, Shresta S. A Mouse Model of Zika Virus Sexual Transmission and Vaginal Viral Replication. *Cell Rep*. dicembre 2016;17(12):3091–8.

## **Chapter 4**

### *General discussions*

At the beginning of this century, ZIKV virus (ZIKV) was a neglected pathogen isolated from a sentinel monkey and mosquitoes in African forests. Since 2007, the year its first outbreak in the Yap Islands, ZIKV has become an emerging global health problem, involving 89 countries worldwide. One of the most concerning features of this pathogen is the ability to cross the placental barrier impairing fetal development in pregnant women. Notably, about 20% of mothers infected by ZIKV during the first trimester of pregnancy reported fetuses with physical and neurological malformations. To date, the most effective strategy to prevent ZIKV infection is the reduction of contact between vectors and susceptible populations since the main ZIKV transmission route is represented by mosquito bites. However, this approach is not always sufficient, because ZIKV can be efficiently transmitted also by other routes, including sexual intercourse and contact with body fluids. For this reason, the scientific community has been spending much effort in developing alternative approaches to fight ZIKV infection. On one hand, researchers have been working on the development of a safe vaccine able to reduce or prevent ZIKV infection in pregnant women and susceptible populations. Secondly, many resources have been invested in finding an effective therapeutic protocol to control ZIKV infection and reduce the possibility of vertical transmission during pregnancy. However, to date no vaccinations or specific antiviral drugs against ZIKV are available.

One of the aspects that hinders the possibility of efficiently preventing or controlling ZIKV infection in pregnant women is the limited knowledge of ZIKV pathogenesis at the level of the placenta, throughout the gestational period. From this perspective, this PhD project aimed to investigate the host and viral determinants capable of affecting ZIKV vertical transmission in the late stages of pregnancy. Unlike ZIKV pathogenesis in the first trimester of pregnancy, which is easily explained by high placental cell susceptibility; in the second and third trimesters, the placenta is supposed to be an efficient barrier able to physically and chemically protect fetus's health; however, ZIKV vertical transmission

occurs. This aspect of ZIKV pathogenesis suggested a remarkable versatility of the mechanism used by this virus to overcome host defenses and prompted us to focus our study on the final stages of the gestational period.

Thanks to the growing body of literature in the flavivirology field, we decided to primarily investigate lipids, among viral and host determinants of ZIKV pathogenesis in placental tissue. In the initial part of this study, for the first time, we created two genetically identical ZIKV viruses, which only differed in the lipid composition of their outer membrane called envelope. This achievement allowed us to define the role of viral lipids in ZIKV replication in placental tissue. We conducted the experiment using *in-vitro* immortalized human placental cell lines, but then we corroborated our findings through a more translational model represented by *ex-vivo* cultures of the full-term placenta. This study revealed the importance of interaction between viral and host cell membranes, determining how the lipid composition of those membranes could significantly affect ZIKV infectivity in placental villous trophoblasts. Moreover, this is the first study that carried out a lipidomic analysis on the envelope of ZIKV, which added further knowledge on viral structural characteristics besides the traditional and widespread genetic data.

Thanks to the previous study, we confirmed the important action of lipids in determining higher or lower ZIKV infectivity in placental tissues. Considering that both viral and host lipids are derived from host nutrients, such as animal and plant fat, we wondered if maternal dietary lipids could affect placental susceptibility to ZIKV infection. In particular, we hypothesized that diet could modulate placenta's host cell membranes, influencing the interaction of ZIKV with this tissue. From this perspective, we designed the second and more complex experiment, based on an *in-vivo* study, of this PhD project. To reach our goal, we first formulated four diets, different for lipid quantity and quality, mimicking the main human dietary patterns. Then, we tailored these diets to the mouse model, and we fed our four groups of female mice before and during the gestation period. Finally, we

analyzed the lipid composition of placental tissues by means of lipidomic assay. Our results showed that lipids of placental cells strictly depend on dietary intake, being affected by both lipid content and the characteristics of fatty acids. Although other few studies reported the influence of diet on cell membrane composition; for the first time, our work demonstrated how minimal variations of lipids in maternal diets were sufficient to change the entire lipidome of placental cells. Moreover, we used this finding to evaluate if a different placental environment, in terms of lipid framework, could affect the susceptibility of this tissue to ZIKV. To reach this goal, we intraperitoneally injected ZIKV into immunocompetent pregnant mice, previously fed with the experimental diets, at the late gestational stage. The choice of this animal model allowed us to mirror ZIKV infection in healthy women during the second or third trimester of pregnancy. Our findings corroborated the hypothesis that the lipid composition of cell membranes significantly influenced ZIKV dynamic in the placental tissues. Importantly, we observed that diets with a low content of fats, most of which consisted of unsaturated fatty acids, conferred the placental tissue resistance to ZIKV infection. On the contrary, placental tissues derived from mothers fed with diets enriched with saturated lipids displayed a relevant susceptibility to ZIKV.

Our results answer the initial questions of this PhD project but open several new issues:

1. Which is the underlying mechanism by which placental lipids affected ZIKV infection?
2. Besides the lipid structure of the placenta, can maternal nutrition change the functional proprieties of this tissue affecting other aspects of the fetal development?
3. Do dietary lipids influence the cell membrane composition of other tissues, such as immune or brain cells, further influencing ZIKV, but also other related *Flaviviruses*, pathogenesis?

4. How much of this *in-vivo* model and the experimental diets can be translated into the human field?

As reported above, several aspects remain to be explored; nevertheless, our findings revealed unprecedented possibilities in the management of ZIKV disease. Among these, we believe that the most important could be the use of the maternal diet as a prophylactic tool to prevent and control ZIKV infection during pregnancy. Since pregnant women often cannot be vaccinated or treated with antiviral drugs to avoid any side-effect to the fetus's health, this kind of approach could be unique in handling this, and similar, infectious diseases.

Concluding, we hope our study has not only presented new perspectives on the neglected interplay between dietary lipids and Flavivirus pathogenesis but has also opened the way to a new line of research in the field of prophylaxis for the control of ZIKV in pregnant women.




# Annex I

Poster presented at the 6th national congress of the Italian Society for Virology - July 3-5, 2022 - Naples

## MATERNAL DIETARY LIPIDS AS RISK FACTOR OF ZIKA VERTICAL TRANSMISSION IN A RODENT MODEL

**Mazzetto E.<sup>1</sup>** Pagliari M.; Baraldo L.; Bovo D.; Morelli G.; Stocchero M.; Mazzacan E.; Fortin A.; Panzarin V.; Claudia Z.; Stefani A.; Giordano G.; Giaquinto C.; Bonfante F.

<sup>1</sup> Department of Mother and Child Health of University of Padova  
If you wish to have more information scan here to find out my profile



---

### BACKGROUND

Zika virus (ZIKV) is a Flavivirus mainly transmitted among human populations by mosquito vectors. In pregnant women, ZIKV is able to replicate and cross the placenta barrier causing adverse consequences to the fetus ranging from miscarriages to fetal malformations called congenital ZIKV syndrome (CZS). Recent works underlined the important role of both host cell membrane and viral envelope lipids, pointing out how the success of host cell infection strictly depends on the type of viral and cell lipids and their reciprocal interactions.

### MAIN QUESTION AND GOALS

Viral and host cell membrane lipids can be considered main determinants in Flavivirus pathogenesis. Since ZIKV envelope lipids derive directly from the infected host cell membranes, and host cells, as placental cells, mainly derive their lipids from dietary fat; we decided to investigate whether dietary lipids could affect ZIKV pathogenesis at the level of placenta in pregnant women. To answer this question we performed a translational in vivo study in immuno-competent mice.

---

### MATERIALS AND METHODS

**WESTERN DIET**  
HIGH FAT  
MOSTLY SATURATED

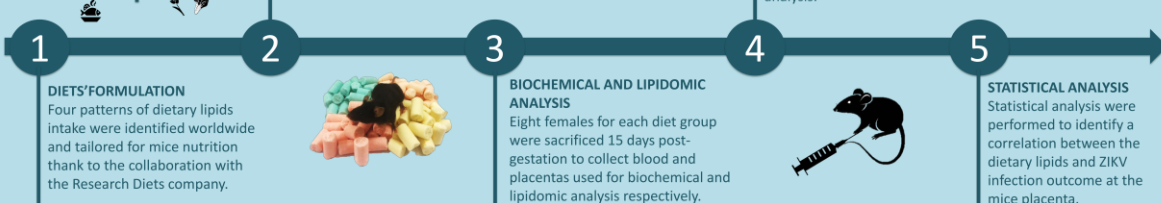
**ASIAN DIET**  
LOW FAT  
MOSTLY SATURATED

**MEDITERRANEAN DIET**  
HIGH FAT  
MOSTLY UNSATURATED

**AFRICAN DIET**  
LOW FAT  
MOSTLY UNSATURATED

**FEMALE MICE FEEDING AND MATING**  
C57BL/6J mice were divided into 4 groups and each group was fed with one of the four experimental feeds before mating and starting pregnancy.


**ZIKV INFECTION**  
Eight females for each diet group were infected with ZIKV 12 days post-gestation and sacrificed 6 days later to collect placentas and fetuses used for virological and immunohistochemical analysis.



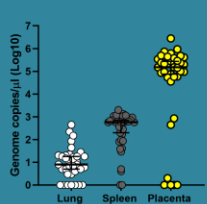
---

### RESULTS

- BIOCHEMICAL PARAMETERS** of pregnant mice resulted comparable among the four diet-groups demonstrating that, despite the different lipid content, the four feed formulations represented diverse but healthy diets suitable for sustaining a normal pregnancy
- LIPIDOMIC ANALYSIS** revealed that the lipid composition of placentas significantly differed among the four diet-groups.
- VIROLOGICAL AND IMMUNOHISTOCHEMICAL ANALYSIS** identified the placenta as the main tissue target of ZIKV. However, animals fed with a low content of saturated fatty acids such as mice in Mediterranean and African diets recorded a significantly lower number of infected placentas compared to mice fed with an Asian and a Western diet.
- STATISTICAL ANALYSIS** showed a significantly correlation between the lipid composition of mice placentas and susceptibility to ZIKV infection ( $r=0,931$ ). Moreover, an univariate approach using an ordinal logistic regression with a 15% false discovery rate determined that protection was positively related to the increase of Glycerophosphoserines.



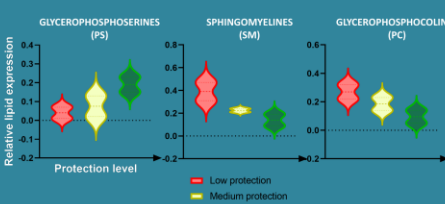
**ZIKV TISSUE TROPISM**



**PERCENTAGE OF INFECTED PLACENTAS PER DIET**

Diet	Non Infected	ZIKV-Infected
Western Diet	77.8%	22.2%
Mediterranean Diet	66.7%	33.3%
Asian Diet	74.9%	25.1%
African Diet	57.9%	42.1%

**CORRELATION OF PROTECTION**




---


### DISCUSSIONS

For the first time, our study has unveiled maternal diet as a fundamental determinant of ZIKV pathogenesis in a pre-clinical animal model of placental infection. These results not only present new perspectives on the neglected interplay between dietary lipids and Flavivirus pathogenesis, but open the way to a new line of research in the field of prophylaxis for the control of ZIKV.

### AKNOWLEDGEMENTS

This work was funded by the European Project ZIKAction and has been supported by the synergic collaboration among Department of Mother and Child Health of University of Padova, the Penta Foundation and the Istituto Zooprofilattico Sperimentale delle Venezie.





## *Acknowledgments*

Ringrazio il prof. Giaquinto per avermi dato la possibilità di intraprendere questo percorso di dottorato. Per me è stata un'opportunità di crescita professionale e personale davvero importante. Mi ha permesso di mettermi in gioco in prima persona su un progetto di ricerca avvincente e complesso, realizzando un desiderio che mi portavo dentro già dagli anni universitari. In particolare ringrazio il Prof. per la fiducia riservatami sin dal primo colloquio, del supporto puntuale nei momenti decisivi e della grande energia che è in grado di trasmettere ad ogni persona coinvolta nella sua sfera collaborativa.

Un ringraziamento speciale va al dott. Bonfante, co-supervisor di questo progetto di dottorato e mio mentore scientifico nella vita di tutti i giorni. Dai primi momenti passati a lavorare assieme, Francesco mi trasmesso la sua passione smisurata per la ricerca scientifica; e con pazienza ed impegno si è speso continuamente per la mia formazione tecnica ed intellettuale. Devo a Francesco non solo tutto ciò che ho appreso in questi anni di ricerca, ma anche la forma mentis che mi ha permesso di camminare con le mie gambe ed iniziare finalmente a costruire qualcosa di mio. Non posso dimenticare come Francesco sia stata la prima persona che ha saputo riconoscere qualcosa in me, spronandomi a capire il mio valore e le mie potenzialità. Credo che senza la sua fiducia non avrei mai saputo armarmi del coraggio e delle doti necessarie ad intraprendere il percorso nel mondo della ricerca, lo stesso mondo che ogni giorno mi rende felice ed orgogliosa del lavoro che ho scelto di fare.

Ringrazio il mio gruppo di lavoro, la "P4" dell'Istituto Zooprofilattico Sperimentale delle Venezie (IZSVE), senza il quale non sarei mai stata in grado di portare a termine questo progetto di ricerca così ambizioso e duraturo. In particolare, ringrazio Elisa, per aver seguito, dalla sierologia alla biologia molecolare, ogni aspetto tecnico di questa ricerca con precisione ineguagliabile e pazienza straordinaria. Alessandra, per aver dedicato il suo tempo di formazione personale a supportarmi nelle prime fasi di questo progetto, rendendosi sempre disponibile durante la validazione di ogni metodica *in-vitro* realizzata per questo studio. Le auguro, ora che anche lei si accinge ad intraprendere un percorso di dottorato, che la sua ricerca le possa riservare le stesse soddisfazioni che la mia ha riservato a me. Ringrazio Matteo per l'enorme supporto datomi in una delle fasi più delicate della sperimentazione *in-vivo*, la sua grande esperienza e l'innato talento per la ricerca, hanno permesso di portare avanti lo studio anche in momenti complessi dettati dall'utilizzo di un modello animale. Ringrazio profondamente Lisa per l'encomiabile aiuto datomi durante l'ultimo anno di dottorato. Nonostante la giovane età, e l'essersi appena affacciata al mondo del lavoro, con la sua professionalità, capacità intuitiva e dedizione inesauribile, ha permesso a questo progetto di raggiungere gli obiettivi più ambiziosi. Infine un grazie speciale anche a tutti gli altri componenti del gruppo, Alessio, Silvia, Daniele per il gioco di squadra e per aver contribuito a livello di feedback costruttivi o di aiuti tecnici ed organizzativi allo sviluppo di questa ricerca.

La conclusione di questo progetto è stato inoltre reso possibile dalla disponibilità e professionalità di molti ricercatori e specialisti afferenti ad altri dipartimenti, i quali hanno arricchito questo lavoro dal punto di vista scientifico rendendolo completo ed esaustivo nella sua versione finale. In particolare, dell'IZSVE, ringrazio Valentina e Andrea per aver curato la parte di biologia molecolare, analisi ed interpretazione dei dati; Claudia e Michela per il costante supporto nella realizzazione dei dati istologici; la dott.ssa Stefani per aver messo a disposizione conoscenze e macchinari inerenti ai profili biochimici. Infine

ringrazio l'amica e collega Diletta per essersi dedicata, con la passione che la caratterizza, alla parte di statistica e analisi dati nonostante i tanti impegni ed il poco tempo a disposizione.

Dell'università di Padova ringrazio Davide, Paola, Gabriele e Matteo per aver accolto e vinto la sfida di applicare la lipidomica alla virologia, aiutandomi sia nel supporto tecnico che morale. Daniela e Sara per aver pazientato nell'accogliermi ad utilizzare il loro fluorimetro. Giada, la dott.ssa Ricci e Mike per l'indispensabile apporto specialistico nello sviluppo di tutta la parte nutrizionale, dall'identificazione delle diete, alla loro formulazione, creazione e analisi. La dott.ssa Gervasi, e le ostetriche per averci aiutato nella raccolta dei campioni in un reparto delicato e riservato come quello di Ostetricia e Ginecologia. In tal ambito, un grazie sentito va a tutte le donne che hanno acconsentito a donare la loro placenta, rendendosi disponibili in uno dei momenti più delicati del loro percorso di gravidanza.

Spero che le pubblicazioni che usciranno da questa impresa collettiva possano dare la giusta soddisfazione a tutti coloro che hanno partecipato a questo progetto di ricerca.

Ringrazio il responsabile del corso dott. Bisogno e il dott. D'agata per la disponibilità e la pazienza con cui hanno accompagnato me, e i miei compagni, in questi anni di dottorato.

Ringrazio la collega e amica Elena per avermi aiutato nella stesura della tesi di dottorato, la sua guida e l'esperienza mi hanno permesso di mettere per iscritto quello che per anni è stato rilegato a quaderni di laboratorio e file archiviati.

Il dottorato mi ha insegnato che, in un bravo ricercatore, la professionalità e l'individualità sono intrinsecamente collegate tra loro, ed ognuno di questi aspetti contribuisce all'evoluzione e allo sviluppo dell'altro. Per questo motivo un grazie sentito va a chi, al di fuori del mondo accademico e istituzionale, ha curato e sostenuto con pazienza e amore la mia crescita personale. In primo luogo ringrazio la mia famiglia, che mi ha vista coinvolta nell'ennesimo percorso di studio, e nonostante questo mi ha sopportato nel continuo susseguirsi di gioie e scoramenti. Ringrazio mia sorella Giorgia e miei amici Matteo, Riccardo, Silvia, Alessandro, Giulia, Ilaria per avermi regalato sia momenti di spensieratezza che di confronto costruttivo. Grazie a Mattias per essermi sempre stato vicino, e a Vito per avermi aiutata a far chiarezza di fronte alle molteplici scelte che ho dovuto affrontare.

Infine l'ultimo ringraziamento, ed il più importante, va a Mattia, il mio compagno di vita e supporto imprescindibile del mio percorso personale e professionale. Grazie ai sacrifici, all'ironia e al grande cuore ha saputo assistermi nei momenti di difficoltà, che spesso caratterizzano imprese di questa portata. Mattia mi ha sempre spinto a dare il giusto peso alle cose, facendomi apprezzare tutti i momenti belli che questo dottorato mi ha regalato. Grazie per avermi accompagnata a crederci fino in fondo.